UNIVERSITY of TASMANIA

AMC
Australian Maritime College

Intelligent Control for Surface Vessels Based on Kalman Filter Variants Trained Radial Basis Function Neural Networks

By

Yuanyuan Wang, M.E. and B.E. (Marine Engineering)

National Centre for Maritime Engineering and Hydrodynamics

Australian Maritime College

University of Tasmania

Submitted in fulfilment of the requirements for the Degree of

Doctor of Philosophy

October 2017

DECLARATIONS AND STATEMENTS

Declaration of Originality

This thesis contains no material which has been accepted for a degree or diploma by the University or any other institutions, except by way of background information and duly acknowledged in the thesis, and to the best of my knowledge and belief no material previously published or written by another person except where due acknowledgement is made in the text of the thesis, nor does the thesis contain any material that infringes copyright.

Authority of Access

This thesis may be made available for loan and limited copying and communication in accordance with the Copyright Act 1968.

_____

Yuanyuan Wang Date:18 October 2017

Statement of Published Work Contained in Thesis

The publishers of the papers comprising Chapter 2 to Chapter 5 hold the copyright for that content, and access to the material should be sought from the respective journals and conference proceedings. The remaining unpublished contents of the thesis are submitted and under review and may be made available for loan and limited copying and communication by the Copyright Act 1968.

Statement of Co-Authorship

The following people and institutions contributed to the publication of work undertaken as part of this thesis:

- Yuanyuan Wang, University of Tasmania (Candidate)
- Dr Hung Duc Nguyen, University of Tasmania (Author 1)
- Assoc.Prof. Shuhong Chai, University of Tasmania (Author 2)
- Prof. Faisal Khan, University of Tasmania (Author 3)

Publications list and proportion of work details

Chapter 2 **'Radial Basis Function Neural Network Based Rudder Roll Stabilisation for Ship Sailing in Waves'** Candidate was the primary author. Author 1, Author 2 and Author 3 assisted with refinement and presentation. [Candidate: 80%, Author 1: 10%, Author 2: 5%, Author 3: 5%]
Chapter 3-- Part A **'Rudder Roll Stabilisation Using Extended Kalman Filter Trained Radial Basis Function Networks for Ship in Waves'** Candidate was the primary author. Author 1, Author 2 and Author 3 assisted with refinement and presentation. [Candidate: 80%, Author 1: 10%, Author 2: 5%, Author 3: 5%]
Chapter 3-- Part B **'Unscented Kalman Filter Trained Neural Networks Based Rudder RollStabilisation System for Ship in Waves'** Candidate was the primary author. Author 1, Author 2 and Author 3 assisted with refinement and presentation. [Candidate: 80%, Author 1: 10%, Author 2: 5%, Author 3: 5%]

Chapter 4 **'Modelling of a Surface Vessel from Free Running Test Using Low Cost Sensors'** Candidate was the primary author. Author 1 and Author 2 assisted with refinement and presentation. [Candidate: 85%, Author 1: 10%, Author 2: 5%]
Chapter 5-- Part A **'Experimental and Numerical Study of Autopilot Using Extended Kalman Filter Trained Neural Networks for Surface Vessels'** Candidate was the primary author. Author 1 and Author 2 assisted with refinement and presentation. [Candidate: 85%, Author 1: 10%, Author 2: 5%]
Chapter 5-- Part B **'Unscented Kalman Filter Trained Neural Network Control Design for Ship Autopilot with Experimental and Numerical Approach'** Candidate was the primary author. Author 1 and Author 2 assisted with refinement and presentation. [Candidate: 85%, Author 1: 10%, Author 2: 5%]

We the undersigned agree with the above stated "proportion of work undertaken" for each of the above published (or submitted) peer-reviewed manuscripts contributing to this thesis

Signed:	Assoc Prof. Shuhong Chai	Prof. Faisal Khan
Dr. Hung Duc Nguyen	Co-supervisor	Co-supervisor
Primary Supervisor NCMEH,	NCMEH, AMC, UTAS	NCMEH, AMC, UTAS
AMC, UTAS Signature:	Signature: _____	Signature: _____
Date: 18/10/2017	Date: 17/10/2017	Date: 17/10/2017

Acknowledgements

Firstly, I would like to express my sincere thankfulness and gratitude to my supervisor Dr. Hung Duc Nguyen, who has been a tremendous mentor for me. I would like to thank him for his continuous support of my PhD study and selfless guidance to my research and this thesis all the time. It is Hung's patience, immense knowledge and insightful discussions and suggestion that enlighten me on the subject of intelligent control for surface vessels, and his brilliant comments and scientific advice which has given me a more profound understanding of the vessel control area. It is no exaggeration to say that Hung is my primary and priceless resource in my study and his supervision has a significant meaning on both my study as well as my future career.

I will also forever be thankful to my Co-supervisor Assoc. Prof. Shuhong Chai for her helpful research advice and suggestions, and also for her insightful comments and hard questions which sparked me to widen my research from many perspectives. Also, I would like to thank the other Co-supervisor Prof. Faisal Khan for his supports during my research project.

Besides my supervisors, I would especially like to acknowledge the AMC Technicians, Michael Underhill, who arranged the free running tests on Lake, and Tim Lilienthal, who gave me a lot of help in the balancing experiment of the newly developed model scaled free running. Without their precious support, it would not be possible to conduct this research. Also, the financial assistance and my scholarship provided by the University of Tasmania are gratefully acknowledged.

Other special thanks go to my family. There is no word to convey how appreciative and grateful I am to my mother, my father and my partner's family for the supporting and sacrifices they have made throughout these years. Their love and care are the driving force for me to move forward. Moreover, the grateful thanks should go to my soul mate and partner, Shurui Wang, who is sticking by my side, sharing all my happiness and sadness, and spending all the sleepless nights with me. She is always my support, both physical and spiritual. She always has faith in me and my intellect even when I felt frustrated and self-doubted.

Last but not the least, I would like to thank all my colleagues in Connell Building, Yuting Jin, Junyi Lee, Wei Zhang and other friends. For their helps, assistance and collaborations with me in different domains, as well as thank them for providing support and friendship that I needed.

Abstract

For decades, there has been a significant increase in the demand of using a ship's autopilot for complicated manoeuvres, such as maritime underway replenishment and sailing in constrained waters. In order to achieve these applications even in the presence of severe sea conditions, new control algorithms are required for the autopilots to control the underactuated ships. The study detailed in this thesis investigates the development of Radial Basis Function Neural Networks (RBFNN) based autopilot to satisfy the functionalities of course keeping, rudder roll damping, and path tracking. Two novel Kalman Filter Variants (KFV) based training algorithms, namely Extended Kalman Filter (EKF) and Unscented Kalman Filter (UKF), were proposed to improve the performance of the autopilot in the aspects of compensating the effects of system nonlinearity and unpredictable external disturbances.

The primary emphasis of this study is in the design of autopilots, analysis of their performances, verification and validation through the experimental and numerical investigations. Considering the better generalisation ability and faster converge performance, modified EKF and UKF were proposed as the alternatives of the Back-Propagation (BP) training method for RBFNN controller to approximate the control law of the ship's motions. The research splits into four phases. In first two phases, the capabilities of the proposed controllers, i.e., course keeping and path tracking controllers incorporating with roll damping controllers, were validated by adopting the mathematical model of a full scale ship with environmental disturbances. In order to enable both the experimental and numerical studies of proposed autopilots, the third phase focused on the modelling of the free running scaled model 'Hoorn', which was newly developed by utilising the embedded open-source hardware and low-cost sensors. In the last phase, the performances of course keeping and path tracking were investigated by conducting experiments using the physical model on Trevallyn Lake (Tasmania, Australia) and simulations using the developed mathematical model.

The simulation results of the full scale ship showed that both EKF RBFNN and UKF RBFNN based control schemes were feasible to maintain the ship advancing on desired course and trajectory while reducing the roll damping only use the rudder as the actuator. The free running tests and system identification were successfully implemented to develop the four Degree of Freedom mathematical model of 'Hoorn', which has been verified by the comparison between experimental data and simulation results. The following experimental and numerical studies

showed that the presented signal processing methods were effectively employed to provide acceptable states estimation, while the KFV trained neural network controllers were adequately making the ship to follow the desired states in the presence of variable external disturbances. Consequently, the ship's robustness and controllability in counteracting environmental disturbances were corroborated.

Based on the above-mentioned investigations, it is concluded that the developed control schemes could effectively determine the deflections of rudder to fulfil the proposed functionalities. The experiment results also demonstrated that the developed autopilots were assisted in effectively tracking desired states and enhancing the ship's controllability with unpredictable disturbances. Moreover, in comparison with the EKF RBFNN based autopilot, the advantages of UKF RBFNN based autopilot consisted in the fast learning rate and smooth control law output while making the ship to meet the predefined requirements. Additionally, the experimental and simulated results have indicated that the developed control schemes have a great potential to be utilised commercially on marine vehicles, while the presented methods in developing free running model supplied a low-cost but efficient way to investigate the ship's hydrodynamic characteristics and intelligent autopilot experimentally.

Table of Contents

List of figures

List of tabels

Nomenclature

$C(v)$	Matrix of Coriolis and centripetal terms
$C_{Roll}\ C_{Rudder}\ C_{Yaw}$	Cost value of Roll, Rudder actions and Yaw deviation
D	damping matrix
$\dot{}_d$	Desired value
E_0	Trajectory deviation
$h(z)$	Activation function in the neuron
$I_x\ I_y\ I_z$	Inertia moments
F_r	Vector of input due to rudder
F_w	Vector of wave disturbance
$g(\eta)$	Vector of restoring forces and moments
$J_x\ J_y\ J_z$	Added inertia moments
$K\ N$	External moment of yaw and roll
M	Inertia item
m	Mass of vessel
$m_x\ m_y\ m_z$	Added masses
n	Shaft speed
η	Position and orientation
P	Covariance matrix of Kalman Filter
Q	Covariance of observation noise
R	Covariance of the process noise
$r\ p$	Roll and yaw displacement
τ	Input vector of the ship
$u\ v$	Surge and sway velocity

$X.'\ Y.'\ K.'\ N.'$	Hydrodynamic coefficients in the degree of surge, sway, yaw and roll
$X\ Y$	Forces in terms of surge and sway
$x\ y\ z$	Body fixed coordinates
δ	Rudder angle
$\widehat{w}$	Weights of the neural networks
$\phi\ \theta\ \psi$	Roll, pitch, yaw angle

Abbreviations

AMC	Australian Maritime College
AUCC	Australian Control Conference
AUV	Autonomous Underwater Vehicle
BP	Back-Propagation
CFD	Computational Fluid Dynamics
DAQ	Data Acquisition
DOF	Degree of Freedom
dps	Degree Per Second
EBS LOS	Enclosure Based Steering Line of Sight
ECDIS	Electronic Chart Display and Information System
EKF	Extended Kalman Filter
FPGA	Field Programmable Gate Array
GNC	Guidance System, Navigation System and Control Systems
GPS	Global Positioning System
I²C	Inter-Integrated Circuit
ICCAR	Conference on Control, Automation and Robotics
IMU	Inertial Measurement Unit
IMO	International Maritime Organisation
KFV	Kalman Filter Variants
LSB	Least Significant Bit
NN	Neural Networks
PD	Proportional-Derivative

PID	Proportional Integral Derivative
PM	Pierson-Moskowitz
PMM	Planar Motion Mechanism
PWM	Pulse-width Modulation
RBFNN	Radial Basis Function Neural Networks
RLS	Recursive Least Square
ROV	Remotely Operated Vehicle
RT	Real-Time
SI	System Identification
SPI	Serial Peripheral Interface
UKF	Unscented Kalman Filter
USV	Unmanned Surface Vessels
UT	Unscented Transformation
UTAS	University of Tasmania

Chapter 1
Introduction

This chapter presents the introductory information about this thesis. The background and the research motivations are described coordinating with the literature review. To address the research questions and fulfil the research objectives, the relevant methodologies, as well as the novel aspects, are briefly introduced. The details of each chapter are outlined in the last section.

1.1 Background

Following the contrivance of the gyrocompass, the automatic steering devices of ships have experienced almost 100 years since the pioneering autopilot developed by Sperry (1922) and Minorsky (1922). After that, it has been widely utilised in various circumstances and occasions.

In recent years, with the comprehensive progress of maritime industry development, autopilots are evolving from basic steering devices to competent systems. They are expected to have the capability of carrying out the special operation tasks, including rudder roll stabilisation, underway replenishment (Fig. 1. 1 a), cable placing, as well as sailing in a dense traffic area like narrow straits and channels. Meanwhile, the increasing requirements of conducting complex manoeuvring, such as maritime search and rescue, mine hunting and monitoring data collection, call for the employment of feasible autopilots. Also, the burgeoning technology of Unmanned Surface Vessels (USV, see Fig. 1. 1 b) demands capable autopilots to fulfil the oceanographic explorations and geographic survey in the sea area where encompassing significant resources to meet the need of humanity.

a. Underway replenishment between Royal Australian Navy and Japanese Maritime Self Defence Force

b. USV made by ASV Global

Fig. 1. 1 Complex manoeuvrings and new technology in maritime industry (Staples, 2013, Haun, 2014)

However, the design of autopilot for the ship remains complicated since ships are nonlinear, time variant and coupled systems. It is worth noting that conventional ships are under-actuated because the number of the actuators is fewer than that of the variables to be controlled. Moreover, the manoeuvring and manipulating would be difficult when the ship subject to severe environmental disturbances such as the wind, waves and current. All of these challenges will influence the control performance of the ship, thus requiring the investigations of advanced motions control systems to guarantee the increasing requirements of controllability and manoeuvrability.

1.2 Problem definition

The autopilot is a control facility for automatically manipulating the actuators to decrease the errors between the desired and the actual sailing states without constant human operations. Generally, the framework of the closed-loop control for maritime vessels can be illustrated in Fig. 1. 2 (Fossen, 2011). It is indicated that three subsystems, i.e. guidance system, navigation system and control systems (GNC system), interact with others via signal and data transmission. Although these three modules can be coupled more tightly with other modules, the loose modularity scheme is widely adopted due to the advantage of allowing software updating from the industrial point of view.

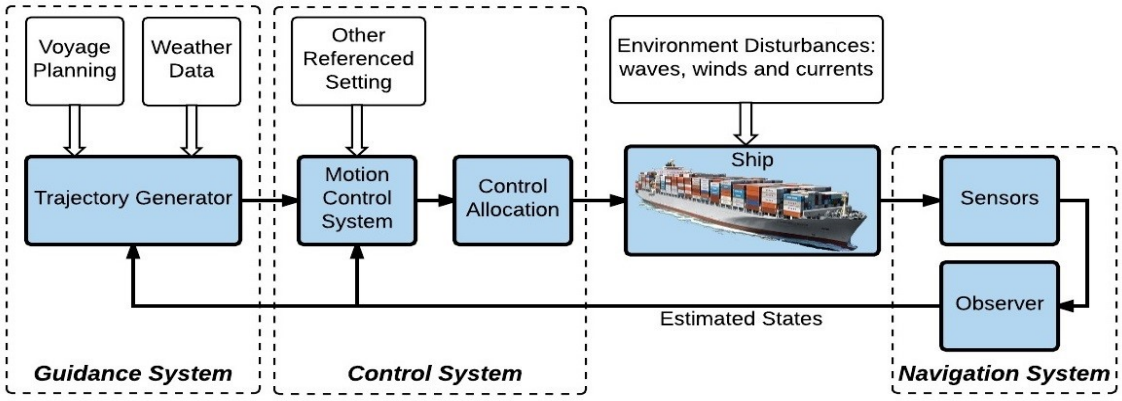

Fig. 1. 2 The signal flow of autopilot control strategy for the maritime vessel

The functionalities of the subsystems can be classified as:

The guidance system is the module which continuously determines the desired position, desired yaw angle and other desired kinematics items for the following module. Deck officers regularly set these reference data according to the voyage planning and weather routing data.

The navigation system is achieved by utilising the Global Navigation Satellite System (GNSS) in conjunction with other sensors including accelerometer, gyroscope and compass. The raw data are processed by the observer to estimate the sailing states.

The control system is typically cooperated with the guidance system. The system aims to calculate the control actions to satisfy the control tasks. General examples of the control tasks are course keeping, path tracking, roll damping etc. Thus, different control strategies can be employed according to the requirements of relevant objectives.

Therefore, for an underway underactuated surface vessel, the estimated states of the ship obtained from the observer are transmitted to the guidance system along with the weather routing data and voyage planning data to determine the online desired states. The error between the desired states and the actual states are utilised by the control system to calculate the necessary angles for the rudder to lead the ship along the desired path. In this process, the control performance is usually depended on the capability of the proposed controller. Thus it drew many attentions from the researchers.

1.3 Research motivations

After the long-term application of mechanical autopilots (Fig. 1. 3 a), the employments of the

inexpensive but efficient microcomputers have made the electronic autopilots practically realisable. Recent years, the electronic autopilots (Fig. 1. 3 b) has been integrated with the Electronic Chart Display and Information System (ECDIS). This progress speeded up the development of autopilots because the application and validation of new control algorithms are easily accessible in use of the corresponding platform. Subsequently, the development of the autopilot experienced a long history along with development of the control theories.

a. Mechanical autopilot b. Electronic autopilot connected with ECDIS

Fig. 1. 3 The front panels of the mechanical autopilot and electronic autopilot made by Sperry (Marine, 2014)

Conventional Autopilot

The types of the autopilot are relatively diverse depending on the control scheme. Benefiting from the availability of the practical Proportional Integral Derivative (PID) controller, the autopilots with improved control performance was developed and extensively accepted until the 1980s. Despite the acceptable performance and comprehensible architecture, the drawback of the PID based autopilot remained that it was qualified in providing optimal performance only at the designed situations (Du et al., 2007, Moreira et al., 2007). However, as a consequence of changes in the sailing states and environmental disturbances, dynamic characteristics will enormously change. To compensate the unpredictable environmental disturbances and cope with the high degree of system nonlinearity, the PID based autopilots usually adopt the manual adjustment (Zirilli et al., 2000) and gain scheduling approaches (Tannuri et al., 2010). Yet, it is complicated and tedious to propose the proper gain scheduling or adjust the parameters on time as the processes require sufficient understanding of control theories and time-consuming tests at sea. Especially, when the ship is sailing in the heavy seas with severe disturbances, it is impossible to use the PID based autopilot for safe manoeuvring. Hence, the deck officers' manual steering is required when the ship is advancing in severe weather.

Robust and adaptive autopilot

The limitations of the conventional PID based controller can be mitigated by adopting the robust control algorithms. The robust control methods algorithms are proposed in the attempt to find the satisfactory parameters which are capable of guaranteeing the control performance in a wide range of operation conditions (Alfi et al., 2015). The robust autopilots have been developed to rectify the diminished controllability of the vessel sailing in severe weathers (Roberts, 1992, Roberts et al., 1997, Zhang et al., 2006, Do et al., 2004, Morawski and Pomirski, 1998). The results indicated that the developed robust autopilots were competent to address the uncertainties in the hydrodynamic and geometric parameters.

Parallel to the investigation of the robust control algorithms, the adaptive control algorithms, where the parameters of the controller are constantly adjusted to determine the optimum of the cost function, were also employed to improve the control capability of the autopilots. In which, the autopilots based on the methods of Self-tuning PID (Källström et al., 1979, Brink et al., 1979), Model Reference Adaptive Control (Zirilli et al., 2000, Van Amerongen, 1984), Linear Quadratic Gaussian (Katebi and Byrne, 1988), Auro-Regressive Model Based Self-tuning Pole Assignment and Optimal Control (Nguyen, 2000), Batch Adaptive (Park et al., 2000), Inverse Kinematics (Antonelli et al., 2004), and Predictive Control (Wu et al., 2012) have been successfully developed to compensate the changes of environmental situations while reducing manual operations. The results indicated that the adaptive autopilots are capable of coping with the unknown disturbances and enhancing the controllability.

Although the benefits of the above-mentioned robust and adaptive autopilots are attractive, some disadvantages are needed to be fixed, including:

- The structure of some controllers are complex, which will lead to computational expensive (Pao, 1989);
- The successful application of some adaptive methods need an enormous amount of prior information (Irwin et al., 1995); and
- The adaptive methods have the risk of unstable when the changing speed of the dynamics is beyond it adapting capability (Sun et al., 2014).

Modern control theory based autopilot

The last decades have witnessed the increasing research efforts in the area of modern control theory. As the sequence of the development, increasingly control strategies with promising

adaptive qualities and robustness have been proposed as the possible successors for the autopilot design:

- The Sliding Mode control algorithm has been adopted to ship's motions control system by Zhang et al. (2000), Antonelli et al. (2001), and Ashrafiuon et al. (2008). Although the developed control systems were efficiency in some extents, the drawback of this approach is that the resulted control actions were highly frequent, which will lead to the energy wastes and may generate unexpected dynamic distortions.
- Some of the autopilots were successfully developed by generating appropriate control input by using the Fuzzy Logic method (Polkinghorne et al., 1995, Gierusz et al., 2007). The drawback of this approach was the difficulties in formulating the fuzzy control rules, which were generally obtained by trial-and-error based human knowledge.
- Autopilots using the Genetic control techniques also have been reported (McGookin et al., 2000, Bruzzone and Signorile, 1998). However the genetic control is complex: apart from the genetic parameters, other items like the fitness function, choice of genetic encoding and genotype to phenotype mapping are also vital in the efficacy of the system. Moreover, it needs a huge number of propagations and generations before getting the proper results.
- The method of back stepping also has been considered as the practical alternative of the challenging control applications, as it provides an efficient way to design the autopilot (Du et al., 2007, Li et al., 2009, Pettersen and Nijmeijer, 2001, Skjetne et al., 2005). It is worth noting that, since the control law is directly related to the states errors, significant control actions and unexpected tracking errors can be generated from the unstable error conditions.

Therefore, to achieve easily accessed controllability and robustness, the other means of control schemes are required.

Neural networks based autopilot

Prompted by the development of computing technology, the sophisticated control algorithms based on Neural Networks (NN) became applicable. The main advantage of using NN is that the dynamics of the vehicles do not need to be completely known as the prior information. Especially, this feature is beneficial to the control of the marine vehicle, whose model is extremely challenging to be determined. Another future of such control method is their capability in 'comprehending' the ship's multi-variable characteristics and mimicking human's operations, which avoids the analytical analysis of the complicated nonlinear differential

equations.

The advantages inspired the design of NN based autopilot. The successful implementation of the NN based autopilot has been reported in Burns (1995), Tee and Ge (2006), Leonessa et al. (2006), Zhang and Zhang (2015), Wang and Er (2015). It is indicated that the NN based controller is capable of minimising the error and enhancing the safety and reliability. Considering the excellent capability of NN in the aspect of ship's motion control, it has been adopted to design the rudder roll stabilisation system (Alarcin and Gulez, 2007, Fang et al., 2010a, Li et al., 2010, Fang et al., 2012a). It is shown that the developed control strategies are feasible to make the ship advancing on predetermined course or trajectory while reducing the roll motion only use the rudder as the actuator.

Among the present multilayer NN, the Radial Basis Function (RBF) NN has the features of simple architecture and good generalisation capability, which is essential to avoid unnecessary and lengthy calculation (Liu, 2013). These merits provide the motivations for Unar and DavidJ (1999), Wu et al. (2012), Zheng and Zou (2016) to adopt the RBFNN based controller to design autopilots. It is demonstrated that the developed control strategies have valuable self-learning capabilities that make it adapt to the variable operating conditions while optimising the tracking performance. Thus, the RBFNN architecture was employed in this study.

Novel NN training algorithms based on Kalman Filter Variants (KFV)

It is well known that the performance of the RBFNN based controller depends on the method for determining the network weights. There are two kinds of NN training algorithms, namely derivative-free method and derivative-based method. The Genetic Method (Chen et al., 1999) and Learning Automata (Narendra and Thathachar, 2012) are the examples of the derivative-based method. The derivative-based methods, including the well-known Back Propagation (BP) method (Simon, 2002), the Fully Supervised Gradient Descent method (Karayiannis, 1999) and Back Stepping method (Li et al., 2004), have been widely utilised to train the neural networks. Although these training algorithms have been proved to be effective for weights estimation, there exist some drawbacks. The disadvantage of the derivative free training methods remains that the converging speed is slow. On the other hand, the derivative based methods have the potential to converge to minima. Moreover, the algorithms are dependence on analysing derivatives, which increased the computational expensive and difficulties in applying the methods to specific types of NN architectures.

Actually, the training of the NN based controller can be viewed as a problem of states estimation. In this situation, representing the model's states by a probability distribution function has distinct advantages. It is the most common way to use Gaussian Random Variables to achieve this process and represent the model state process and measurement noises. A practical training algorithm based upon the Extended Kalman Filter (EKF) for multilayer feed forward networks was proposed and have exhibited substantial improvements relative to standard BP (Puskorius and Feldkamp, 1992). Unlike other high order approaches, the EKF based algorithms for NN training does not require batch processing, which makes it more suitable for online use (Puskorius and Feldkamp, 1994). It is indicated that, with EKF training, the learning speed is improved and the number of tuning parameters is reduced (Sum et al., 1999a).

However, in the EKF, the state distribution is approximated and propagated through the first order linearization of the system. This process can introduce error in the posterior mean and covariance when transforming the GRV, which may lead to sub-optimal performance and sometimes divergence. Especially, the performance using EKF estimation method will degrade greatly when the nonlinearity is severe (Zhan and Wan, 2006). For the UKF, which is firstly developed by Julier and Uhlmann (1997b), the state distributions are also approximated by GRV, but it addressed the propagated error by using the deterministic sampling approach, namely Unscented transformation sigma points, which are chosen based on the square root decomposition of the prior state covariance. These sampling points are capable of capturing the mean and covariance of the GRV and propagating through the true nonlinear system (Wan and Van Der Merwe, 2000). The UKF estimator for NN training has been presented by Choi et al. (2003) and de Oliveira (2012a) with results exceed the performance of the linear state estimation. It is obvious that this method gave a more accurate estimation of the weights, which led to an improvement of the convergence performance (Van Der Merwe and Wan, 2001, Julier, 2002).

1.4 Research questions and objectives

As outlined above, modern control methods have been adopted to design automatic control to assist in the manoeuvrability of the vehicle in the presence of unpredictable disturbances. However, there is a huge space for improvement. This study aims to improve the capability of the conventional RBFNN based controller and to develop the ship’s motions control system

with the functions of course keeping, course changing, path tracking and rudder-roll damping. The proposed control scheme in this project can be illustrated in the Fig. 1. 4. The motivation behind this study is to improve the control convergence speed and the capability in counteracting the external disturbance.

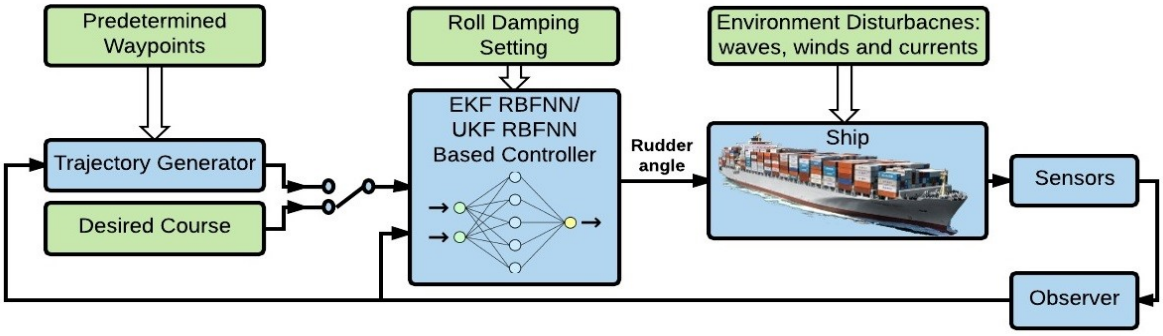

Fig. 1. 4 Ship's control system employing EKF/UKF RBFNN based control algorithms.

The key objectives of the research project include the following components:

- Investigating the capability of modified BP RBFNN based controller regarding course keeping, path tracking and roll damping with different sailing states. Comparing the performance of the proposed controllers with the conventional PID controllers to characterise the efficiency;
- Development of the RBFNN based control system which adopts the EKF and UKF algorithms for weights training to improve the learning speed and enhance the robustness against external disturbances in use of a full scale mathematical model (see Appendix I);
- Updating a free running scaled mode named 'Hoorn' (see Appendix II) with new embedded hardware and conducting the system identification to establish the four Degree of Freedom (DOF) mathematical model (see Appendix III); and
- Implementation of the developed control systems on both the physical ship and numerical model. Validating the efficiencies of the autopilots through considering different sailing conditions and environmental disturbances.

Moreover, each objective is executed by answering the corresponding research question. Therefore, the questions for this project are expressed as follows:

- How is RBFNN based autopilot designed to reduce the deviation of course keeping and path tracking while stabilising the roll motion when vessel sailing at rough sea?

- Whether the EKF and UKF based training algorithms are competent to improve the capability of the ship in compensating the external disturbance generated by waves and the winds when developing the autopilot system?
- How can a low-cost but effective free running scaled model be established to enable the experimental and numerical validations of the developed control systems? and
- Whether the developed autopilots are efficient and robust in comparison with the conventional autopilot system during the experimental tests?

1.5 Methodology and novel aspects

To solve the research questions, both experimental studies (using a physical model), and numerical studies (using the mathematical models of full scaled and model scaled vessels) have been conducted to investigate the performance of the designed motion control systems. The proposed research project contains four successive phases as follows. The phases are outlined in Fig. 1. 5.

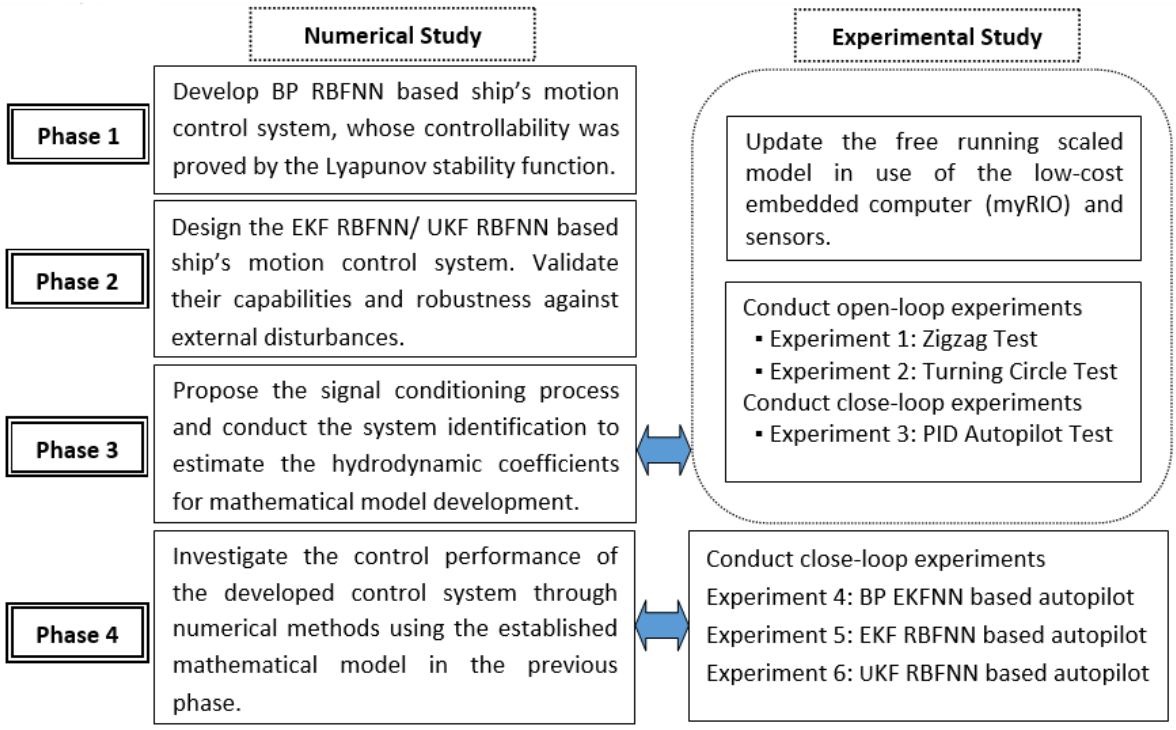

Fig. 1. 5 Research methodology in the four phases

1.5.1 Research methodology

Phase 1: Development of BP RBFNN based ship's motions control system

The RBFNN control algorithm was modified and employed to realise course keeping and roll damping while the external disturbances were applied. For the developed control scheme, the most commonly used BP training method was adopted to update the weights online. Considering the effectiveness of the proposed control algorithm, the ship's conventional control system, in consideration of the course keeping and path tracking, was extended to stabilise the roll motion simultaneously only use the rudder as the actuator.

Phase 2: Development of EKF/ UKF RBFNN based ship's motions control system

In this phase, the EKF and UKF methods were investigated to train the proposed RBFNN. Nonlinear waves disturbances were employed to effect on the motion responses of the ship. In addition, Enclosure Based Steering Line of Sight (EBS LOS) path tracking method was studied to ensure that the ship can sail according to the preset waypoints. The control performances, including the course keeping, path tracking and rudder roll damping, were investigated. The performances of proposed control systems were thoroughly evaluated and analysed.

Phase 3: Modelling of the newly developed free running model scaled vessel 'Hoorn'

In order to enable both experimental and numerical studies of the developed controllers, the free running scaled model 'Hoorn' was developed by using the 'myRIO' as the embedded computer and Data Acquisition (DAQ) card. The signal processing of the low-cost sensors and the system identification were carried out to develop the mathematical model of the physical ship.

Phase 4: Experimental and numerical tests of the developed control system

At this stage, the performances of the autopilot using EKF and UKF trained neural networks for surface vessels were verified by conducting experiments with the physical model on Trevallyn Lake and simulations using the developed mathematical model. The improvements of the developed EKF/UKF RBFNN based autopilot were validated by the comparison with that of the BP RBFNN based one.

1.5.2 Novel aspects

There are three novelty aspects in which this project provides original contributions to the design of intelligent autopilots.

The development of ship's motion control system based on EKF trained RBFNN

Although the PB algorithm has been widely applied in training the NN based controller, there remain some potential drawbacks including the low converge speed and the complicated structure due to the analysis of the system derivatives. This project is the pioneering work that investigates the design of the ship's control motion control system in use of the EKF as the training algorithm, which was treated as the parameter identification problem for a nonlinear dynamic system. Theoretically, this algorithm updates parameters in a way that is consistent with the previously measured data and generally converges in a few iterations. The experimental and numerical results indicated that the EKF RBFNN based control system was competent in course keeping, path tracking, as well as rudder-roll damping by using the rudder only as the main actuator. Also, its robustness against the environmental disturbances was demonstrated.

The development of ship's motion control system based on UKF trained RBFNN

Although the EKF training algorithm has the merits of straightforward and simple, it owns drawbacks, including instability due to linearization and the biased nature of its estimates. Thus the novel UKF is proposed to improve the capability further. Rather than using the linearization approximation approaches, the UKF algorithm involves using the unscented sigma points for calculating the state predictions and the relevant covariance, and then a weighted mean and covariance is taken. The control technique developed in this project was initially examined within a simulated environment by employing a full scale ship's mathematical model to achieve the tasks of path tracking, course keeping and roll damping. In addition, the efficacy and utility of the developed control system were illustrated through experimental approaches. The results demonstrate that the UKF RBFNN based autopilot leads to faster settling time and higher quality solutions without over-sizing computational expensive.

The capabilities of EKF RBFNN and UKF RBFNN based autopilot in the aspects of faster learning and good disturbance rejection can be analysed from the numerical and experimental results. It can be observed that the UKF training algorithm has increased computational complexity and expense, but its performance obviously increased in comparison with EKF based one. Therefore, the selection of the EKF or UKF training algorithms can be determined by considering the specification of the control tasks as well as the hardware computational capability.

The approach of conducting intelligent autopilot investigation using low-cost free running model scaled ship

To investigate the above-mentioned motions control system through the experimental approaches, a free running model scaled vessel was developed and the corresponding signal processing algorithms, working as the observer, was introduced. In addition, the 4DOF mathematical model with full coefficients, which is essential to carry out the study through numerical approaches, was proposed.

The configuration of the free running model scaled ship was firstly presented with attractive advantages. In order to avoid incompatibility amongst every component and to ensure satisfactory performance of the designed platform, the device 'myRIO', which is operated through using the software LabVIEW, was utilised as the embedded computer. It integrates the dual-core processor, the Xilinx programmable gate array (FPGA) and real-time (RT) I/O platform together, which has qualified the connection from DAQ to sensors and actuators.

The experimental results have demonstrated the capability of 'myRIO' in overcoming the computational expensive, as the complicated NN based control algorithms could be implemented and processed within this device. In addition, the functionality of RT operation allows the users to remotely deploy advanced observer methods to conduct signal processing and investigate the control algorithms through a low-cost but efficient manner. It is well-known that, when the geometric and kinetic similarity principles are preserved during the construction of the scaled model, the results of experiments can easily be recalculated to refer to real objects by using public relations (Morawski and Pomirski, 1998). Thus, the experimental can be referred for sea trails of full scaled ship.

1.6 Thesis outline

This thesis is written in a 'chapterised thesis' structure, in which the core chapters 2 to 5 are based upon the papers which have been published and are under review. To some extent, these chapters comprising scientific papers provide complete components and can be read individually. The details of each chapter are outlined below.

Chapter 1: the introductory chapter presents the problem definition, the background of the project as well as the motivations for applying the proposed control algorithms. It also clarifies the research objectives and the corresponding research questions for solving. Moreover, the

structure of this thesis is outlined.

Chapter 2: presents the development of feedback control algorithm based on modified RBFNN, which is used to approximate the control law for the control of the ship's motions, including yaw angle and roll motions. In the designed control scheme, conventional Back-Propagation (BP) is utilised to train the neural network controller for the steering of surface vessels. The Lyapunov stability theory is chosen to prove the controllability of the system from the theoretical aspect. To validate the robustness of the developed controller, the nonlinear wave spectrum is adopted to reflect the unpredicted environmental disturbances influencing on the hull. The superiority of RBFNN control over the conventional Proportional-Integral-Derivative (PID) control is validated by utilising the mathematical model of a full scale container ship with variable disturbances.

Chapter 3: introduces the principles of the Kalman Filter Variants (i.e. EKF and UKF) trained RBFNN control system. In this chapter, the EKF and UKF are adopted as the alternatives for neural networks training to improve the capability in dealing with the environmental uncertainties and system nonlinearities. The capacity of the proposed controllers, including course keeping and path tracking controllers incorporating with roll damping controllers, have been validated by designing the scenarios with different sailing states and environmental disturbances. The results indicate that both of EKF and UKF methods are effective for control and steering due to their functionalities in the aspects of robustness in the presence of a variable external disturbance.

Chapter 4: concerns the modelling of a newly developed free running scaled model named 'Hoorn'. A brief description of the ship's characteristics is given, focusing on the configurations of the embedded open-source hardware and low-cost sensors. It is well known that the measured data from low-cost sensors are easily subject to the effects of white noise and other disturbances generated from the hardware and environmental changes. Therefore, the signal processing methods are outlined to estimate the sailing states, which are used in the following process of system identification for hydrodynamic coefficients estimation. Finally, the 4 DOF mathematical model is presented and verified by the comparison between experimental data and simulated results.

Chapter 5: presents the experimental and numerical studies of autopilot using EKF and UKF trained neural networks for surface vessels. The performances of course keeping, course

changing and path tracking are shown by conducting experiments with the physical model on Trevallyn Lake and simulations using developed mathematical model. The results indicate that the proposed signal processing methods are effectively employed to provide acceptable states estimation, while the KFV trained neural network controllers are adequately making the ship to follow the desired states. It is indicated that the performances of the autopilot based on EKF and UFK trained RBFNNs are superior to that of the BP RBFNN based autopilot in the aspects of the fast learning speed and smooth control law output. Consequently, the robustness and controllability in counteracting environmental disturbances are corroborated experimentally. Moreover, in comparison with the EKF RBFNN based autopilot, the merit of the UKF RBFNN based control scheme remains the improved control accuracy and 'softer' control law with acceptable computational expensive.

Chapter 6: concludes the overall summary of this project and the relevant findings of each phase, and highlights main conclusions drawn from corresponding findings. It also discusses the implications of these investigations. Also, several potential research respects are presented for future works.

Appendices:

Appendix I -- Mathematical model of a full scale container ship's mathematical model coding in MATLAB S-function

Appendix II -- Electronic configuration of scaled model 'Hoorn' Coding in MATLAB S-function

Appendix III -- Mathematical model of 'Hoorn'

Appendix IV -- Path tracking methods coding in MATLAB S-function

Chapter 2

Conventional RBFNN Based Control Scheme for Surface Vessels

This chapter is about the development of a modified RBFNN based control system for ship's steering to deal with the uncertainty of external environment, the nonlinear characteristics of the ship. In the proposed control scheme, the adaptive BP algorithm is adopted to train the RBFNN based control system to achieve the course keeping and rudder-roll damping simultaneously. The advantages of developed RBFNN based control system are highlighted through the comparison with that of the PID based control system. This is a starting point to realise a new control algorithm, and to answer research question 1 as stated in **Chapter 1**.

This chapter has been published and presented at the Australia Control Conference (2015). The citation for the research article is:

Wang, Y., Nguyen, H. D., Chai, S., & Khan, F. (2015). *Radial basis function neural network based rudder roll stabilisation for ship sailing in waves*. In 2015 5th Australian Control Conference (AUCC) (pp. 158-163).IEEE.

Abstract: This paper presents a rudder-roll stabilisation system utilising Radial Basis Function neural network (RBFNN) for course keeping and roll damping. Roll motion of a vessel sailing under severe weather conditions has adverse effects on crews' health, cargoes and safety. Thus it must be damped as much as possible. A new control algorithm for both course keeping and roll damping is proposed based on the RBFNNs. To realise the proposed rudder roll stabilisation system, a nonlinear mathematical model of a container vessel with effects of wave disturbance is used to simulate the proposed rudder roll stabilisation system which consists of two controllers implemented in parallel, one is the autopilot for course keeping, and the other is roll damping controller. The performance and robustness of the proposed control system are investigated by taking consideration of the effects of external disturbance. The simulation studies are designed to verify the improved performance of the proposed rudder roll stabilisation system and to validate its efficiency of course keeping and roll motion reduction.

2.1 Introduction

Nowadays, as the cheapest means of transportation, the cargo ships carrying goods from and to a definite country play a vital role in the development of the world. Since the ships have to sail at rough seas, such as the Indian Ocean route in summer and Northern Pacific route in winter, they always suffering in severe roll motion and yaw motion generated by the rough sea. From the perspective of safety, roll motion is regarded as the most serious problem for ships sailing in the seaway, because the acute roll motion generally affects the stability of the ship and the reliability of machines and electrical facilities. Also, it will result in the worse working environment for sailor because of the seasickness and may even lead to ship's capsizing. Therefore, more effective methods and facilities need to be utilised to reduce the roll motion, thus to maintain the stability of the ship.

Some facilities have been applied to reduce roll reduction, e.g. bilge keels, anti-roll tanks, gyroscopic stabilisers, moving weights, and stabilising fins(Treakle et al., 2000). Although most of the devices were validated to be effective, additional facilities and additional power supply will increase the tonnage of the ship and change the structural strength. Also, the installation and maintenance costs will be raised and the vessel's seaworthiness may be affected by the additional devices.

Usually, when a rudder is used as the manoeuvring device, it is found that the rudder steering will create additional roll force and moment. Therefore the rudder can be utilised as a roll

reduction facility (Fossen, 1994a). In recent years, with the merit of development of modern control theory, various control methods have been applied to the design of rudder roll damping system (Nejim, 2000, Zhang et al., 2006, Fang and Luo, 2007a). Considering the excellent capability in approximating, neural networks have successfully been applied to the design of rudder roll stabilisation by many scholars (Alarcin and Gulez, 2007, Li et al., 2010, Fang et al., 2010a, Fang et al., 2012a). Compared with the multilayer feed forward neural network, RBFNNs have the advantages of good generalisation ability and simple neural network architecture which can avoid unnecessary and lengthy calculation (Liu, 2013), therefore it is employed in this study.

In the paper, section 2 outlines the 4 degree of freedom (DOF) mathematical model which is necessary for the description of ship motion as well as for the simulations. The wave model is also considered in this section. The general configuration of RBFNN is addressed in section 3. In section 4, the process of designing RBFNN based rudder roll stabilisation system is presented. The simulation results of the proposed stabilisation system are discussed in section 5. Conclusions are presented in the last section.

2.2 Equations of Motion in Waves

The equation of motion and external disturbance for the surface vessel are introduced in this section.

The equation of motion for the vessel has been deduced from Newton's second law. And the representative coordinate for the vessel is expressed in Fig. 2. 1 (Fossen, 2011). Thus, a 6 DOF dynamic equation for surface vessel can be presented as:

$$M\dot{\nu} + C(\nu)\nu + D(\nu)\nu + g(\eta) = \tau + \tau_E \qquad (2.1)$$

where M is the inertia item which includes added mass; ν is the translated motion and rotation motion velocity of the vessel; $C(\nu)$ is the matrix of Coriolis and centripetal terms including added mass; D is the damping matrix; $g(\eta)$ is the vector of restoring forces and moments attribute to gravity and buoyancy; η is the position and orientation of the vessel; τ is the vector of input due to actuator; τ_E is the vector of input due to wave disturbance.

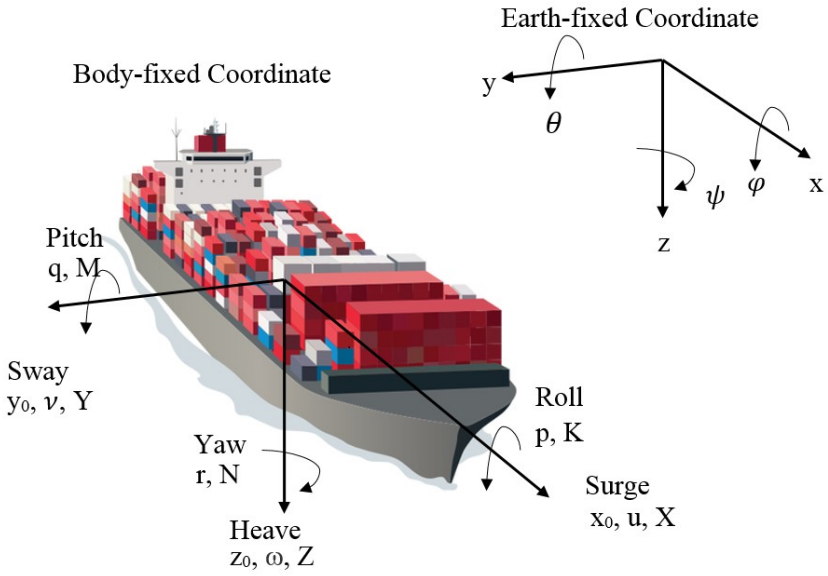

Fig. 2. 1 Body-fixed frame and inertial frame for surface vessel

2.2.1 Four DOF Ship Motion Equations

The approach stated above can be adopted to describe the motion of the vessel in the body-fixed frame. However, for the most conventional vessels, their dynamic motion can be considered in 4 DOF (surge, sway, yaw, and roll) because the motion of pitch and heave can be ignored compared with others. A 4 DOF non-dimensional model using the prime system (SNAME, 1950) was developed to design roll stabilisation for surface vessels (Perez and Blanke, 2002):

$$(m' + m'_x)\dot{u}' - (m' + m'_y)v'r' = X' \tag{2.2}$$

$$(m' + m'_y)\dot{v}' + (m' + m'_x)u'r' + m'_y\alpha'_y\dot{r}' - m'_y l'_y\dot{p}' = Y' \tag{2.3}$$

$$(I'_x + J'_x)\dot{p}' - m'_y l'_y\dot{v}' - m'_x l'_x u'r' + W'\bar{G}\bar{M}'\phi' = K' \tag{2.4}$$

$$(I'_z + J'_z)\dot{r}' + m'_y\alpha'_y\dot{v}' = N' - Y'x'_G \tag{2.5}$$

where m′ is the mass of vessel. I'_x and I'_z are the inertia moments of roll and yaw. The terms m'_x and m'_y donate the added masses in the x and y direction, respectively. The added inertia moments in the x-z axes are represented by J'_x and J'_z. Surge and sway velocity are donated by u and v, respectively. Roll and yaw displacement are expressed by r and p. Furthermore, α'_y is the center of m'_y in x-coordinate, and the center of m'_x and m'_y are indicated by l'_x and l'_y. The

items X' and Y′ are the forces in terms of surge and sway. K' and N' are respectively external moment of yaw and roll motion.

2.2.2 Wave Forces and Moments

The response of a vessel to waves is quite complicated because the wave force and moment are determined by the complex characters of waves and the states of the sailing vessel. This section outlines the method used to describe the spectrum of waves and the motion responses of the marine vehicle in waves.

In order to predict the response of vessel in open sea, the modified Pierson- Moskowitz (PM) wave spectrum model has been recommended by ITTC as:

$$S(\omega_w) = \frac{173h_{1/3}^2}{\omega_i^5 T_w^4} e^{\left(\frac{-691}{\omega_w^5 T_w^4}\right)} \qquad (2.6)$$

where

$h_{1/3}$: the significant wave height;

T_w: the average period of waves;

ω_i: the wave frequency of the *i*th wave component.

For the vessel with certain advancing velocity of U, the inherent frequency of waves should be replaced by the encounter frequency ω_e. The relation between two terms can be expressed as follows:

$$\omega_e = \omega_0 - \frac{\omega_0^2}{g} U cos\beta \qquad (2.7)$$

where

ω_e: encounter frequency (rad/s)

ω_0: initial wave frequency (rad/s) which equals to $\sqrt{kg}$

U: forward speed of the vessel

β: encounter angle of the vessel in waves as shown in Fig. 2. 2.

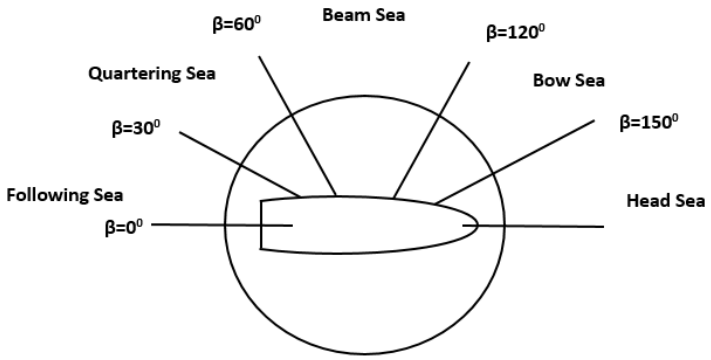

Fig. 2. 2 Body-fixed frame and inertial frame for surface vessel

Based on the above method, the forces and moments generated by the wave disturbance can be derived and expressed as (Sgobbo and Parsons, 1999a):

$$X_w = m\overline{a_1}S$$

$$Y_w = m\overline{a_2}S$$

$$K_w = mL\overline{a_3}S$$

$$N_w = mL\overline{a_4}S \qquad (2.8)$$

where

X_w: the wave forces with respect to surge;

Y_w: the wave forces with respect to sway;

K_w: the roll moment generated by waves;

N_w: the yaw moment generated by waves;

$\bar{a}$ with four subscripts: the filter parameters;

S: the wave spectrum.

2.3 General Configuration of RBFNN

The RBFNN was firstly formulated by Broomhead and Lowe in (Broomhead and Lowe, 1988)

and has been verified as an effective method for time series prediction and classification. It is a kind of artificial neural network with three layers as shown in Fig. 2. 3.

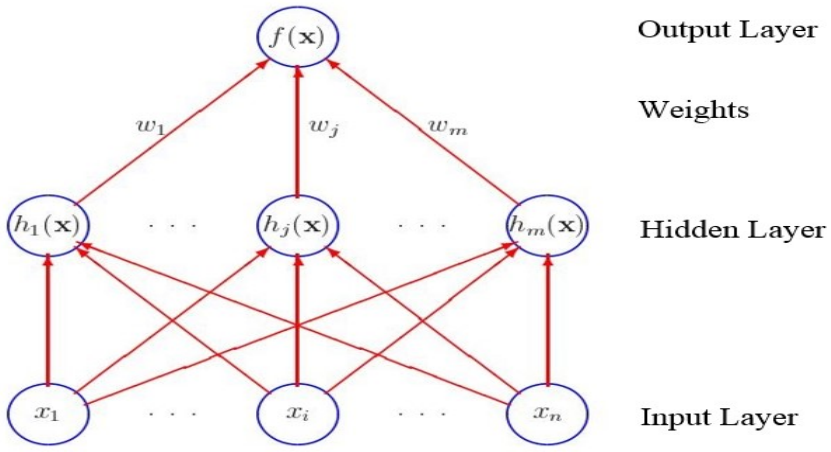

Fig. 2. 3 Architecture of RBFNN.

In the hidden layer, radial basis functions are employed as the activation functions, which are expressed by the distance of the input from a given vector of centres. Therefore, the output of the neural network can be expressed by a combination of parameters and radial basis functions.

It has been demonstrated that RBFNN is capable of approximating an arbitrary function by transferring a real number of vector R^n to the output of R as a scalar function (Park and Sandberg, 1991). The approximate function can be expressed as

$$u(x) = w^T h(x) = w_1 h_1 + w_2 h_2 + \cdots + w_j h_j + \cdots + w_m h_m \qquad (2.9)$$

where x is the input and $x \in \boldsymbol{R}^n$, m is the node of the hidden layer, the weights vector is represented by $w = [w_1; w_2; \ldots; w_j; \ldots; w_m]$, $h(x) = [h_1(x);\ h_2(x); \ldots;\ h_j(x); \ldots; h_m(x)]$ is the activation functions in the hidden layer.

Generally, Gaussian function is chosen as the activation function $h(x)$:

$$h(x) = exp(-\frac{\|x-c\|^2}{2b^2}) \qquad (2.10)$$

where

x: input of network

c: coordinate value of Gaussian function center

b: width value of Gaussian function

So the selected continuous function is approximated as

$$F^*(x) = w^{*T} h(x) + \gamma \qquad (2.11)$$

where w^* is the ideal weights vector, and h is the radial basis function vector. The item γ is the approximation error satisfying $|\gamma| \leq \gamma_0$ and $w^* = \arg\min\left\{\sup_{x \in R^n} |w^T h(x) - F^*(x)|\right\}$.

2.4 RBFNN Based Rudder Roll Stabilisation Design

This section presents the rudder roll stabilisation system based on the control algorithm proposed in (Ge et al., 2010) and robust adaptive control which is approximated by RBFNN.

2.4.1 Adaptive Control by RBF

Let's consider a second order nonlinear system as follows:

$$\dot{x}_1 = x_2$$

$$\dot{x}_2 = \alpha(x) + \beta(x) u_{sys}$$

$$y_{sys} = x_1 \qquad (2.12)$$

where $x_{sys} = [x_1\ x_2]^T \in R^2$, $u_{sys} \in R$ and $y_{sys} \in R$ are system states, input and output, respectively. The items $\alpha(x)$ and $\beta(x)$ represent the unknown functions. Here it is assumed that the sign of $\beta(x)$ is positive. Furthermore, there exists a known limitation $\bar{\beta}$ such that $|\beta(x)| \leq \bar{\beta}$ and $\beta(x)/\bar{\beta}$ is independent of the state x_{sys}.

If the desired state vector x_d is defined, the error vector $\boldsymbol{e}$ and an augmented system s are

$$x_d = [y_d\ \dot{y}_d]^T$$

$$\boldsymbol{e} = x - x_d = [e\ \dot{e}]^T$$

$$s = [\zeta\ 1]\boldsymbol{e} = \zeta e + \dot{e} \qquad (2.13)$$

where ζ is positive such that the polynomial $s + \zeta$ is Hurwitz (Ge et al., 1999).

It is convenient to define that $v_{sys} = \zeta\dot{e} + \ddot{y}_d$, thus (2.13) is rewritten as

$$\dot{s} = \zeta\dot{e} + \ddot{e} = \zeta\dot{e} + \ddot{y}_d - \ddot{x}_1$$

$$= \zeta\dot{e} + \ddot{y}_d - \alpha(x) - \beta(x)u_{sys}$$

$$= v_{sys} - \alpha(x) - \beta(x)u_{sys} \qquad (2.14)$$

If the desired feedback control law is chosen as

$$u_{sys}{}^* = -\frac{1}{\beta(x)}\left(\alpha(x) - v_{sys}\right) - \left(\frac{\dot{\beta}(x)}{2\beta(x)^2} - \frac{1}{\varepsilon\beta(x)} - \frac{1}{\varepsilon\beta(x)^2}\right)$$

$$\mathbf{z} = [\boldsymbol{x}^T \; s \; \frac{s}{\varepsilon} \; v_{sys}]^T \qquad (2.15)$$

where $\varepsilon > 0$ is the design parameter, then $\lim_{n\to\infty}\|e\| = 0$. And from (2.15), the control law can be expressed as a matrix with $\boldsymbol{x}$, s and v_{sys}

Proof. *(Stability of the RBFNN control scheme) Submitting $u_{sys} = u_{sys}{}^*$ into the equation (2.14) yields*

$$\dot{s} = v_{sys} - \alpha(x) - \beta(x)\left[-\frac{1}{\beta(x)}\left(\alpha(x) - v_{sys}\right) - \left(\frac{\dot{\beta}(x)}{2\beta(x)^2} - \frac{1}{\varepsilon\beta(x)} - \frac{1}{\varepsilon\beta(x)^2}\right)\right]$$

$$= -s\left(\frac{1}{\varepsilon\beta(x)} + \frac{1}{\varepsilon} + \frac{\dot{\beta}(x)}{2\beta(x)}\right)$$

$$= -s\left(\tfrac{1}{\varepsilon\beta(x)} + \tfrac{1}{\varepsilon}\right) + s\tfrac{\dot{\beta}(x)}{2\beta(x)} \qquad (2.16)$$

If the Lyapunov function is chosen as $V = \frac{1}{2\beta(x)}s^2$, the following is obtained

$$\dot{V} = \frac{1}{\beta(x)}s\dot{s} - \frac{\dot{\beta}(x)}{2\beta(x)^2}s^2$$

$$= -\frac{1}{\beta(x)}s\left[-\left(\frac{1}{\varepsilon\beta(x)} + \frac{1}{\varepsilon\beta(x)^2}\right)s + \frac{\dot{\beta}(x)}{2\beta(x)}s\right] - \frac{\dot{\beta}(x)}{2\beta(x)}s^2$$

$$= -\left(\tfrac{1}{\varepsilon\beta(x)} + \tfrac{1}{\varepsilon\beta(x)^2}\right)s^2 \leq 0 \qquad (2.17)$$

and it indicates that $\lim_{t\to\infty}|s| = 0$*, correspondingly, we have* $\lim_{t\to\infty}|e| = 0$.

Since the nonlinear function $\alpha(x)$ and $\beta(x)$ are unknown, the control law u^* is unavailable. Here the RBFNN is applied to approximate the function.

The direct robust adaptive control law can be proposed as

$$u(x) = \frac{1}{\hat{\beta}}\hat{w}^T h(x) \qquad (2.18)$$

where $\hat{w}$ as the estimation of the ideal weights w^*. The weights updating method is proposed as a modified back-propagation method:

$$\dot{\hat{w}}_t = -\Gamma(h(x)s + \alpha_{RBF}\hat{w}_{t-1}) \qquad (2.19)$$

where Γ denotes the positive adaption gain matrix and α_{RBF} is a constant which is used to eliminate the approximation error and external disturbance.

2.4.2 Design of Rudder Roll Stabilisation System

The rudder roll stabilisation is an effective means for roll motion damping using only a rudder. It has been shown that the rudder controller can be developed by designing the roll damping controller and course keeping controller separately as shown in Fig. 2. 4.

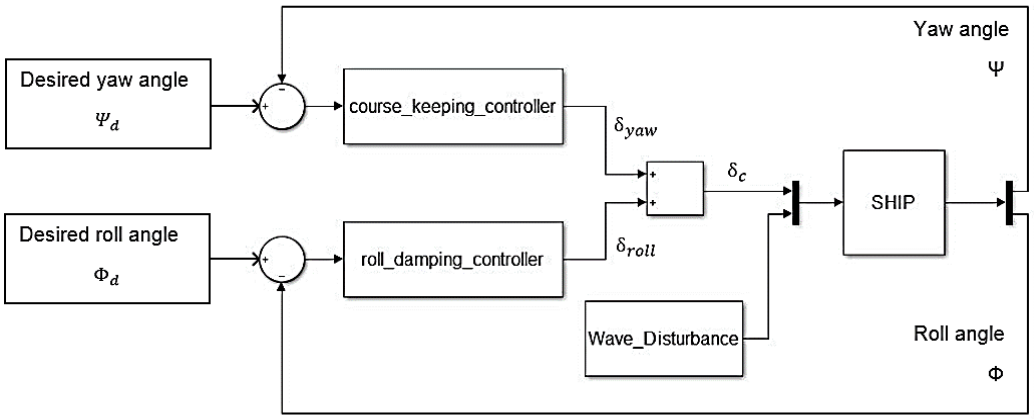

Fig. 2. 4 Block diagram of RBFNN based rudder roll stabilisation.

The commanded rudder angle is presented as follows

$$\delta_c = \delta_{roll} + \delta_{yaw} \quad (2.20)$$

where δ_c is the rudder control signal, δ_{roll} is the output of roll damping controller and δ_{yaw} is the output of course keeping controller.

2.5 Simulation Results

In this section, in order to verify the efficiency of RBFNN based rudder roll stabilisation, the 4 DOF nonlinear model of container ship developed in (Fossen, 1994a) is used. The main characters of the container ship are shown in Table 2.1. The shaft speed of the engine is set to 80 rpm, the limitation of the steering machine are $\delta_{max} = 20\ deg$ and $\dot{\delta}_{max} = 5\ deg/s$.

Table 2. 1 The Main Characters of the Container Ship (Principal Dimensions)

Length (m)		175.00
Breath (m)		25.40
Draft (m)	fore(d_F)	8.00
	aft(d_A)	9.00
	mean(d)	8.50
Displacement volume (m^3)		21,222
Height from keel to transverse metacentre (m)		10.39
Height from keel to the centre of buoyancy (m)		4.6154
Block coefficient		0.559
Rudder area (m^2)		33.037

In order to simplify the process of simulating wave spectra, the second-order transfer function $h(s)$, which is generated by a Gaussian white noise process, can be utilised to approximate the Pierson-Moskowitz spectral density function $S(\omega_w)$. The transfer function can be expressed as

$$h(s) = \frac{K_\omega s}{s^2 + 2\zeta\omega_e s + \omega_e^2} \quad (2.21)$$

where ζ is damping coefficient with general value 0.1~0.3, ω_e is the wave encounter frequency stated in (*2.6*), the gain matrix is defined as $K_\omega = 2\zeta\omega_e\delta$ with δ indicating the wave intensity.

To evaluate the performance of rudder roll stabilisation, the formulating method was proposed in (Oda et al., 1992) as:

$$Roll\ reduction = \frac{d_{BEF} - d_{AFT}}{d_{BEF}} \qquad (2.22)$$

where d_{BEF} is the standard deviation of roll rate before using rudder roll stabilisation control system and d_{AFT} is that after using roll stabilisation control system.

The performance of course keeping and roll damping of RBFNN based rudder roll stabilisation according to simulations are shown in Fig. 2. 5 and Fig. 2. 6.

For the first case study, the desired course is set to *30°* and the encounter angle is approximate *30°*. It can be found from Fig. 2. 5 that, before 1000s, when RBFNN based stabilisation is switched off, the course keeping controller works good, but the roll motion is severe. During 1000s to 2000s, when the rudder roll stabilisation is activated, the roll angle decreases significantly. The roll reduction for this case by equation *(2.22)* is 51.15%. Compared with the results in (Nguyen and Jung, 2007) at approximate 39%, for the same mathematic model, the proposed algorithm has better performance in terms of roll damping.

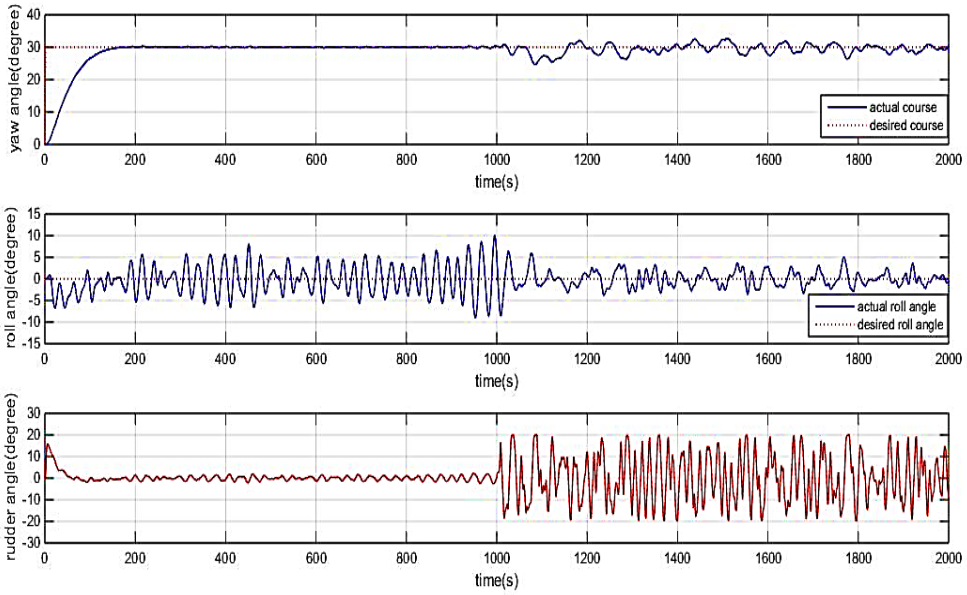

Fig. 2. 5 Simulation result of the RBFNN rudder roll stabilisation controller when setting course is 30°

To test the performance of proposed controller in different sailing status, the desired course is changed to 0°and the significant waves are assumed to come from the beam sea, it is observed from the Fig. 2. 6 that, when the rudder roll stabilisation is switched on, the roll motion reduces significantly. The roll reduction of this study is 51.54%.

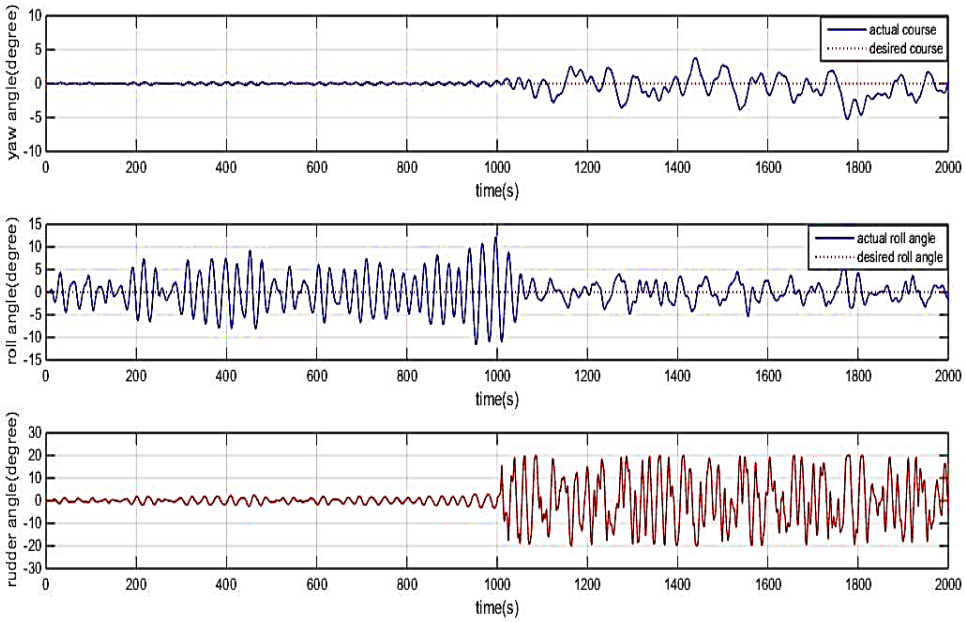

Fig. 2. 6 Simulation result of the RBFNN rudder roll stabilisation controller when setting course is 0°

To validate the merits of the RBFNN based rudder roll stabilisation system to the conventional PID based rudder roll stabilization system with regard to the robustness and adaptiveness, the following two scenarios were conducted. In the first scenario, the performance of RBFNN based roll stabilisation system was compared with that of PID based roll stabilisation system with the same sailing status and wave disturbance. The differences between their performance are presented in Fig. 2. 7. It can be found that the average roll angle has been reduced from $\pm 2.1°$ to $\pm 1.6°$ and the standard deviation of roll rate decreases from 0.01145 to 0.00625.

The second scenario was conducted to validate the adaptiveness of the proposed control system. To be more specific, the random white noises was added into the feedback-loop to act as the sensors' measurement uncertain. The performance of the controller can be found from Fig. 2. 8. It indicates that, compared with the PID based roll damping stabilisation system, the roll rate standard deviation of RBFNN based rudder roll stabilisation system is reduced from 0.01224 to 0.00776. Although the roll angle and the roll rate were increased correspondingly due to the additional disturbance, the results indicated that the roll motion amplitudes and roll rate by using RBFNN based controller is far smaller than that by using PID based one. Thus, the RBFNN based system has a better robustness and adaptiveness in terms of compensating undesired disturbance when reducing roll motion compared with PID based controller.

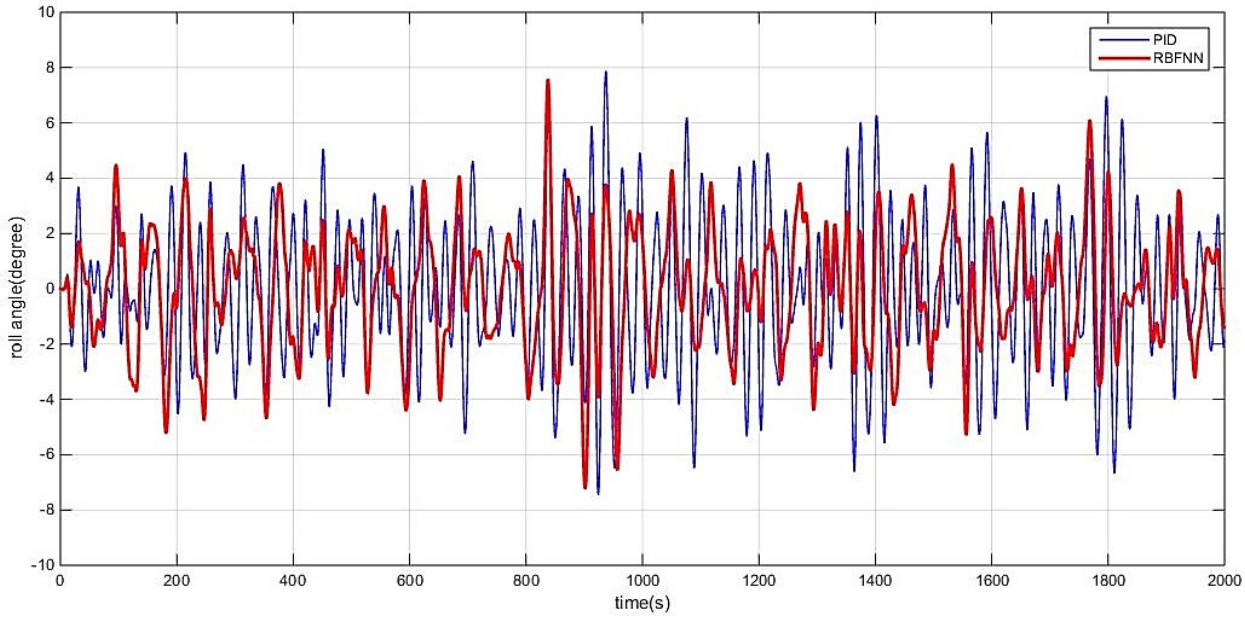

Fig. 2. 7 Simulation result of roll motion reduction in use of the RBFNN rudder roll damping controller and PID based rudder roll damping controller when setting course 0°

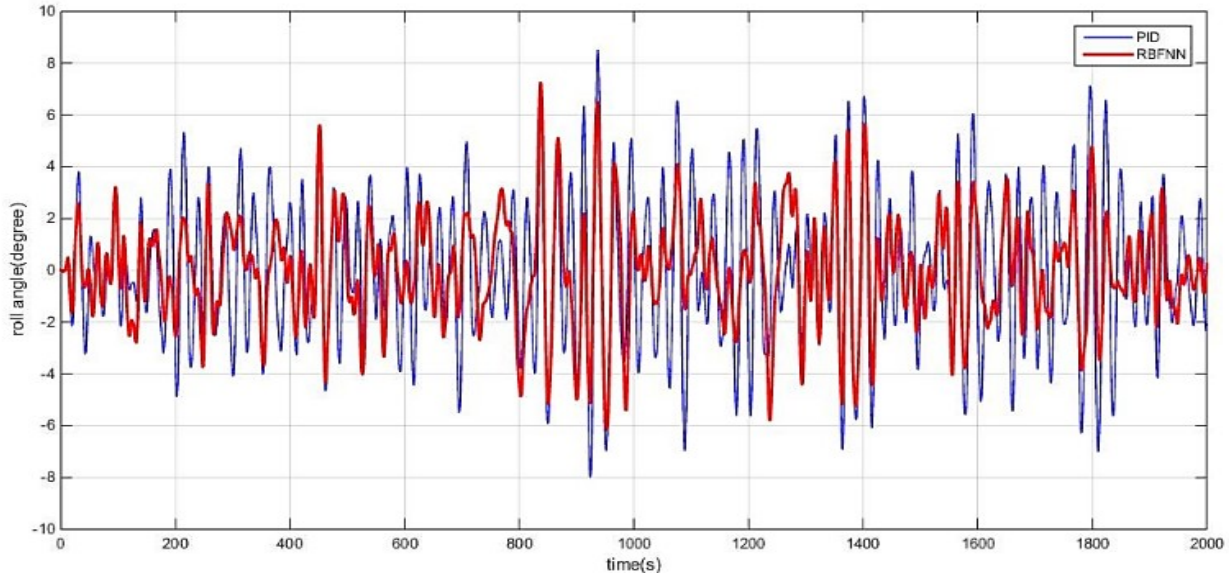

Fig. 2. 8 Simulation result of roll motion reduction in use of the RBFNN rudder roll damping controller and PID based rudder roll damping controller with random input noise when setting course 0°

Generally, the case studies outlined above show that the proposed RBFNN based rudder roll stabilisation proved to be effective in maintaining course and reducing roll motion in different sailing conditions. Furthermore, it achieved better performance than the conventional PID based roll damping controller when coping with the external disturbance.

2.6 Conclusion

In this paper, an RBFNN based rudder roll stabilisation system, which contains course keeping controller and roll damping controller, has been developed. The nonlinear mathematical model with manoeuvring features presented above is successful to simulate the motion response of vessel in waves.

Simulation scenarios have validated the effectiveness and the flexibility of the proposed control algorithm when the rudder is used as the only manoeuvre actuator. It is proved that the RBFNN based rudder roll stabilisation system can maintain the ship sailing on the desired orientation and regulate the roll motion in variable sailing conditions. According to a series of comparison and calculation, the RBFNN based controller can fulfil faster response and less overshot when reducing roll motion substantially. Also, the robustness and performance under the effects of disturbances indicate that it is capable of eliminating the effects of external disturbance.

Further study will be conducted to investigate the capability of the RBFNN based rudder roll stabilisation system in more complex environmental conditions, i.e. wave, wind, and current effects. Other algorithm will be applied to optimise the design parameters in order to achieve a more simplified and practical control system.

Chapter 3

KFV RBFNN Based Control Scheme for Surface Vessels

This chapter comprises two parts, in which the EKF and UKF based training methods are presented to replicate the previous training method for RBFNN based controllers in **Chapter 2**. The first part of this chapter presents the EKF RBFNN based steering control system while the second part focuses on the development of the UKF RBFNN based control algorithm which is able to improve the controllability of the surface vessel. The functionalities of the proposed control system, including course keeping, course changing, path tracking, as well as rudder-roll damping, are validated by using a 4 DOF mathematical model of a full scaled containership. The improved control performance of the proposed control systems have been demonstrated, which answered the second research question as stated in **Chapter 1**.

Part A: This subchapter has been submitted for publication in 'Journal of Ocean Engineering' and at the time of writing is under review. The citation for the research article is:

Wang, Y., Nguyen, H. D., Chai, S., & Khan, F. (2016). *Rudder Roll Stabilisation Using Extended Kalman Filter Trained Radial Basis Function Networks for Ship in Waves*. Ocean Engineering.

Part B: This subchapter has been published in 'Applied Ocean Research'. The citation for the research article is:

Wang, Y., Chai, S., Khan, F., & Nguyen, H. D. (2016). *Unscented Kalman Filter trained neural networks based rudder roll stabilisation system for ship in waves*. Applied Ocean Research,68, 26-38.

Chapter3 - Part A. EKF Trained RBFNN Control System for Surface Vessels

Abstract: The roll motion of ships advancing in heavy seas has severe impacts on the safety of crews, vessel and cargoes, thus it must be damped. This paper presents the design of a rudder roll stabilization system by utilizing the Extended Kalman Filter (EKF) trained Radial Basis Function Neural Networks (RBFNN) control algorithm to reduce the roll motion for ships sailing in waves only through rudder actions. The stabilization system is composed of two parts implemented in parallel, i.e. the controller of course keeping and the controller of roll reduction. The neural network control design, which is accomplished by adopting the modified EKF training algorithm, is utilized in the control system. To validate the performance of proposed stabilization system, the nonlinear mathematical model including manoeuvring characteristics and effects of wave disturbance was employed. Moreover, the Enclosure Based Steering Line of Sight (EBS LOS) guidance method was adopted in this study to fulfil the functions of path tracking. The performance and robustness of the stabilization system, as well as the speed reductions, were investigated by considering the effects of external disturbances and different sailing states. The results indicate that the designed controller is practical and efficient to reduce roll motions in comparison with back-propagation (BP) trained neural network controller and proportional-derivative (PD) based controller for ship advancing in waves.

3A.1. Introduction

At present, marine transportation is indispensable for the development of the world. Ocean-going ships carrying cargoes from and to a definite port have to sail at rough seas and endure large disturbances owing to external environmental impacts including waves, winds and currents. These disturbances usually result in enormous impacts on ship's roll motion and path tracking. Dramatic roll motion will affect the efficiency and comfort of seafarers and passengers because of seasickness. Also, it may lead to the instability of the ship and the unsafety of the cargoes. Even worse, the ship might be in danger of capsizing due to the severe roll motions. Hence, from the perspective of safety, roll motions are especially dangerous for ships. Thus it must be damped as much as possible.

Practically, when the ship encountering the severe weather, the deck officer with good seamanship will perform a course changing and speed reduction to prevent the large amplitude

of roll motions. Yet, for the ship in special conditions, such as operating with a strict linear schedule or advancing in the area of traffic separation, the roll damping facilities or roll motion control strategies are needed. Some methods and devices, e.g. moving weights (Treakle et al., 2000), bilge keels, anti-roll tanks, and stabilizing fins, have successfully been adopted to reduce roll motions. Although these facilities have been validated to be efficient, the additional equipment will affect ship's carrying capacity, seaworthiness, structure strength and costs of shipbuilding and maintenance. Therefore, other approaches are needed to maintain the orientation and stability.

It is well known that altering rudder angle will generate additional roll force and moment to the hull. Consequently, besides being used as the manoeuvring facility, the rudder could be employed in reducing roll motion. However, using the rudder for course keeping and roll reduction simultaneously is not a simple task due to the coupling between the motions of yaw and roll. Therefore, the qualified control strategies are required to handle the trade-offs regarding two aims with disturbance rejection. The conventional rudder roll stabilizer based on the proportional-integrative-derivative (PID) control method was firstly developed for its simplification and reliability. However, this kind of controller was designed with fixed parameters, and did not work well in heavy seas (Van Amerongen and Van Nauta Lemke, 1978). Thus, other adaptive methods have been adopted to design the rudder roll stabilizer (Messina et al., 1997, Lauvdal and Fossen, 1998, Sgobbo and Parsons, 1999b). With the development of modern control theory, various control methods, e.g. fuzzy logic control (Nejim, 2000), receding horizon control (Perez, 2005), H∞ robust control (Xianku et al., 2006) and sliding mode control (Fang and Luo, 2007b) have been adopted in this domain. However, there existed some drawbacks in adopting these methods, such as difficulties in formulating the fuzzy control rules, the risk of unstable when the changing speed of the dynamics was beyond the adapting capability, and high frequency of control actions leading to the unexpected dynamic distortions (Sun et al., 2014).

Impelled by the development of computing technology, the control algorithms based on Neural Networks became applicable. The advantages of the neural network based control lie in the capability in unknown approximating and robustness against system noises. Another future of the neural network is the capability in 'comprehending' the system's multi-variable characteristics by adjusting the weights, which avoids the analytical analysis of the complicated nonlinear differential equations. Therefore, neural network based control algorithms have been

investigated to design the rudder roll stabilizer (Alarcin and Gulez, 2007, Li et al., 2010, Fang et al., 2010b, Fang et al., 2012b). Amongst the multilayer feed-forward neural networks, the RBFNN has been proved to have the merits of good generalization capability and simple architecture to avoid unnecessary and lengthy calculations (Liu, 2013), thus it is adopted in this study. When the RBFNN is employed in the design of the rudder roll stabilizer, a training algorithm is essential to train the proposed neural networks. Apart from the well-known BP training algorithm (Duro and Reyes, 1999), other training methods, including gradient descent (Karayiannis, 1999) and back-stepping (Yahui et al., 2004), have been extensively utilized.

Although these methods are sufficient to train the proposed neural networks, the related difficulties have hindered the exploitation of the neural network based controller. Firstly, the calculation of dynamic derivatives regarding the networks' output concerning the relative weights is computationally expensive (Sum et al., 1999b). Secondly, the training of networks with gradient descent methods tends slowly and poorly in approaching satisfactory results (Trebatický, 2005). Addressing these flaws became the motivation of investigating more efficient network training algorithm.

Actually, the training algorithm of neural networks can be viewed as a parameter estimation problem. The EKF algorithm, which is capable of achieving second order accuracy for nonlinearity (Medagam and Pourboghrat, 2009), can provide an online mechanism for training neural networks in which the parameters can be updated immediately (Simon, 2002). This algorithm updates parameters in the way that is consistent with the previous measurements and converges in the following iterations. Contrary to some other higher-order training methods, the EKF based training algorithm for networks do not require batch processing, making it more suitable for online usage. It is demonstrated that, with the application of the EKF training algorithm, the converging speed was improved and the design complexity was decreased (Sanchez et al., 2008).

The main task of this study is to investigate the control performance of RBFNN based rudder roll stabilization system with modified EKF training algorithm. The key objectives of this research are:

- to formulate the modified EKF based training method for feedback RBFNN control scheme;
- to develop the EKF RBFNN based rudder roll stabilization system for surface vessels

advancing in waves;

- to fulfil the roll damping and path tracking/course keeping simultaneously only use the rudder as the actuator; and
- to verify the proposed stabilization system with numerical simulations, and validate the efficiency of the system by considering nonlinear disturbance and different sailing conditions.

This paper is organized as follows: the four degree of freedom (DOF) mathematical model including manoeuvring characteristics for ships sailing with wave disturbances is introduced in the 2nd section. In the 3rd section, the EKF training method is presented to train the RBFNN based controller. The EKF RBFNN based control algorithm is proposed to design the rudder roll stabilization system with the functions of course keeping, path tracking as well as roll damping. The simulation scenarios and results are presented in the 5th section to investigate the efficiency of the system. Finally, the conclusion is made in the last section.

3A.2. Equations of Motions in Waves

The mathematical model of ship, which is deduced from Newton's second law, is the description of ship's motions. The typical coordinate system for the surface ship is presented in Fig. 2. 1. The six DOF dynamic equation (Fossen, 1991) can be developed and shown as:

$$M\dot{\nu} + C(\nu)\nu + D(\nu)\nu + g(\eta) = \tau + \tau_E \qquad (3A.1)$$

where the inertia terms including added mass are represented by M, $\nu = (u, v, w, p, q, r)^T$ indicates the velocities of the vessel's translated motion and rotation motion; the matrix of Coriolis and centripetal terms containing the added mass is denoted by $C(\nu)$; D represents the matrix of damping terms; $g(\eta)$ denotes the vector of restoring forces and moments arisen from gravity and buoyancy; η represents ship's position and orientation; τ is the control vector from the actuator; τ_E is the vector of external disturbances.

The equations of 4 DOF mathematical model for under actuated ship can be seen in **Chapter 2.2**, where the waves forces and moments influencing on the ship's hull are also presented.

3A.3. Control Algorithm Based on EKF Trained RBFNN

The RBFNN was firstly performed by Broomhead and Lowe (1988) and its capability of

approximating unknown functions has been demonstrated by Park and Sandberg (1991). It is a kind of artificial neural networks with three layers (i.e. input layer, hidden layer and output layer) and the obvious feature is that the radial basis function is adopted in the hidden layer as the activation function, shown in Fig. 3A. 1. In this section, the RBFNN based feedback control design as well as the modified EKF training algorithm are presented.

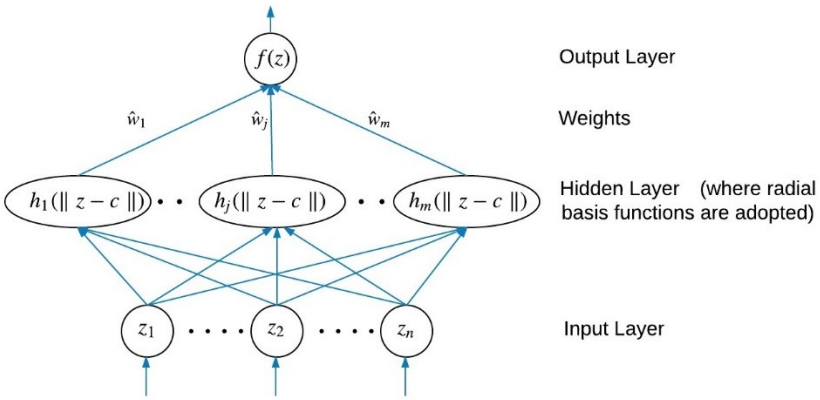

Fig. 3A. 1 Architecture of RBFNN

3A.3.1. RBFNN Based Feedback Control and Function Approximation

The details of the adopted RBFNN control scheme can be seen in **Chapter 2.3**. The forward calculation expression can be simplified as:

$$u(z) = \sum_{j=1}^{m} \hat{w}_j^T h_j(z) = \hat{w}_1 h_1 + \hat{w}_2 h_2 + \cdots + \hat{w}_j h_j + \cdots + \hat{w}_m h_m \qquad (3A.2)$$

$$z = [x\ s\ \frac{s}{\varepsilon}\ v_{sys}]^T \qquad (3A.3)$$

where $\hat{w}_j (j = 1\ to\ m)$ are the estimations of the ideal weights and $h_j (j = 1\ to\ m)$ denote the activation functions, z is the input matrix contenting the desired signals, the system states and their relevant derivatives

3A.3.2. The Modified EKF Training Algorithm

In this study, the EKF training algorithm is adopted and slightly modified. The proposed training algorithm is an application of using Kalman Filter variant for parameters estimation, which can be simply described by the state equation and observation equation containing the process noise and measurement noise. The weights of the network are regarded as the filter states, and the output is regarded as the filter output (Haykin, 2001, Zhao et al., 2013). The

difference between EKF and conventional BP training algorithm is that the former method requires the updating and storage of the approximate error covariance as well as weights matrix, whereas the BP method only updates the weights. The EKF training algorithm for the RBFNN based controller is presented below:

- **Initialization at $\boldsymbol{k = 0}$**

  $\widehat{w}_0 = E[\widehat{w}_0], P_0 = E[(\widehat{w} - \widehat{w}_0)(\widehat{w} - \widehat{w}_0)^T]$,

  At this step, the weights are initialized as small random values (e.g. magnitude of 0.1), and the initial value of P_0 can be a diagonal matrix with diagonal components.

- **Recursively executing for $\boldsymbol{k = 1, 2, \ldots, \infty}$**

  (I). Prediction transformation

  Weights Predicted: $\widehat{w}_{k|k-1} = f(\widehat{w}_{k-1})$

  Jacobin Matrix: $F_{k-1} = \partial f / \partial \widehat{w}_{k-1}$

  Covariance of predicted weights: $P_{k|k-1} = F_{k-1} P_{k-1} {F_{k-1}}^T$

  (II). Observation transformation:

  Jacobin Matrix: $H_k = \frac{\partial u}{\partial \widehat{w}_{k-1}} |_{\widehat{w}_{k|k-1}} = (h_m)_k$

  Covariance of measurement: $P_k^1 = H_k P_{k|k-1} {H_k}^T + R$

  $P_k^2 = P_{k|k-1} {H_k}^T$

  (III). Extended Kalman Filter calculation and update functions

  $K_k = P_k^2 / P_k^1$

  $\widehat{w}_k = \widehat{w}_{k|k-1} + K_k s$

  $P_{k+1} = P_{k|k-1} - K_k {H_k}^T P_k + Q$

where K_k is Kalman gain matrix for weights group, P_{k+1} denotes the approximate error covariance matrix for the next step, $\widehat{w}_k$ is the estimated weights for RBFNN based controller, R is a diagonal matrix with components equal to or slightly less than 1, Q is the artificial process noise which is useful to avoid numerical divergence, s is the item of augmented error.

Therefore, based on the above-mentioned theories, the EKF trained RBFNN control system can be illustrated by the Fig. 3A. 2. In which, the target value and the actual value are utilised to build up the input matrix. After the work of the proposed RBFNN based controller, where EKF algorithm is employed as the training method, the control law can be used to make the plant converge to target value recursively.

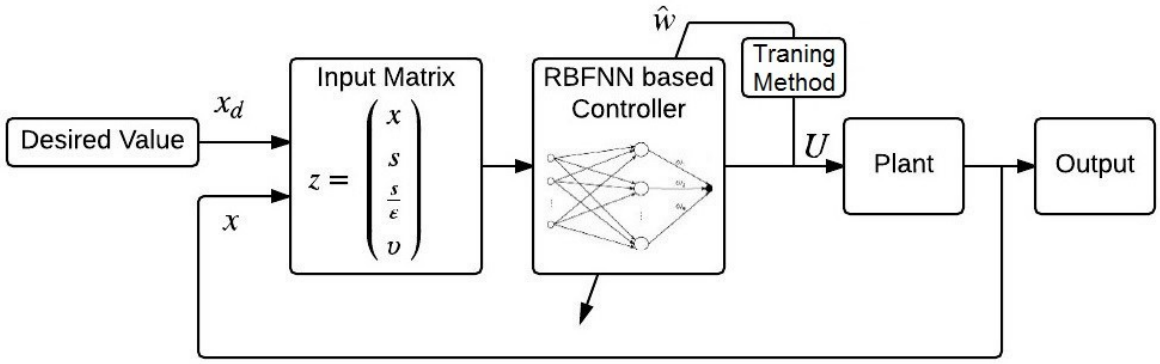

Fig. 3A. 2 Architecture of EKF trained RBFNN control system

3A.4. Rudder Roll Damping Control System

The rudder roll stabiliser is an efficient strategy to reduce roll motion using only the rudder as the actuator. It has been demonstrated that the rudder roll stabilisation system can be designed through developing the course keeping controller as well as the roll damping controller separately, and conducting them in parallel (Perez and Blanke, 2012). Based on the control scheme developed by Wang et al. (2015) concerning the objective of path tracking, the EKF trained RBFNN based rudder roll stabiliser is developed as shown in Fig. 3A. 3.

In this control system, the objectives of course keeping and path tracking can be achieved. When it is switched to the course keeping loop, the actual yaw angle ψ is compared with the desired yaw angle ψ_d to build up the input matrix z_ψ for the course keeping controller. Simultaneously, the roll damping controller will calculate the relevant control output based on the actual roll angle ϕ. On the other side, when the system is switched to the path tracking loop,

the actual position is utilised in the EBS LOS guidance block to calculate the instantaneous course angle.

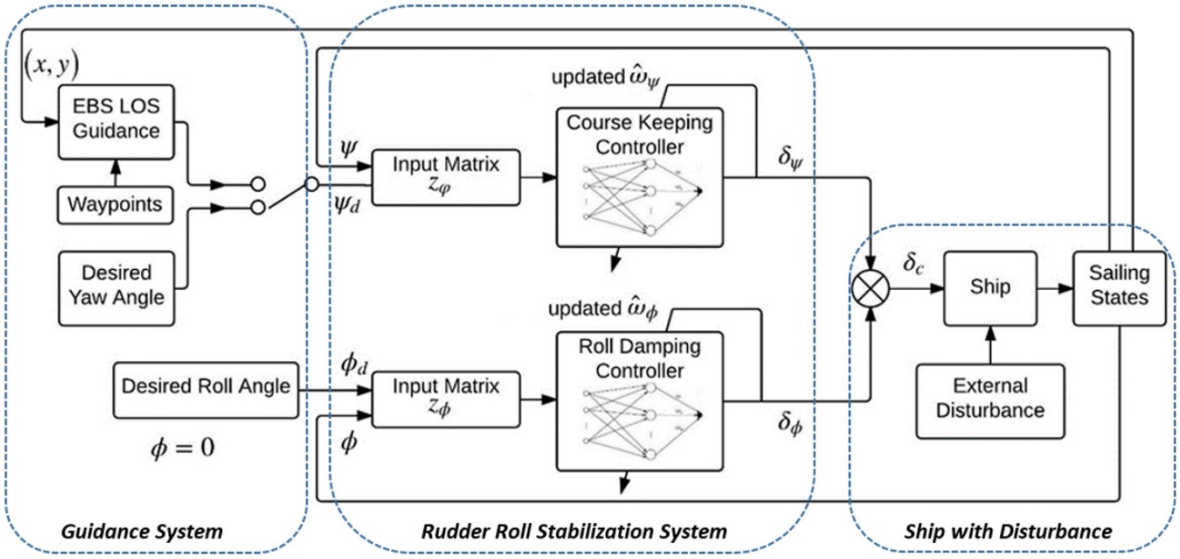

Fig. 3A. 3 The scheme of proposed rudder roll stabilisation

In order to make the ship sail based on the pre-set trajectory, the EBS LOS method is adopted in this paper as the guidance means and can be described as follows: when the vessel sails between two pre-set waypoints $p_k(x_k, y_k)$ and $p_{k+1}(x_{k+1}, y_{k+1})$, a virtual circle with radius R (which normally equals to 2 times of ship's length) exists around the vessel, the circle will intersect the desired track and the one near p_{k+1} represents the LOS point, see Fig. 3A. 4 (Fossen, 2011).

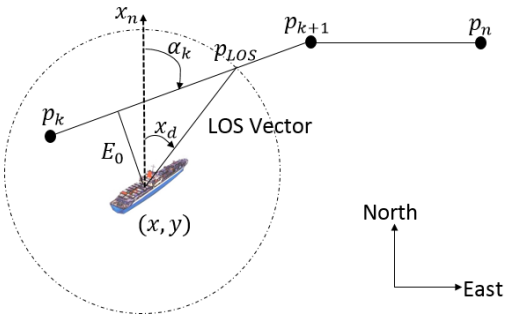

Fig. 3A. 4 EBS LOS guidance method

In order to calculate the instantaneous LOS point $p_{LOS}(x_{los}, y_{los})$, the following two equations can be utilised.

$$(x_{los} - x)^2 + (y_{los} - y)^2 = R^2 \quad (3A.4)$$

$$tan(\alpha_k) = \frac{y_{k+1} - y_k}{x_{k+1} - x_k} = \frac{y_{los} - y_k}{x_{los} - x_k} = constant \quad (3A.5)$$

Thus the instantaneous desired course angle x_d can be computed as

$$x_d = arcatan(\frac{y_{los} - y}{x_{los} - x}) \quad (3A.6)$$

The tracking error between ship's actual position and the pre-set trajectory can be counted by the following equation:

$$E_0 = (y - y_k)cos(\alpha_k) - (x - x_k)sin(\alpha_k) \quad (3A.7)$$

where E_0 is the tracking error, α_k is the angle of the desired trajectory. More details about the calculation code can be seen in Appendix IV.

This desired course angle will be transited to the following parts of the system to fulfil the aim recursively. For the ship's command rudder angle, it is formulated by the summation of the control outputs from both controllers:

$$\delta_c = c_\psi \delta_\psi + c_\phi \delta_\phi \quad (3A.8)$$

where δ_c is the rudder command signal, δ_ψ and δ_ϕ are the control output of course keeping controller and roll damping controller, c_ψ and c_ϕ are the parameters reflecting the emphasis of control performance. It is worth noting that determining the importance of the yaw control and roll damping control is depended on the sailing conditions and stabilization requirements. In this study, both yaw control and roll damping control were assumed to be equivalent important, thus the same weights (i.e. 1) are used in the equation (Fossen, 2011).

The output of the course keeping controller has the following forms:

$$\delta_\psi = \hat{u}_\psi(z_\psi) = \sum_{i=1}^{m} \hat{w}_{\psi(EKF)}^T h(z_\psi)$$

$$= \hat{w}_{\psi 1(EKF)} h_1(z_\psi) + \hat{w}_{\psi 2(EKF)} h_2(z_\psi) + \cdots + \hat{w}_{\psi m(EKF)} h_m(z_\psi) \quad (3A.9)$$

$$\hat{w}_{\psi(EKF)}(n) = \hat{w}_{\psi(EKF)}(n-1) + K_{c(EKF)} s_\psi \quad (3A.10)$$

where z_ψ represents the input matrix of the course keeping controller and it can be derived from equation *(3A.3)*, m is the amount of neuron nodes in the hidden layer, $\hat{w}_{\psi(EKF)}(n)$ is the estimated weights of course keeping controller updated by EKF algorithm at *n*th time step, and s_ψ denotes the augmented error matrix of yaw error.

Also, the output of the roll damping controller has the form as follows:

$$\delta_\phi = \hat{u}_\phi(z_\phi) = \sum_{i=1}^{m} \hat{w}_{\phi(EKF)}^T h(z_\phi)$$

$$= \hat{w}_{\phi 1(EKF)} h_1(z_\phi) + \hat{w}_{\phi 2(EKF)} h_2(z_\phi) + \cdots + \hat{w}_{\phi m(EKF)} h_m(z_\phi) \qquad (3A.11)$$

$$\hat{w}_{\phi(EKF)}(n) = \hat{w}_{\phi(EKF)}(n-1) + K_{r(EKF)} s_{\phi(EKF)} \qquad (3A.12)$$

where z_ϕ represents the input matrix of the roll damping controller and the details is expressed in equation *(3A.3)*, m is the amount of neuron nodes in the hidden layer, $\hat{w}_{\phi(EKF)}(n)$ is the estimated weights of roll damping controller updated by EKF algorithm at *n*th time step, s_ϕ represents the augmented error matrix of roll motion.

In order to evaluate the feasibility of the proposed rudder roll stabilisation system, the formula of roll reduction is expressed as follows

$$Roll\ Reduction = \frac{d_{BEF} - d_{AFT}}{d_{BEF}} \times 100\% \qquad (3A.13)$$

where d_{BEF} denotes the standard deviation of roll rate before the roll damping controller is activated and d_{AFT} denotes the standard deviation of roll rate with the control of roll damping (Fossen, 1994a).

In addition, the cost functions of yaw error C_{Yaw}, roll motion C_{Roll} and rudder angle C_{Rudder} presented by McGookin et al. (2000) are adopted in this study to judge the quality of operation as follows:

$$C_{Yaw} = \sum_{i=0}^{N} (\Delta\psi_i)^2$$

$$C_{Roll} = \sum_{i=0}^{N} \phi_i^2$$

$$C_{Rudder} = \sum_{i=0}^{N} \delta_i^2 \qquad (3A.14)$$

where N is the amount of the total iterations, $\Delta\psi_i$, ϕ_i and δ respectively represent the yaw angle error, roll angle and rudder angle of the ith iteration.

3A.5. Simulation Results and Discussion

In order to validate the efficiency of the proposed EKF trained RBFNN based rudder roll stabilization system, the four DOF nonlinear mathematical model of a full-scale container ship developed by Fossen (1994a) is adopted in this study (see Table 2.1). The inputs of the mathematical model include rudder angle, shaft speed of propeller and the Pierson-Moskowitz wave spectrum. The response of rudder's motion was expressed by using the model $\dot{\delta} = \delta_c - \delta$ (where δ is actual rudder angle and δ_c is the commanded rudder angle). Practically, in order to avoid huge steering, the rudder angle range of the conventional autopilot would be set within $\pm 15°$. Considering the fact that the rudder is utilized as the only actuator to control both the course and roll motion in the rudder roll stabilization system, larger force and moment are required from the rudder action to compensate the huge disturbances generated from rough sea. Therefore, the rudder angle range is extended to $\delta_{max} = \pm 20\,°$ corespondingly. It is well known that roll reduction is affected by the characteristics of the rudder as a high slew rate steering system has better damping performance Oda et al. (1999). However, the controller design for the ship with conventional rudder system is more essential from the perspective of engineering practice. Thus, the slew rate limit was set to $\pm 5\, degree/s$ regarding the characteristics of normal servo motors as well as the requirement of IMO. The ship was advancing in random waves with significant heights $h_{1/3} = 3\ m$ and average period $T_w = 10\ s$, and the depth of the water was assumed to be infinite. The shaft speed of the propeller was set to $80\ rpm$ with initial speed at $8\ m/s$. The Bogacki-Shampine algorithm was employed to solve the time history simulation of the ship motions, including the velocity of surge, sway, yaw rate and roll rate, the angle of yaw and roll, the position of the ship and the actual rudder angle.

3A.5.1. Roll Damping of the Ship Sailing with Course Keeping

In this part, the study aims to investigate the roll damping performance of ship sailing on the desired course. The working mode of the designed system was turned to the 'Course Keeping Loop'. The desired courses $\psi_d = 30°, 60°$ are adopted in this study with waves coming from

true east. The adopted courses are utilised to guide the ship advancing with the heading angle tracking the desired angle, which is represent by the rotation around Z axis. In order to highlight the capability of the proposed control system, the BP RBFNN based and PD based rudder roll stabilization system developed by Wang et al. (2015) were employed in this study for comparison.

In the first case, the container ship is desired to sail forward with $\psi_d = 30^0$. The Fig. 3A. 5 illustrates the deviation between desired yaw angle and actual angle, the roll angle and the actual rudder angle for four types of control systems (i.e. without roll damping control, with EKF RBFNN roll damping control, with BP RBFNN roll damping control and PD roll damping control). It is observed that, without the roll damping controller, the EKF RBFNN based course keeping controller was capable of making the ship sails on desired course steady. However, the roll angle of the ship is huge due to the environmental disturbances. When the roll damping controller being activated, the rudder roll stabilization system achieved the tasks of course keeping and roll damping synchronously. The figures also indicate that the EKF RBFNN based control system uses less rudder action, but it performed better in course keeping and roll damping in comparison with that of the BP RBFNN and PD based control algorithms. Although the yaw angle errors increased, they are the price paid for roll damping added to the complicated coupling system. Moreover, the advancing speed of the ship is shown as well. The results indicate that the ship's speed reduction using EKF RBFNN based control system is smaller than that of others. The value of cost functions for yaw deviation, roll motion and rudder angle of both stabilizer are summarized in

Table 3A. 1. The roll reduction percentage of the proposed rudder roll stabilization systems are calculated as 55.30%, 50.99% and 44.78%, respectively. It is easy to observe that, in comparison with the BP RBFNN and PD based stabilizer, the EKF RBFNN stabilizer is capable of providing effective rudder actions with better roll damping performance and speed maintenance.

Table 3A. 1 The value of cost function and roll reduction percentage at yaw angle 30°

Controller types	Yaw error cost	Roll angle cost	Rudder angle cost	Roll reduction percentage
EKF RBFNN	876	17704	204558	55.30%
BP RBFNN	3270	26870	267957	50.99%
PD	2837	40109	329786	44.78%

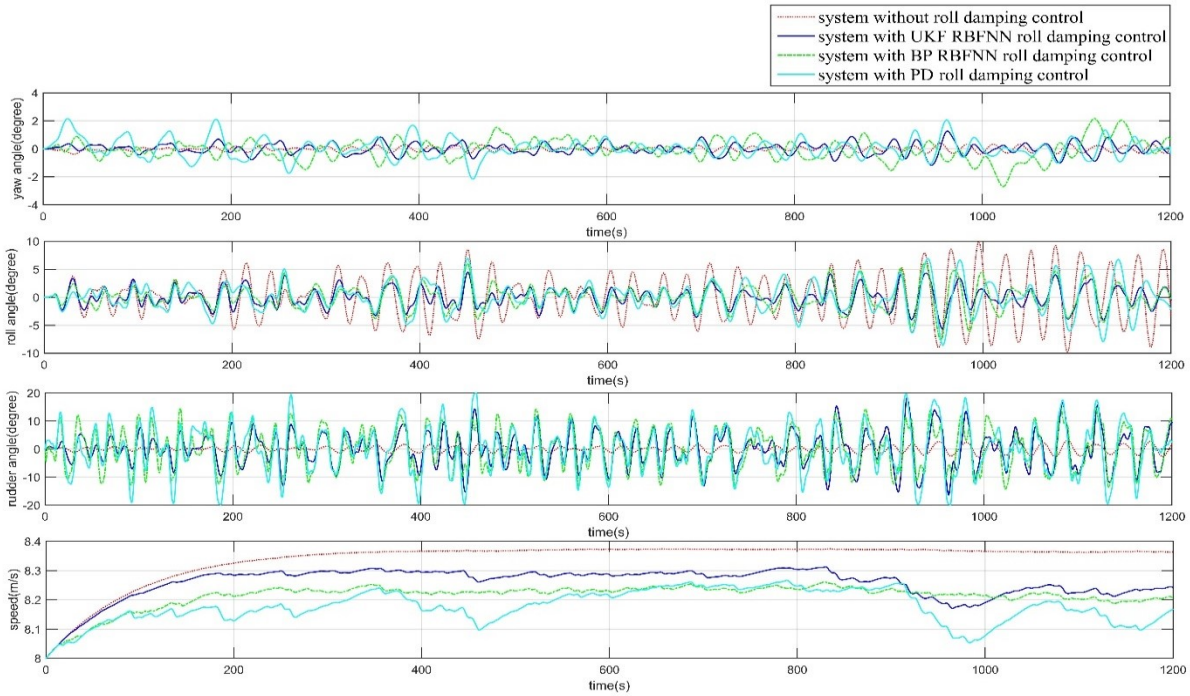

Fig. 3A. 5 The ship response of the rudder roll stabilizer when setting course is 30°

The same conclusions as the above-mentioned case can be applied to the scenario with the desired course $\psi_d = 60^0$. The sailing states of the ship, including course keeping deviation, roll angle, actual rudder angle and advancing speed, are shown in Fig. 3A. 6. It is seen that the designed stabilizer has good performance in course keeping and roll damping. While reducing the roll motion obviously, the yaw tracking error is acceptable. The relevant results of cost functions and roll reduction rate are outlined in

Table 3A. 2. It can be observed that the yaw error cost of EKF RBFNN is 60% smaller than that of BP RBFNN and PD based stabilization systems. Meanwhile, the roll cost and the rudder cost of the former control system are also smaller than that of the latter ones. In addition, the roll reduction rate of the EKF RBFNN based stabilizer (i.e. 49.54%) is bigger than that of the BP RBFNN stabilizer at 47.28% and PD stabilizer at 44.25%.

Table 3A. 2 The value of cost function and roll reduction percentage at yaw angle 60°

Controller types	Yaw error cost	Roll angle cost	Rudder angle cost	Roll reduction percentage
EKF RBFNN	1129	8146	125683	49.54%
BP RBFNN	2561	12937	177772	47.28%
PD	2575	19796	291788	44.25%

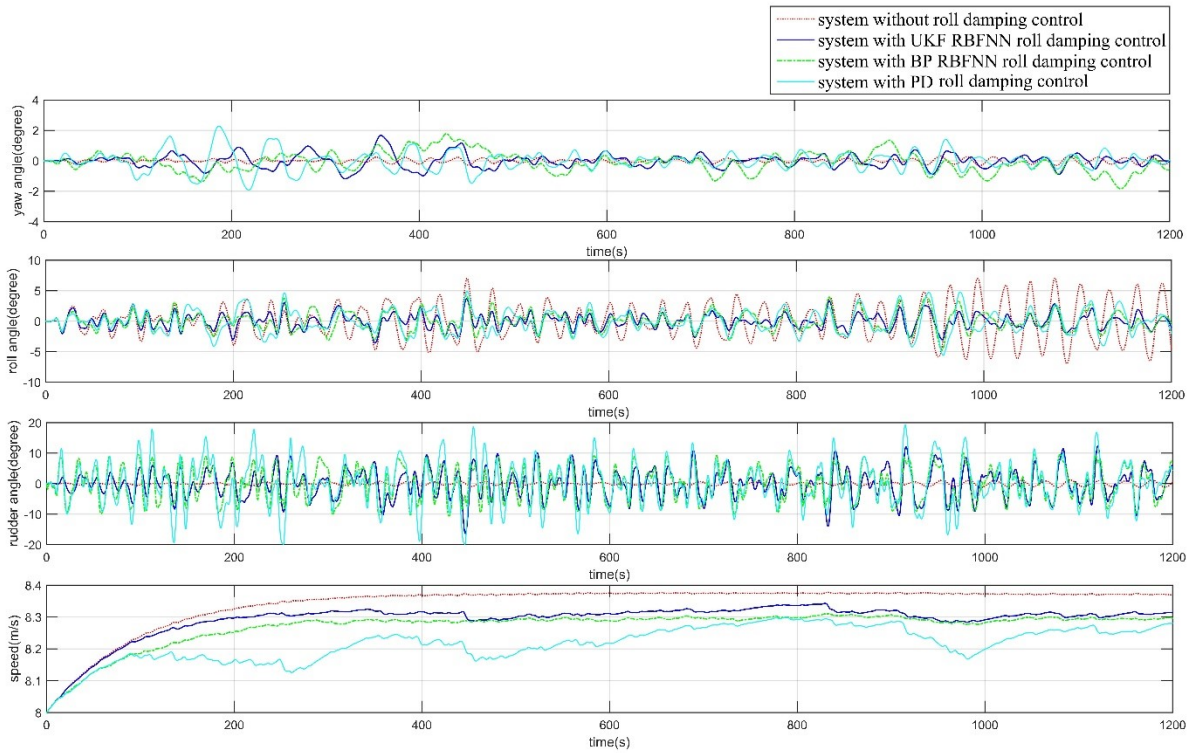

Fig. 3A. 6 The ship response of the rudder roll stabilizer when setting course is 60°

From the investigations concerning different course angles and waves encounter angles, the EKF RBFNN based rudder roll stabilization system was demonstrated to be effective in maintaining the ship advancing on the desired course and reducing the roll motions at the same time. In comparison with the BP RBFNN and PD based control systems, the designed system has low costs and better roll reduction performance.

3A.5.2. Roll Damping of the Ship Sailing with Path tracking

This part focuses on the investigation of ship's dynamic behaviours when sailing based on the pre-set waypoints. In order to realize the objective of path tracking control, the working mode of the control system was switched to the 'Path tracking Loop' with the EBS LOS guidance algorithm adopted as the guidance method. Two different pre-set trajectories are adopted in this part to validate the capability of the proposed control system. As the efficiency of the EKF RBFNN control system has been proved through the comparison with BP RBFNN and PD based system in the previous section, the capability regarding path tracking and roll damping were directly validated through the investigations of the system with and without EKF RBFNN based roll damping controller.

The initial heading angle of the ship is set to 0^0, the ship is requested to sail from the initial

waypoint (0, 0) to the waypoint (4000, 0), and then heading to the next point at (8000, 1200) before advancing to the waypoint (12000, 1200) (defined as Trajectory 1). In this process, the dynamic performances of steering to both port side and starboard side were considered. The trajectory and the deviation of path tracking are expressed in Fig. 3A. 7 and Fig. 3A. 8. It is shown that the ship is capable of sailing on the desired trajectory without significant tracking errors when using the proposed rudder roll stabilization system. The roll motion is distinctly reduced as illustrated in Fig. 3A. 9. In comparison with the system without roll damping control, when the roll damping controller is activated, the tracking deviation is slightly increased due to the rudder's force and moment added to the complicated coupling system. According to the analysis of this case study, before arriving at the same position at (11178,1200), the actual sailed distance of the ship under the control of EKF RBFNN based roll damping controller (i.e. 11344m) is approximately similar to that of the ship without roll damping controller (i.e. 11348m). The time consumption of the ship with and without roll damping controller are 1400s and 1369s, which means 2.21% reduction of the 'effective sailing speed' in covering the same length of predetermined trajectory. Therefore, it is shown that the roll damping performance is promising and the fuel consumption of the main engine in driving propeller is reasonable when adopting the designed rudder roll stabilization system.

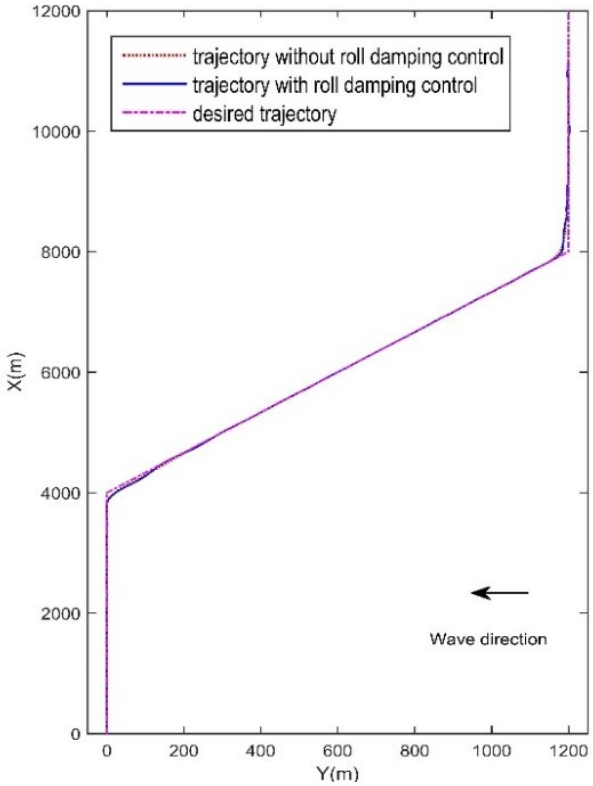

Fig. 3A. 7 The results of path tracking for ship sailing with and without roll damping control on Trajectory 1

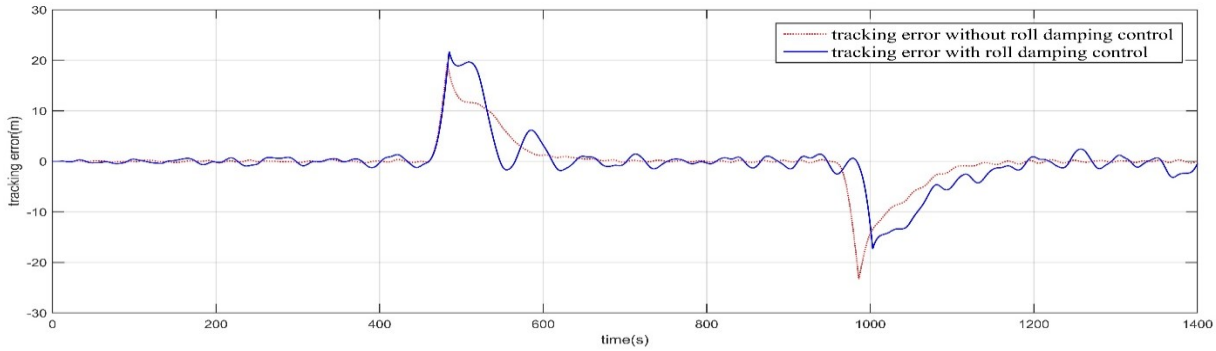

Fig. 3A. 8 The results of path tracking error for ship sailing with and without roll damping control on Trajectory 1

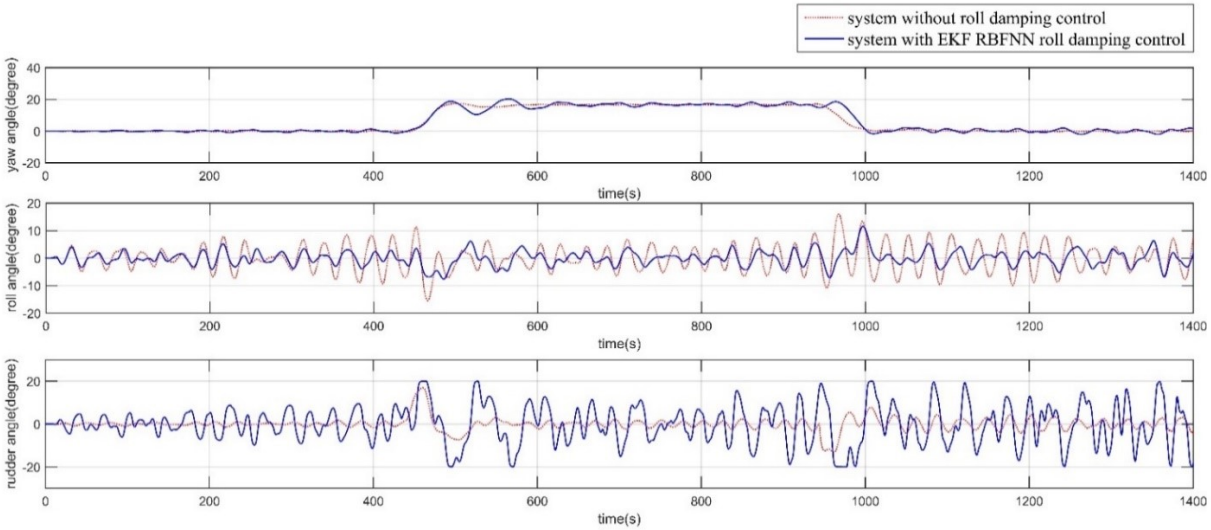

Fig. 3A. 9 The ship response with and without roll damping control when sailing based on the Trajectory 1

The similar conclusion can be applied to the scenario with different waves encounter angles, in which the voyage (Trajectory 2) of the ship is designed from the initial waypoint (0, 0) to (3600, 2160), and then to (5920, 6120) before arriving at the waypoint (5920, 9600). From Fig. 3A. 10, Fig. 3A. 11 and Fig. 3A. 12, it is shown that the proposed rudder roll stabilization system is capable of making the ship converge to the desired trajectory and reduce the roll motion. For the ship with and without roll damping controller, the actual sailed distances before arriving at the same position at (5950, 8590) are calculated to be $11237m$ and $11234m$, taking 1400s and 1377s. The result indicates that the difference between the two sets of actual sailed length can be ignored. In addition, the 'effective sailing speed' in covering the same length on predetermined trajectory under the control of roll damping controller is almost not affected. Thus, the roll damping and path tracking, as well as the sailing efficiency were validated.

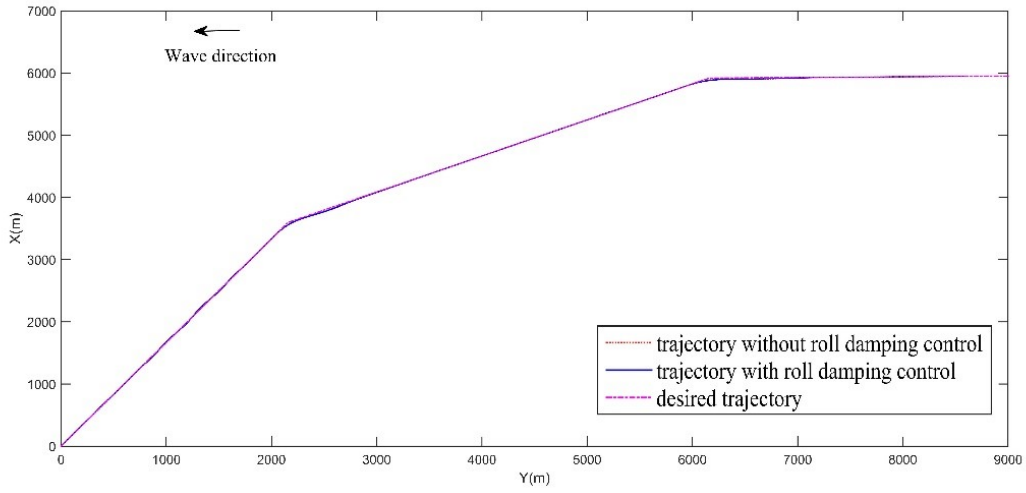

Fig. 3A. 10 The results of path tracking for ship sailing with and without roll damping control on Trajectory 2

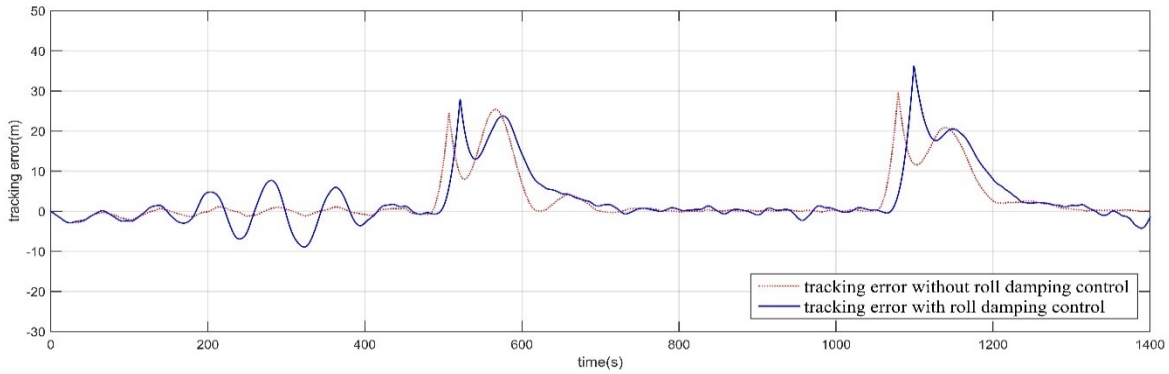

Fig. 3A. 11 The results of path tracking error for ship sailing with and without roll damping control on Trajectory 2

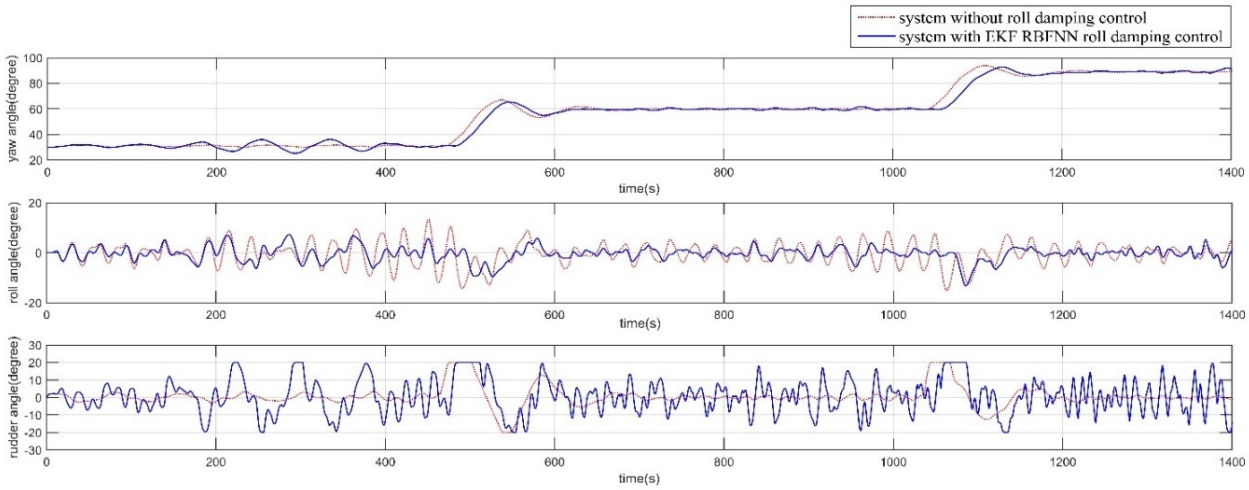

Fig. 3A. 12 The ship response with and without roll damping control when sailing based on the Trajectory 2

The above cases have indicated that the EKF RBFNN based rudder roll stabilization system was verified to be feasible regarding path tracking and roll reducing concerning the dynamic sailing conditions. The advantages of the proposed system consisted in its capability in counteracting roll motions generated from external disturbances and the stability in rapidly coping with dynamical change.

3A.6. Conclusion

In this paper, the EKF RBFNN algorithm has been adopted to develop the rudder roll stabilization system, which contains course keeping controller and roll damping controller implemented in parallel. The rudder roll stabilization system incorporated with the nonlinear mathematical model has been applied to verify the control performance of the ship only use the rudder as the steering actuator. It is found that the designed control system is feasible to maintain the ship advancing on the desired track or course while reducing the roll motion at the same time with the effects of environmental disturbances. It is worth noting that the designed EKF RBFNN based control algorithm involved fewer design parameters and avoided complicated gradient calculation regarding the output in every iteration in comparison with the design of BP RBFNN based one. Also, the speed reduction generated by the rudder actions under the control of EKF RBFNN based rudder roll stabilization system was smaller than that of using the other two roll damping control methods. Therefore, in comparison with the BP RBFNN and conventional PD based stabilization system, the EKF RBFNN based stabilization system is more efficient to reduce roll motions and robustness against the external disturbances generated by random waves

Further investigations will be carried out to validate the capability of the proposed EKF RBFNN based rudder roll stabilization system through experimental approaches. To improve the accuracy of the weights estimation and the robustness in coping with the environmental variables, more training algorithms will be further investigated to apply on the neural network training in the following studies.

Chapter3 - Part B. UKF Trained RBFNN Control System for Surface Vessels

Abstract: The large roll motion of ships sailing in the seaway is undesirable because it may lead to the seasickness of crew and unsafety of vessels and cargoes, thus it needs to be reduced. The aim of this study is to design a rudder roll stabilisation system based on Radial Basis Function Neural Network (RBFNN) control algorithm for ship advancing in the seaway only through rudder actions. In the proposed stabilisation system, the course keeping controller and the roll damping controller were accomplished by utilising modified Unscented Kalman Filter (UKF) training algorithm, and implemented in parallel to maintain the orientation and reduce roll motion simultaneously. The nonlinear mathematical model, which includes manoeuvring characteristics and wave disturbances, was adopted to analyse ship's responses. Various sailing states and the external wave disturbances were considered to validate the performance and robustness of the proposed roll stabiliser. The results indicate that the designed control system performs better than the Back Propagation (BP) neural networks based control system and conventional Proportional-Derivative (PD) based control system in terms of reducing roll motion for the ship in waves.

3B.1. Introduction

For most ships, it is unavoidable to encounter severe sea conditions when they carry cargoes from and to the port of destination. When these ships are advancing in rough seas under severe weather conditions, the large roll motion would be occurred due to the external environmental disturbances, such as strong winds, waves and currents. As one of the most undesired phenomena, the severe roll motion will enormously affect the safety of crew, cargoes and ships. Generally, it may lead to the working inefficiency of seafarers and results in the discomfort of the passengers because of the seasickness. In addition, the huge roll movement may cause stability loss and cargos damage to ships. Even worse, the vessel might be in danger of capsizing because of the severe roll motion. Therefore, reducing roll motion is very important for the ship advancing in the seaway from the perspective of safety.

Conventionally, course altering or heaving to is a good choice for the deck officers to reduce the large roll motions. However, for the ship which is in special conditions, such as executing maritime search and rescue mission, sailing in the area of traffic separation scheme, or having

strict liner shipping schedule, it is necessary to maintain course and advancing while reducing roll motion. Thus, apart from the seamanship, roll damping facilities are needed in some cases. Many attempts have been previously carried out to reduce the roll motion, such as the application of moving weights, bilge keels, anti-roll tanks, gyroscopic stabilisers, and stabilising fins. Although the above-mentioned method and facilities have been validated to be efficient, the ship's carrying capacity would be affected by the weight increase and space decrease. The installations of additional devices and appendages also impact on the hydrodynamic performance, seaworthiness and structural strength of the ship. Besides, the costs of ship building and maintenance will be raised. Thus, other rational and feasible methods are demanded for ships to maintain orientation and stability.

As the rudder is usually located after and under the ship's centre of gravity, apart from yaw movement, altering rudder angle will generate additional roll force and moment to the hull. Thus, besides being used as the yaw control facility, the rudder could be employed to reduce the roll motion of the ship whose rudder is capable of generating enough roll moments. Especially, when the range of rudder area is larger than 3% of $L \times T$ (i.e. $Ship's\ Length \times Draught$), it would be more efficient to supply moment and force to reduce roll motion in use of rudder. But the challenge is how to select the effective control method for the ship to maintain the tracking and reduce roll motion synchronously only through altering the deflections of rudder. The background of the rudder roll stabilisation design was reviewed by Lloyd (1975). Although the conventional Proportional-Integrative-Derivative (PID) based rudder roll stabiliser was effective and reliable in some cases, it could not work well in heavy seas because its fixed parameters were optimized corresponding to specific operating conditions (Van Amerongen and Van Nauta Lemke, 1978). In order to improve the performance of the control systems, various adaptive control methods had been adopted to stabilise the roll motion of ships (Messina et al., 1997, Lauvdal and Fossen, 1998, Sgobbo and Parsons, 1999b, Oda and Ohtsu, 1991). At present, with the development of modern control theory, rudder roll stabilisation systems accomplished with batch-adaptive control (Park et al., 2000), fuzzy logic control (Nejim, 2000), receding horizon control (Perez, 2005), H_∞ robust control (Xianku et al., 2006), and sliding mode control (Fang and Luo, 2007b) have been developed. Considering the excellent capability in approximating, neural network control algorithms have been widely utilised by Alarcin and Gulez (2007), Fang et al. (2010b), Li et al. (2010) and Fang et al. (2012b) to design the rudder roll stabiliser. In comparison with some multilayer feed forward neural network controller, it is indicated that the RBFNN controller

has the advantages of good generalization capability and simple architecture, which are beneficial to avoid unnecessary and lengthy calculations (Liu, 2013), therefore it is applied to design the rudder roll stabilisation system in this study.

The training algorithm plays an important role in designing the neural network based control system. Some commonly employed training algorithms, e.g. BP (Duro and Reyes, 1999), gradient descent (Karayiannis, 1999) and back-stepping (Yahui et al., 2004) have been validated to be effective to optimize the artificial neural network controller, but the performance of the proposed controller might be plagued by converging to poor local optimal and low learning velocity (Choi et al., 2005b). In order to overcome the above-mentioned flaws, the Kalman Filter variants could be the alternatives to train the neural networks based controllers (de Oliveira, 2012b). In comparison with the Extended Kalman Filter (EKF), which has the potential to propagate errors through its linearization, the UKF used deterministic sampling method and achieved a better level of estimation accuracy (Wan and Van Der Merwe, 2000).

The main objectives of this study are

- to formulate the desired feedback RBFNN based control algorithm whose weights are updated by a modified UKF method;
- to propose the rudder roll stabilisation system utilising UKF RBFNN for ship advancing in waves;
- to achieve roll damping and path tracking simultaneously only through rudder actions; and
- to validate the superiority of the designed roll stabilisation system in comparison with the BP RBFNN and PD based control system.

This paper is organized as follows: the 2nd section briefly presents the mathematical model including manoeuvring characteristics for ships sailing in waves. The following sections focus on the design of rudder roll stabilisation system. In the 3rd section, the principle of feedback RBFNN control method and UKF training algorithm are addressed. The UKF RBFNN based controller is applied to develop the rudder roll stabilisation system for roll damping and track keeping. In the following section, different sailing conditions are adopted to investigate the yaw control ability and roll reduction performance. Finally, the conclusions are presented in the last section.

3B.2. Mathematical Model of Ship Motions in Waves

In this section, the nonlinear model containing steering and sea-keeping characteristics for the ship with external wave disturbances is introduced. The motion equations, which can be utilised to describe the responses of the ship under rudder actions, are given in the Inertial and Body-fixed coordinate systems as shown in Fig. 2. 1.

Deduced from Newton's second law, the six degrees of freedom (DOF) dynamic equations of ship represented by Fossen (1994a) can be expressed as:

$$M\dot{\nu} + C(\nu)\nu + D(\nu)\nu + g(\eta) = \tau + \tau_E \qquad (3B.1)$$

where $\nu = (u, v, w, p, q, r)^T$ is the velocities of the vessel's translated motion and rotation motion; $M$is the inertia matrix; τ is the vector of control inputs; τ_E is the vector of environment forces and moments; $C(\nu)$ is the matrix of Coriolis and centripetal terms containing the added mass; D is the matrix of damping terms; $g(\eta)$ is the vector of restoring forces and moments arisen from gravity and buoyancy; η represents ship's position and orientation.

Considering the aims of roll damping and path tracking, the motions of pitch and heave can be overlooked in comparison with the motions of surge, sway, yaw and roll. Thus the nonlinear four DOF non-dimensional model can be employed to describe the dynamic motions of the proposed vessel, see in Son and Nomoto (1982).

In this study, the modified Pierson-Moskowitz (PM) wave spectrum model recommended by ITTC and outlined in Perez (2006) is utilised to simulate ship's response in random waves. According to the research of Sgobbo and Parsons (1999b), the forces and moments generated by waves can be added to the right hands of the motion equations to represent the environmental forces and moments.

3B.3. UKF Trained RBFNN Control Algorithm

In this section, the feedback control method based on the RBFNN is presented. In order to get higher training velocity and mapping accuracy, the modified UKF is employed as the training algorithm for the neural network controller.

3B.3.1. RBFNN Based Feedback Control Scheme

In this section, the same scheme of RBFNN (see the details in **Chapter 2.3**) was applied to approximate the function of control law as

$$u(z) = \sum_{j=1}^{m} \hat{w}_j^T h_j(z) = \hat{w}_1 h_1 + \hat{w}_2 h_2 + \cdots + \hat{w}_j h_j + \cdots + \hat{w}_m h_m \quad (3B.2)$$

$$z = [x\ s\ \frac{s}{\varepsilon}\ v_{sys}]^T \quad (3B.3)$$

where $\hat{w}_j (j = 1\ to\ m)$ are the estimations of the ideal weights and $h_j (j = 1\ to\ m)$ denote the activation functions. The input of the neural network is defined by the matrix z, which contains the values of desired signals, the system states, and their relevant derivatives.

By using the above-mentioned control algorithm, when a proper training algorithm is employed to update the relevant weights, the unknown nonlinear system can be controlled according to the observation of desired states and actual states of the plant.

3B.3.2. The Modified UKF Training Algorithm

The training algorithm of neural networks can be viewed as a parameters estimation problem and represented as a weighted least squares minimization problem. The Kalman Filter Variant algorithm provides an online mechanism in which the states of the networks can be updated immediately. The KF and its variants used for training NN are an application of parameters estimation. The estimation problem was usually described by the state equation and observation equation containing the process noise and measurement noise. There is an assumption that the noises are zero mean white Gaussian noise. In the most common used EKF, the probability distribution function is propagated through its linearization, which may induce errors and lead the states to diverge over time (Kandepu et al., 2008). The UKF, which was firstly proposed by Julier and Uhlmann (1997a), addressed the drawbacks of EKF by using a set of carefully selected 'sigma points'. This algorithm is capable of capturing the true mean and covariance of the Gaussian random variables through the system dynamics. When these points were propagated through the nonlinear system, it was accurate up to 3rd order in capturing the mean and covariance with high training velocity (Hongli et al., 2010).

The main difference between UKF and BP training algorithm is that an additional item, named error covariance matrix $P(n)$, needs to be updated and stored for the UKF algorithm apart from

the updating of weights matrix $\widehat{w}(n)$. The covariance provides a form of averaging on the output function, which prevents the parameters from going to the minimum of the error surface (Wan and van der Merwe, 2002). In this study, by employing the slightly modified UKF, the weights updating of the proposed neural network controller is achieved.

As the core technique of the UKF, the Unscented Transformation (UT) is used to cope with the nonlinearity. For the RBFNN with m neurons in the hidden layers, the UT can be fully expressed by three parameters, in which the parameter α concludes the spread of the sigma points, the second parameter β reflects the information of the prior distribution, and the tertiary parameter is denoted by κ, more details can be found in Rhudy and Gu (2013). Base on the above outlined scaling parameters, the weights vectors are defined as:

$$\lambda = \alpha^2(m + \kappa) - m$$

$$\eta_1^M = \frac{\lambda}{m+\lambda}, \eta_i^M = \frac{\lambda}{2(m+\lambda)}, i = 2, \dots, 2m + 1$$

$$\eta_1^C = \frac{\lambda}{m+\lambda} + 1 - \alpha^2 + \beta, \eta_i^C = \frac{\lambda}{2(m+\lambda)}, i = 2, \dots, 2m + 1 \qquad (3B.4)$$

where λ is the additional scaling parameter, η^M and η^c are the weight vectors of mean and covariance respectively.

Using the prior mean w and covariance P_W, the $2m + 1$ sigma points are generated as

$$W = \left[w, w + \left(\sqrt{m + \lambda}\sqrt{P}\right)_i, w - \left(\sqrt{m + \lambda}\sqrt{P}\right)_i\right], i = 1, \dots, m \qquad (3B.5)$$

where $\sqrt{P}$ is a lower triangular matrix calculated by Cholesky decomposition. Once the points with corresponding weights are generated, they can then applied to propagate through the nonlinearity of the UKF as shown as following:

- **Initialization at $k = 0$**

  (I). Define the weights vector: $\eta^M = \left[\frac{\lambda}{m+\lambda}, \left(\frac{\lambda}{2(m+\lambda)}\right)_i\right], i = 2, \dots, 2m + 1;$

  $$\eta^C = [\frac{\lambda}{m+\lambda} + 1 - \alpha^2 + \beta, \left(\frac{\lambda}{2(m+\lambda)}\right)_i], i = 2, \dots, 2m + 1$$

  (II). Initialize with: $W_0 = E[w], P_{W_0} = E[(w - w_0)(w - w_0)^T]$

- **Recursively executing for $\boldsymbol{k = 1, 2, \ldots, \infty}$**

(III). Generate sigma points: $W = \left[w, w + \left(\sqrt{m+\lambda}\sqrt{P}\right)_i, w - \left(\sqrt{m+\lambda}\sqrt{P}\right)_i\right]$

(IV). Prediction transformation

Mean of predicted weights: $W_{Mean} = \sum_{i=1}^{2m+1} W_i \eta_i^M$

Covariance of predicted weights:

$$P_W = \sum_{i=1}^{2m+1} \eta_i^M (W_i - W_{Mean})(W_i - W_{Mean})^T + Q$$

(V). Measurement update transformation

Mean of propagated sigma points: $U_{Mean} = \sum_{i=1}^{2m+1} U_i \eta_i^M$

Covariance of measurement: $P_{UU} = \sum_{i=1}^{2m+1} \eta_i^C (U_i - U_{Mean})(U_i - U_{Mean})^T$+R

Cross-covariance of measurement: $P_{WU} = \sum_{i=1}^{2m+1} \eta_i^C (W_i - W_{Mean})(U_i - U_{Mean})^T$

(VI). Unscented Kalman Filter calculation and update functions

$$K = P_{WU}/P_{UU}$$

$$\widehat{w} = W_{Mean} + Ks$$

$$P = P_W - KP_{UU}K^T$$

where the item K denotes the Kalman gain matrix for weights group, P is the approximate error covariance matrix, the estimated weights is represented by $\widehat{w}$ and it will be used in the next iteration to generate sigma points, Q and R are the artificial process noise and observation noise which is useful to avoid numerical divergence, s is the augmented error item which has been expressed in equation *(3B.3)*. For the conventional UKF trained Neural Network, the error between the actual value and desired value is used to update the weights directly. Considering the under-actuation and high inertia of surface vessel, the derivative of the error is also used in the UKF training process to guarantee the control performance. The following case studies demonstrated the efficiency of this method.

Therefore, the working principle of RBFNN based control system incorporating with UKF training algorithm can be referred in Fig. 3A. 2. In the proposed working loop, the target value and the actual value are utilised to construct the input matrix of neural networks. Accomplished with UKF training method, the control law will be calculated by the controller and then used to make the plant converge to target value recursively.

3B.4. Rudder Roll Damping Control System

In comparison with other methods, the rudder roll stabiliser is an efficient strategy to reduce roll motion only by altering the angle of the rudder. It has been demonstrated that the rudder roll stabilisation system can be designed through separating the steering and roll characteristics and then designing the corresponding controllers separately (Perez and Blanke, 2012). One advantage of this kind of control system is that the roll damping controller can be switched off when the roll motions are small and the roll reduction is not necessary. Based on the control scheme developed by Wang et al. (2015), the UKF trained RBFNN based rudder roll stabiliser was developed with the function of path tracking. The architecture of the system can be illustrated in Fig. 3A. 3.

The proposed rudder roll stabilisation system aims to realise the roll damping and path tracking simultaneously by conducting the course keeping controller and roll damping controller in parallel. For the roll damping controller, it can be switched on when large roll angle is detected. The objectives of course keeping and path tracking can be achieved by switching to different blocks. When the system is switched to the course keeping loop, the input matrix z_ψ for the course keeping controller can be constructed by the actual yaw angle ψ and the desired yaw angle ψ_d. Meanwhile, the actual roll angle ϕ is used to get the roll damping control output according to the work of roll damping controller. When the system is switched to the path tracking loop mode, the instantaneous desired course angle can then be calculated by EBS LOS guidance technique. The control law for the rudder, which will make the ship controllable recursively, is formulated by the summation of the control outputs from both controllers:

$$\delta_c = \delta_\psi + \delta_\phi \qquad (3B.6)$$

where δ_c is the rudder command signal, δ_ψ represents the control output of course keeping controller while δ_ϕ denotes the control output of roll damping controller (Fossen, 1994a). As it is difficult to determine the importance of the yaw control and roll damping control, they are

assumed to be equivalent important, and the same weights (i.e. 1) are used in the equation.

The output of the course keeping controller has the following forms:

$$\delta_{\psi} = \hat{U}_{\psi}(z_{\psi}) = \sum_{i=1}^{m} \hat{w}_{\psi(UKF)}^{T} h(z_{\psi})$$

$$= \hat{w}_{\psi 1(UKF)} h_1(z_{\psi}) + \hat{w}_{\psi 2(UKF)} h_2(z_{\psi}) + \cdots + \hat{w}_{\psi m(UKF)} h_m(z_{\psi}) \quad (3B.7)$$

$$\hat{w}_{\psi(UKF)} = W_{\psi\, Mean(UKF)} + K_{c(UKF)} s_{\psi} \quad (3B.8)$$

where z_{ψ} represents the input matrix of the course keeping controller and it can be derived from equation *(3B.3)*, m is the amount of neuron nodes in the hidden layer, $\hat{w}_{\psi(UKF)}$ is the estimated weights of course keeping controller updated by UKF algorithm, $W_{\psi\, Mean(UKF)}$ is the item derived from the weights of the previous iteration, $K_{c(UKF)}$ denotes the Kalman gains of the UKF training method for course keeping controller, and s_{ψ} is the augmented yaw error matrix.

Also, the output of the roll damping controller has the form as follows:

$$\delta_{\phi} = \hat{U}_{\phi}(z_{\phi}) = \sum_{i=1}^{m} \hat{w}_{\phi(UKF)}^{T} h(z_{\phi})$$

$$= \hat{w}_{\phi 1(UKF)} h_1(z_{\phi}) + \hat{w}_{\phi 2(UKF)} h_2(z_{\phi}) + \cdots + \hat{w}_{\phi m(UKF)} h_m(z_{\phi}) \quad (3B.9)$$

$$\hat{w}_{\phi(UKF)} = W_{\phi\, Mean(UKF)} + K_{r(UKF)} s_{\phi} \quad (3B.10)$$

where z_{ϕ} represents the input matrix of the roll damping controller and the details is expressed in equation *(3B.3)*, $\hat{w}_{\phi(UKF)}$ is the estimated weights of roll damping controller updated through UKF algorithm, $W_{\phi\, Mean(UKF)}$is the mean of weights and can be calculated from the sigma points and covariance of the previous iteration, $K_{r(UKF)}$ denotes the Kalman gains of the UKF training method for roll damping controller, and s_{ϕ} represents the augmented error matrix of roll motion.

As one of the reliable guidance methods, the Enclosure-Based Steering Line of Sight (EBS LOS) algorithm is adopted in this paper to maintain the ship sails on the pre-set tracking. This

method can be represented by considering a virtual circle with radius R, which normally equals to 2 times of ship's length (Alfi et al., 2015). The details can be seen in **Chapter 3A.3** with further MATLAB coding attached in Appendix IV.

In order to evaluate the roll damping performance of the proposed systems. The roll reduction percentage shown in equation *(3A.13)* was used. Further evaluation items using the costs value functions, including the values of yaw error, roll motion and rudder angle were employed as well, the details can be seen in equation *(3A.14)*.

3B.5. Simulation Results and Discussion

In this study, a container ship introduced by Fossen (1994a) was selected to investigate the performance of the proposed UKF RBFNN based rudder roll stabilisation system. The main characters of the employed ship can be seen in the Table 2.1. For the adopted mathematical model, the inputs were rudder angle, shaft speed of propeller and the Pierson-Moskowitz wave spectrum. The response model of rudder actions ($\dot{\delta} = \delta_c - \delta$, where δ is actual rudder angle and δ_c is the commanded rudder angle) was utilised in this study. Generally, the rudder angle range of the conventional autopilot would be limited within 15° to avoid huge steering. However, for the ship utilising rudder roll stabilisation, rudder the is the only actuator to control both the course and roll motion. In order to compensate the huge disturbances generated from rough sea, large force and moment is required from the rudder action. Thus, the rudder angle range is extended to $\delta_{max} = \pm 20$ ° corespondingly. Although roll reduction is affected by the characteristics of the rudder as a high slew rate steering system has better damping performanceOda et al. (1999), the conventional rudder system was used to validate the performance of proposed controller. Moreover, in order to meet the requirement of International Maritime Organization (IMO), the slew rate limit was set to $5\ °/s$. The ship was advancing in random waves with significant heights $h_{1/3} = 3\ m$ and average period $T_w = 10\ s$, and the depth of the water was assumed to be infinite for simplification. The shaft speed of the propeller was set to $80\ rpm$. The Bogacki-Shampine method was applied to solve the time history simulation of the ship motion response, including the velocity of surge, sway, yaw and roll, the angle of yaw and roll, the position of ship and the actual rudder angle.

3B.5.1. Ship Sailing in Waves Based on Desired Course

In this section, the working mode was switched to the Course Keeping Loop. The desired

courses $\psi_d = 10°, 45°, 80°, 180°$ were adopted to validate the course keeping and roll reduction performance of designed stabiliser. The courses adopted are straight directions to guide the ship sailing forward with different waves encounter angle, and the heading of the ship was desired to stabilise on the corresponding yaw angle, which is expressed by the rotation around Z axis in Fig. 2. 1. The ship was steered by rudder only with random waves coming from true North. In order to demonstrate the advantages of the proposed control system, the BP RBFNN based rudder roll stabilisation system and PD based rudder roll stabilisation system, developed by Wang et al. (2015), were employed for comparison.

When the ship is sailing with the desired course at 10°, the time history of the yaw angle, roll angle and rudder actions for three kinds of control systems are illustrated in Fig. 3B. 1. Comparing with the control system without roll reduction function, it is shown that the roll motion is obviously reduced when the roll damping controller is included. Although the yaw angle error is consequently increased and the rudder actions become bigger, it can be explained by complicated coupling effects between reduced roll motions, and yaw response. The cost value of yaw error, roll motion and rudder angle of three stabilisers are summarized in Table 3B. 1. It is easy to observe that the UKF RBFNN stabiliser can use the rudder more effectively to reduce roll motion while making the ship sail on the desired course in comparison with the BP RBFNN control system and PD control system. Based on equation *(3A.13)*, the roll reduction rate of the UKF RBFNN based rudder roll stabilisation system is calculated to be 56.33%, which is higher than that of the BP RBFNN based and PD based stabiliser. In addition, the time series obtained data, including yaw rate, roll rate, speed and force generated from external waves under different control algorithm are presented in the Fig. 3B. 2 to show the simulation results in details. Moreover, it is indicated that, as the rudder altering of using UKF RBFNN based roll stabilisation system are small and efficient, the proposed control system has less effect on ship's controllability and speed maintenance.

Table 3B. 1 The value of cost functions and roll reduction percentages at yaw angle 10°

Controller types	**Yaw error cost**	**Roll angle cost**	**Rudder angle cost**	**Roll reduction percentage**
UKF RBFNN	3898	13983	124116	56.33%
BP RBFNN	3849	25992	335010	44.47%
PD	3960	31614	345248	41.20%

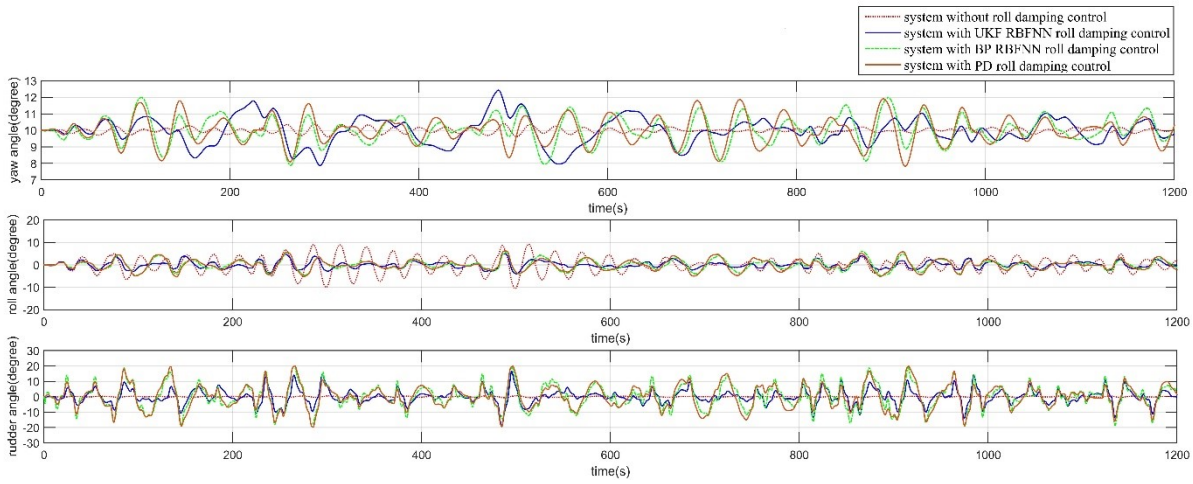

Fig. 3B. 1 The ship response of the rudder roll stabiliser when desired course is 10°

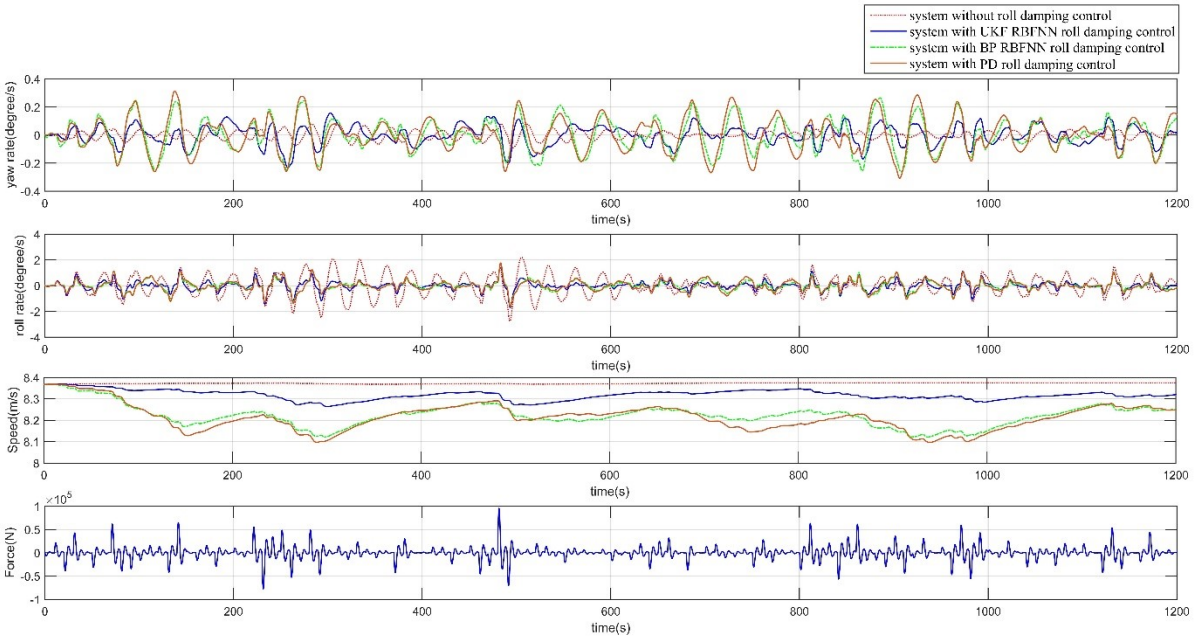

Fig. 3B. 2 The motions and force generated from external waves under different control algorithm when desired course is 10°

The dynamic responses of the ship are shown in the Fig. 3B. 3 when the desired course is set at $\psi_d = 45^0$. It is observed that the roll motion of the proposed ship is quite high when utilising the controller without roll damping function. Whereas, after the activation of the roll reduction controller, the rudder roll stabiliser is capable of making the ship maintain the orientation and reduce the roll motion synchronously. Considering the values of the cost summarized in Table 3B. 2, the superiority of the UKF RBFNN based stabiliser on the aspect of roll damping and yaw keeping can then be evaluated in comparison with that of the BP RBFNN and PD control based one. And it shows that the roll reduction rate of the UKF RBFNN based stabiliser (i.e.

53.00%) is higher than that of the BP RBFNN stabiliser at 48.34% and PD stabiliser at 43.53%.

Table 3B. 2 The value of cost functions and roll reduction percentages at yaw angle 45°

Controller types	Yaw error cost	Roll angle cost	Rudder angle cost	Roll reduction percentage
UKF RBFNN	1634	17807	156191	53.00%
BP RBFNN	4899	28046	376728	48.34%
PD	4784	34923	386137	43.53%

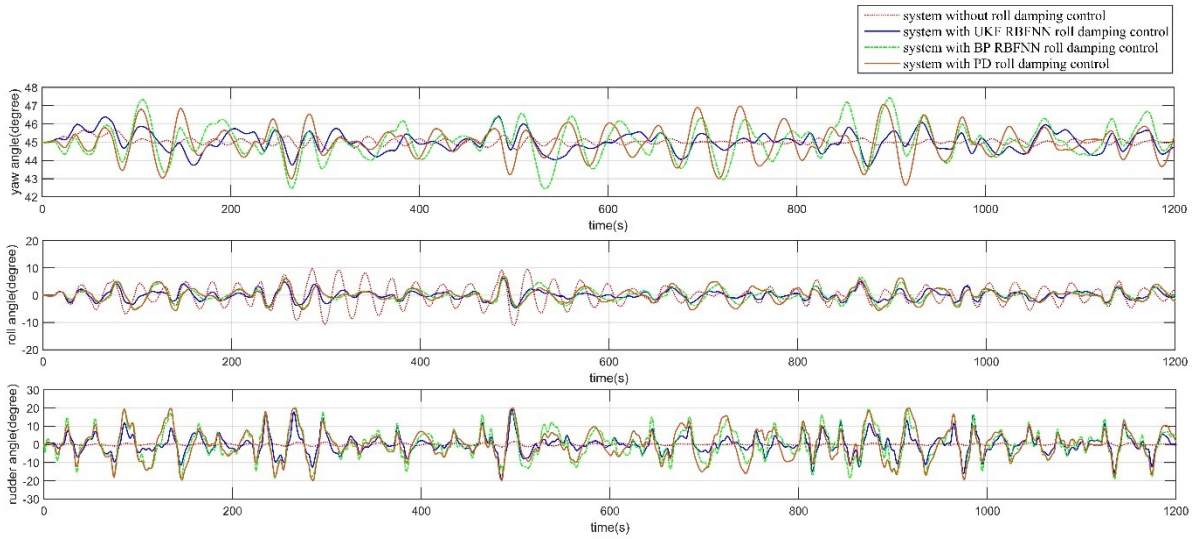

Fig. 3B. 3 The ship response of the rudder roll stabiliser when setting course is 45°

The similar conclusions expressed previously can be applied to the scenario with the desired course $\psi_d = 80^0$. The ship responses including yaw angle, roll angle, and rudder angles are illustrated in Fig. 3B. 4. It is indicated that the function of proposed stabiliser in course keeping and roll damping can still be handled well even with the waves from beam seas. Although the yaw error is increased when using the roll stabiliser, they are the price paid for roll damping added to the coupling system. The relevant results of cost and roll reduction percentage are outlined in Table 3B. 3. The roll reduction percentage for three kinds of stabilisation system is approximately 56.79%, 54.99% and 48.93%, respectively.

Table 3B. 3 The value of cost functions and roll reduction percentages at yaw angle 80°

Controller types	Yaw error cost	Roll angle cost	Rudder angle cost	Roll reduction percentage
UKF RBFNN	8290	29457	275978	56.79%
BP RBFNN	10078	34067	476941	54.99%
PD	8676	50078	639578	48.93%

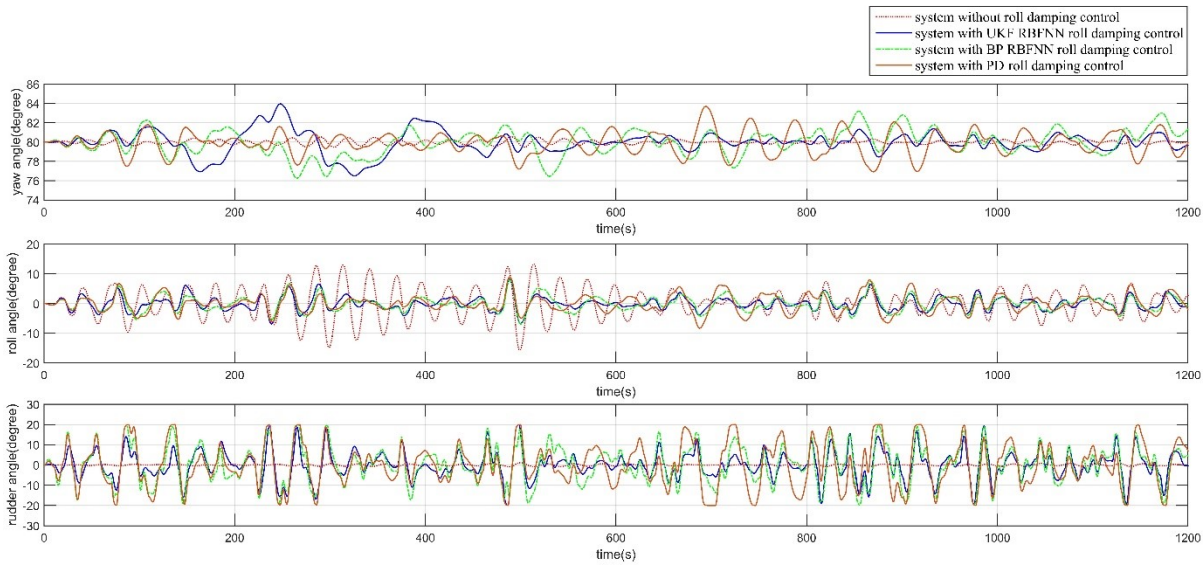

Fig. 3B. 4 The ship response of the rudder roll stabiliser when setting course is 80°

It is known that the waves coming from the following sea may generate huge roll motion, even lead to the parametric roll motion. When the desired course is set at 180° with waves coming from the following sea, the ship responses including yaw angle, roll angle, and rudder angles are illustrated in Fig. 3B. 5. In this study, the large roll motion amplitude at 35° existed. In order to make further analysis under this extreme conditions, the angle of flooding is assumed to be larger than 40° and the corresponding righting arm is sufficient. Although the yaw error is increased accordingly, it is indicated that the roll reduction by using UKF RBFNN based stabilisation system is calculated to be 49.79%, which is a little higher than that of using BP RBFNN and PD based ones. The cost value of roll motions, yaw error and rudder actions are summaries in Table 3B. 4. Thus, the control performance of proposed rudder roll stabilisation system was verified with waves coming from the stern of the ship.

Table 3B. 4 The value of cost functions and roll reduction percentages at yaw angle 180°

Controller types	Yaw error cost	Roll angle cost	Rudder angle cost	Roll reduction percentage
UKF RBFNN	7330	200659	550914	49.79%
BP RBFNN	9545	222582	553533	48.92%
PD	8676	237629	639578	48.52%

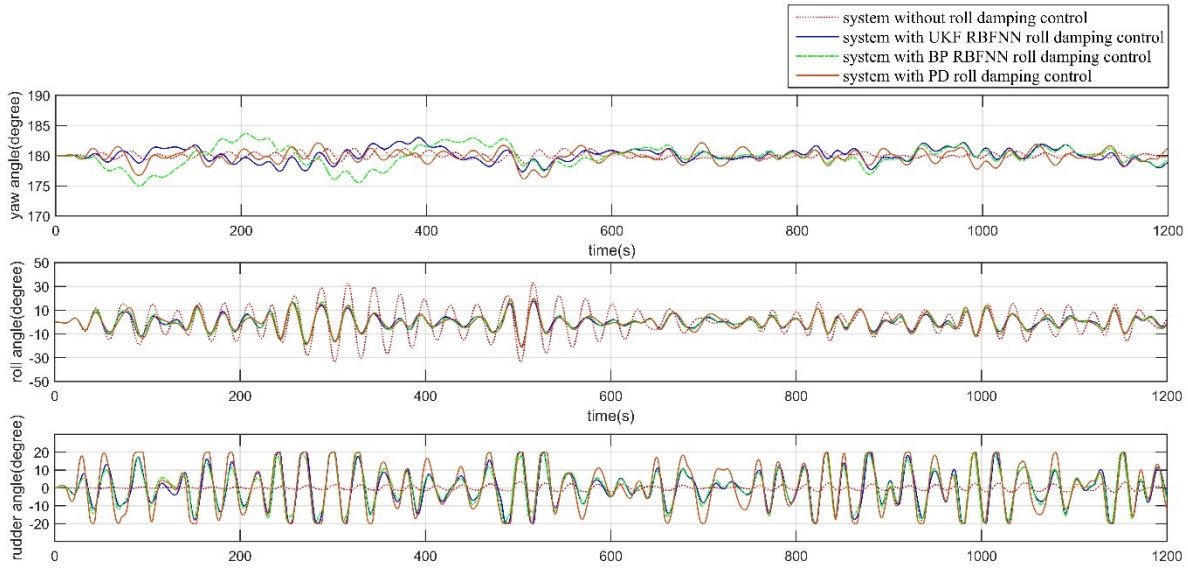

Fig. 3B. 5 The ship response of the rudder roll stabiliser when setting course is 180°

From the overall investigations with respect to different heading and waves encounter angles, the capability of UKF RBFNN based rudder roll stabilisation in keeping course and reducing the roll motion was validated. In comparison with the BP RBFNN control system and PD control system, the proposed system could use the rudder more effectively to get better roll reduction performance.

3B.5.2. Ship Advancing in Waves Based on Pre-set Waypoints

In this section, the working mode was switched to the Path tracking Loop. The dynamic behaviours of the proposed ship navigated by the EBS LOS guidance technique were investigated. Two sets of pre-set waypoints were utilised to generate the desired trajectories, which are then used in this part to validate the path tracking capability of the proposed control system. Because the advantages of the UKF RBFNN based stabiliser have been demonstrated in the former section by comparing with the BP RBFNN based stabiliser, the responses of the

ship with and without UKF RBFNN based roll damping control were analysed to verify the feasibility of the proposed rudder roll stabilisation in coping dynamic sailing states.

Trajectory 1 is constructed from the initial waypoint (0, 0) to the following waypoint (1450, 2500), and then to the waypoint (4950, 6000) before heading to the next point at (7450, 7450). When the ship is sailing on the desired trajectory with the initial heading angle at 60^0, the trajectory and the error of path tracking are shown in Fig. 3B. 6 and Fig. 3B. 7. What still needs to be explained is that the unsmooth inflexion points in Fig. 3B. 7 are generated from the change of newly referred tracking. According to the illustration of the figure, it is indicated that the UKF RBFNN based stabiliser system works well on the roll reduction apart from the path tracking. The differences in the two trajectories can be explained as the ship's heading is consequently affected by the additional roll motion. The results in Fig. 3B. 8 show that the roll motion is distinctly reduced. Based on the above simulation, for the ship with and without roll damping controller, the sailed distances before arriving at the same position near the last waypoint are calculated to be 9853.6m and 9856.9m, taking 1200 seconds and 1188.8 seconds respectively. The actual speed of covering the same length on the desired trajectory by using the proposed stabilisation system is 0.93% smaller than that of without using it, which can be accepted in some cases. Therefore, the fuel consumption is reasonable when using the stabiliser for path tracking and roll reduction.

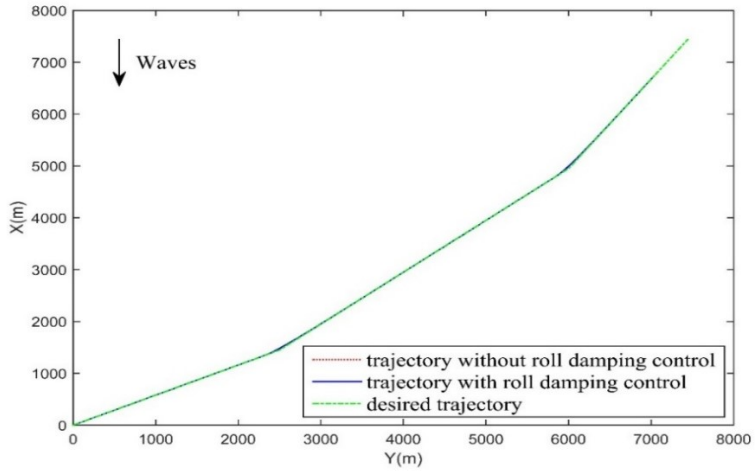

Fig. 3B. 6 The results of path tracking for ship sailing with and without roll damping control on Trajectory 1

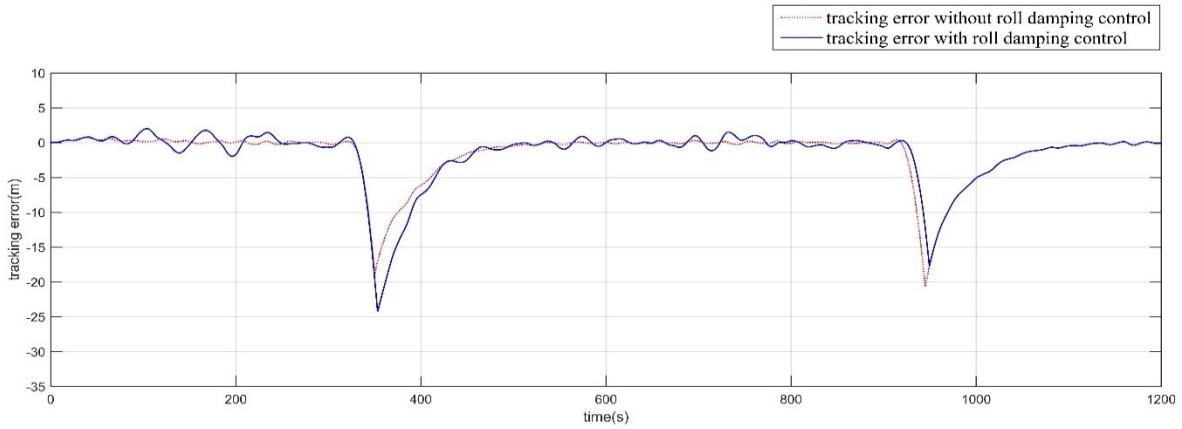

Fig. 3B. 7 The results of path tracking error for ship sailing with and without roll damping control on Trajectory 1

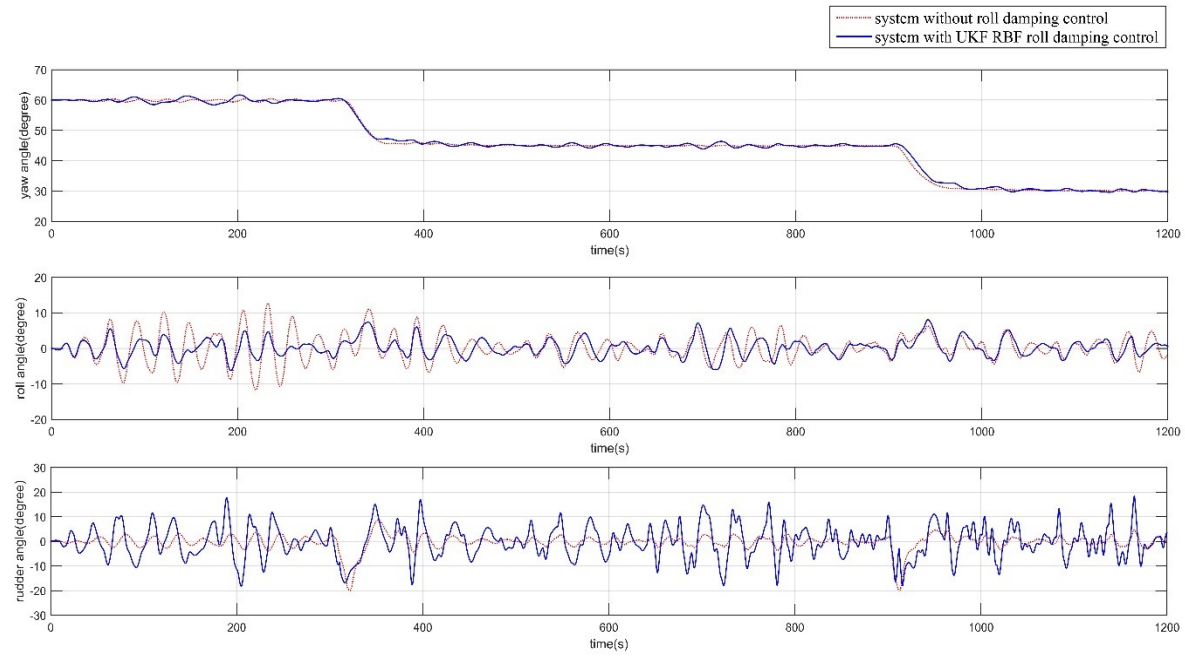

Fig. 3B. 8 The ship response with and without roll damping control when sailing based on the Trajectory 1

The similar conclusion can be applied to the scenario of the ship sailing on *Trajectory 2* from the initial waypoint (0, 0) to (600, 3500) and then to (2050, 6000) before arriving at (2950, 11000). The ship's dynamic responses in Fig. 3B. 9, Fig. 3B. 10 and Fig. 3B. 11 show that the proposed rudder roll stabilisation system is able to guide the ship sailing on the desired trajectory while reducing the roll motion synchronously. It should be noted that, before the ship arriving at the same position near the last waypoint, the sailed distance of the ship using rudder roll stabilisation system (i.e. 9760.9m) is similar as that of the ship without using roll damping

controller (i.e. 9759.6m). In addition, the time consumption for the ship using the UKF RBFNN based roll stabilisation system and without using it are respectively 1184.4s and 1200s, which means 1.3% of speed reduction is generated by using the proposed rudder roll stabilisation system. Thus, the extra fuel consumption of the ship utilising roll stabiliser is acceptable while achieving roll reduction.

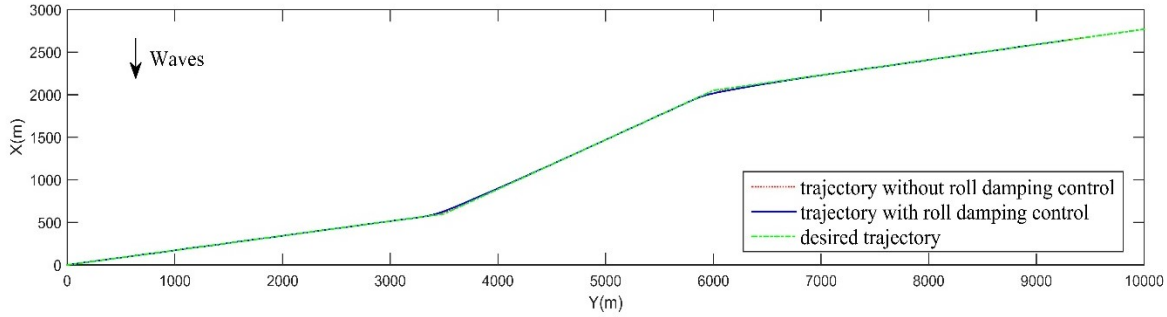

Fig. 3B. 9 The results of path tracking for ship sailing with and without roll damping control on Trajectory 2

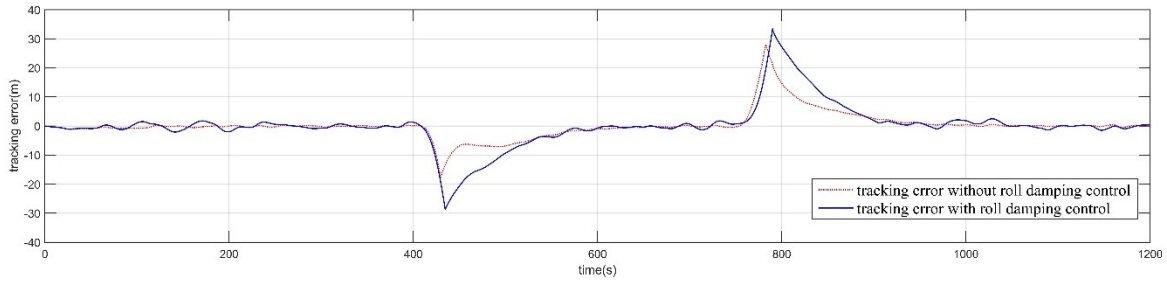

Fig. 3B. 10 The results of path tracking error for ship sailing with and without roll damping control on Trajectory 2

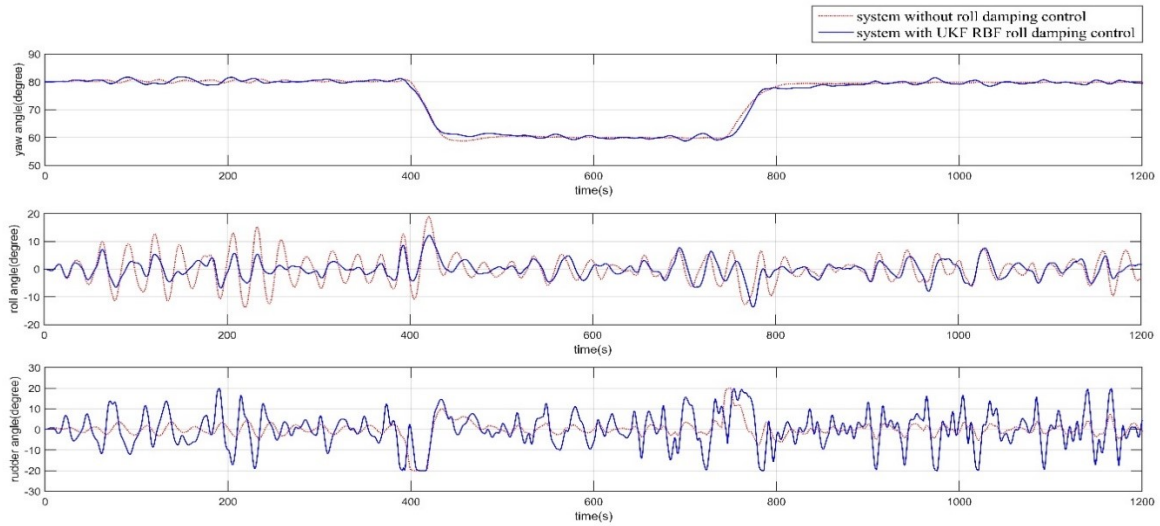

Fig. 3B. 11 The ship response with and without roll damping control when sailing based on the Trajectory 2

Based on the above-mentioned investigations, the feasibility of the proposed UKF RBFNN based rudder roll stabilisation system on the aspects of path tracking and roll damping was verified. The priorities of the proposed system consist of its capability of eliminating external disturbance and the robustness of coping with dynamical changes.

3B.6. Conclusion

The design of the UKF trained RBFNN based rudder roll stabilisation system has been presented. The performance of the developed stabiliser has been verified by employing a container ship sailing in random waves and analysing its motion responses. The results in this investigation indicate that the UKF RBFNN based roll stabilisation system is capable and flexible to accomplish the purposes of path tracking and roll reduction simultaneously only through rudder actions. Besides, the robustness of the proposed control method in terms of rapidly responding dynamical sailing states, which including head-sea, beam-sea and following-sea, has been demonstrated. According to the comparison with the BP RBFNN based stabiliser and PD based stabiliser, the significant advantages of the UKF RBFNN based stabiliser have been clearly justified. Based on the analysis, the reductions of actual speed generated by the rudder actions under the control of UKF RBFNN based stabiliser are acceptable. It is indicated that the proposed control system is much more effective to use rudder for roll reduction and course keeping in comparison with the BP RBFNN based control system.

In the future studies, other training algorithms with higher estimation accuracy and lower computational expense will be adopted to improve the capability of the control system. In addition, further investigations will be carried out to validate the capability of the proposed rudder roll stabilisation system by experiments using a model scaled container ship.

Chapter 4

Modelling of a Surface Vessels from Free Running Tests

Chapter 4 presents the modelling of a free running model scaled surface vessel. The electronic and mechanical components are described to show the configuration of the ship. Free running tests are carried out to collect the raw data from the corresponding sensors. After the implementation of the KF based data filtering, the hydrodynamic coefficients are identified by the RLS method. This chapter provides a low-cost but effective approach to develop free running model scaled ship and answers the third research question stated in **Chapter 1**.

This chapter has been published and presented in 'the 3rd International Conference on Control, Automation and Robotics'. The citation for the research article is:

Wang, Y., Chai, S. & Nguyen, H. D. (2017). *Modelling of a surface vessel from free running test using low-cost sensors.* 3rd International Conference on Control, Automation and Robotics (ICCAR), 2017. IEEE

Abstract: Identification of hydrodynamic coefficients and accessibility of accurate mathematical model to predict actual responses of vessels has practical significance to design computer-based simulators and apply new control algorithms, thus effective methods and proper devices should be investigated to do the modelling. The aim of this study was to estimate hydrodynamic coefficients of a surface vessel from the free running test using an experimental modelling method. Working as the embedded platform and data acquisition card, myRIO was utilised to control the scaled model, namely 'P&O Nedlloyd Hoorn', and measure her motion states using low cost sensors including a Global Positioning System (GPS) receiver, accelerometer, gyroscope and digital compass. System identification was conducted utilising the processed experimental data with Kalman filter to estimate the hydrodynamic coefficients of a mathematical model in four degree of freedom (DOF) including surge, sway, yaw and roll. The developed mathematical model of the scaled model was validated through the comparison between the experimental data and simulation results. It has demonstrated that the proposed low-cost hardware and system identification algorithm is capable of estimating hydrodynamic coefficients of the proposed mathematical model of the scaled surface vessel.

4.1 Introduction

Nowadays, the developments of the control engineering call for the competent mathematical models with which the new algorithms can be verified by simulations to describe the responses of vessels with high accuracy. In addition, due to the ever-increasing demands for developing computer-based simulators, creating accurate mathematical models is of key importance to describe manoeuvring characteristics of vessels. Whereas, for the underway surface vessels, the systems always have a high degree of complexity thus it is not easy to identify their mathematical models by theoretical modelling (Moreno-Salinas et al., 2013). Therefore, it is important to employ effective methods and proper devices to get mathematical models for various purposes.

Traditionally, estimation of hydrodynamic coefficients can be made by using Planar Motion Mechanism (PMM). Whereas, any changes to the ship's configuration might decrease the usefulness of these measurements (Pereira and Duncan, 2000). When the roll motion is considered, the number of PMM tests will dramatically increase (Yoon et al., 2007). Although the computational fluid dynamics (CFD) method can be extended for free running tests and measure the data of ship manoeuvres, the capabilities of the cluster, propulsion modelling and

size of the mesh are more than essential(Araki et al., 2012). In comparison with the above-mentioned methods, the system identification (SI) method provides a more practical alternative. Once the structure of the mathematical model and the experimental input-output are determined, the parameters of the model can be estimated then.

The main objectives of this study are

- to propose a 4 DOF mathematical model for a model scaled free running surface vessel, namely Hoorn, with a number of hydrodynamic coefficients to be estimated;
- to conduct free running tests utilising myRIO as the embedded computer and data acquisition card (DAQ) connected with low-cost sensors including a GPS receiver, accelerometer, gyroscope and digital compass to get data including displacements in x, y, and z-axes, linear and angular rates;
- to introduce the procedure of signal processing and filtering;
- to estimate the hydrodynamic coefficients of the proposed mathematical model using SI algorithm; and
- to verify the developed 4DOF mathematical model by comparing the simulated responses and actual ones.

This paper is organized as follows: the 4 DOF nonlinear mathematical model is presented in the 2nd section, followed by the introduction of the scaled model and free running tests. The 4th section introduces the method of data acquisition and processing. In the following section, SI algorithm is applied to identify the hydrodynamic coefficients and the accuracy of the mathematical is validated. Conclusions are drawn in the last section.

4.2 Equation of Ship's Motion

Generally, to describe a surface ship's motions, a body-fixed frame and inertial frame as shown in Fig. 4. 1 are used. The 4 DOF non-dimensional model of ship's motion based on Newton-Euler formulation can be represented as:

$$X'_H = (m' + m'_x)\dot{u}' - (m' + m'_y)v'r' - X'_P - X'_R \quad (4.1)$$

$$Y'_H = (m' + m'_y)\dot{v}' + (\mathrm{m}' + m'_x)u'r' + m'_y\alpha'_y\dot{\mathrm{r}}' - m'_y l'_y\dot{\mathrm{p}}' + Y'_R \quad (4.2)$$

$$K_H{}' = (I'_x + J'_x)\dot{p}' - m'_y l'_y\dot{v}' - m'_x l'_x u'r' + W'GM'\varphi' + + K'_R \quad (4.3)$$

$$N_H{}' = (I_z' + J_z')\dot{r}' + m_y'\alpha_y'\dot{v} + Y'x_G' - N_R' \quad (4.4)$$

where the items with H subscript are the hydrodynamic forces and moments; the items with R subscript are the rudder forces and moments; X_P' is the drag force in surge dimensional; m', m_x' and m_y' are the mass and added masses of vessel respectively; I_x' and I_z' are the inertia moments of roll and yaw; J_x' and J_z' are the added inertia moments in the x-z axes; u and v are surge and sway velocity; r and p are roll and yaw displacement. More details can be found in (Nomoto, 1972).

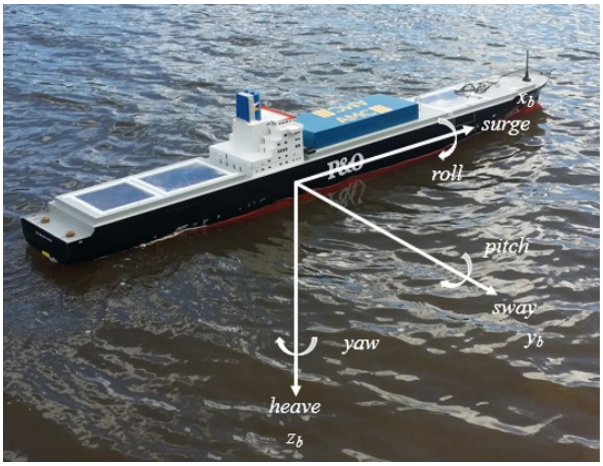

Fig. 4. 1 Body-fixed frame and inertial frame for surface vessel

The hydrodynamic forces and moments can be represented as the function of kinematic items and corresponding hydrodynamic coefficients as (Fossen, 1994a):

$$\begin{bmatrix} X_H \\ Y_H \\ K_H \\ N_H \end{bmatrix} = [\Phi_X \quad \Phi_Y \quad \Phi_K \quad \Phi_N] \begin{bmatrix} Para_X \\ Para_Y \\ Para_K \\ Para_N \end{bmatrix} \quad (4.5)$$

where Φ with four subscripts are matrices composed by kinematic items u, v, p, r,φ and ϕ; $Para$ with four subscripts are the matrices of relevant hydrodynamic coefficients, in this paper the 3rd order system was employed.

4.3 Free Running Model Tests

4.3.1Free Running Model

The physical model utilised in this study is a 1：100 scaled model of ‘P&O Nedlloyd Hoorn’.

The main characters of the vessel and scaled model are outlined in Table 4. 1.

Table 4. 1 Main Characters of Motor Vessel Hoorn and the Scale Model

Items	Values	
	Vessel	**Scale Model**
Length between perpendiculars (L_{pp})	247 m	2470 mm
Breadth (B)	32 m	320 mm
Draft (D)	12 m	120 mm
Mass (Δ)	64000 Tonnes	63.4 kg
Metacentric height (GM)	0.875 m	8.75 mm

The scaled model was equipped with the following five sub-systems: power supply system, the sensors, the propeller and manoeuvring system, embedded computer myRIO containing real-time I/O platform and the host PC with LabVIEW installed. The layout of the configuration is shown in Fig. 4. 2.

Fig. 4. 2 The configuration of the free running model Hoorn

4.3.2 Free Running Tests

The free running tests were carried out in a lake in Tasmania. The experiments were standard manoeuvring tests: the rudder angle was set to $10°, 20°, 30°$ for portside and starboard turning circle tests, and $-20°/20°$ for zig-zag tests. The proposed tests can be seen in Fig. 4. 3.

Fig. 4. 3 $20°$ starboard turning circle of Hoorn in Trevallyn Lake

4.4 Signal Acquisition and Processing

The proposed maneuvering experiments aimed to measure the data from the inertial measurement unit (IMU) and GPS sensors. The measured data from corresponding sensors are outlined in Table 4. 2.

Table 4. 2 Employed Sensors and Corresponding Measured Data

Sensors	Chip	Measurements
Digital compass	HMC5883L	Yaw angle
Accelerometer	ADXL345	Linear rate
Gyroscope	L3G4200D	Yaw rate, Roll rate
GPS	MTK3339	Position, Speed

Generally, the data collected from the low-cost sensor cannot be used directly without calibration as the measurement will be subjected to coloured noise and distortion. This section will introduce the methods of signal processing for the following estimation of hydrodynamic coefficients.

4.4.1 Data Acquisition, Calibration and Conversion

In order to get accurate yaw angle from the digital compass, calibration is needed to compensate the declination and magnetic distortions existed in raw data.

Magnetic declination is the angle between magnetic north and true north. Referring to the position of the experiment, the magnetic declination can be got as $\varphi_{declination} = 0.2467\, rad$. In addition, the magnetic distortions, which include hard iron distortions and the soft iron distortions, need to be eliminated. The hard iron distortions are generated by the change of magnetic fields around the sensor (such as electronic devices and wires) and the measurement offsets, while the soft iron distortions are produced by the existing ferromagnetic materials around the sensor. By introducing a vector of bias and a corresponding transformation matrix, the magnetometer data in least significant bit (LSB) by default can be calibrated as:

$$D_c = M \times (D_{nc} - B) \tag{4.6}$$

where $D_c = [x_c \;\; y_c \;\; z_c]$ are the calibrated magnetometer data, D_{nc} is the non-calibrated magnetometer data, the transformation matrix is calculated as M, the bias vector is calculated

as B.

Based on the above-mentioned calibration, the heading angle can be calculated as follows:

$$\varphi = \arctan\left(\frac{y_c}{x_c}\right) + \varphi_{declination} \tag{4.7}$$

As the gyroscope gives data in LSB by default as well, in order to get the yaw rate and roll rate, the data need to be converted into the data in degree per second (*dps*) by multiplying the value calculated by the following equation:

$$dps = \frac{R}{2^N} \tag{4.8}$$

where R is the full range of the chip and N is the value of bit-rate.

In order to convert the GPS data into relative displacement in meters, the distance (in meters) per degree of longitude and latitude in the experiments area need to be used in this conversion.

4.4.2 Data Filtering Using Kalman Filter

The Kalman filter has demonstrated its excellent capability in many engineering applications. It is widely utilised across many areas as it is capable of estimating the states of a system. Its working principle can be stated as taking the observation of the current states and using the previous calculations to estimate the most likely current states. The other advantage of Kalman filter is that it is capable of combining data from different sensors to do the estimation.

In this study, as several low-cost IMU sensors were employed, the Kalman filters were developed by using two kinds of observations for state estimation. Due to space constraints, the filtering of roll angle by using gyroscope and accelerometer data is demonstrated in this paper.

Filtering method: execution of roll angle filtering:

- Predict states

  $$\hat{\phi}_t^- = \hat{\phi}_{t-1} + \Delta t \times \omega_x$$

  where $\hat{\phi}_t^-$ is the predicted roll angle, $\hat{\phi}_{t-1}$ is the previous roll angle, Δt is the time interval, ω_x is the roll rate measured by the gyroscope.
- Predict estimate covariance

$$P_t^- = P_{t-1} + Q$$

where P_t^- is the predicted error covariance, Q is the covariance of the process noise.

- Calculate observation data

$$z_\phi = \arctan(ax/az)$$

where z_ϕ is the observed roll angle calculated by the data from the accelerometer, ax and az are the x-axis and z-axis data from the accelerometer respectively.

- Calculate Kalman gain

$$K_\phi = \frac{P_t^-}{P_t^- + R}$$

where K_ϕ is the Kalman gain, R is the covariance of observation noise.

- Update state estimate

$$\hat{\phi}_t = \hat{\phi}_t^- + K_\phi \times (z_\phi - \hat{\phi}_t^-)$$

where $\hat{\phi}_t$ is the estimated roll angle.

- Update estimate covariance

$$P_t = (1 - K_\phi)P_t^-$$

where P_t is the updated covariance which can be used for the next step.

After the signal processing and data filtering, it is available to get the smoothed and continuous values of displacement, angle and angle rate, which can be used to describe the motion states of the free running model.

4.5 System Identification and Modelling

In this section, the recursive least square (RLS) based system identification method was implemented to identify the hydrodynamic coefficients. Based on the estimated parameters, the mathematical model of the proposed model was developed and validated.

4.5.1 System Identification

RLS is an adaptive filtering method for parameter estimation in a deterministic system. It is an online implementation of the least square method and the basic idea is to minimize the cost function, more details can be found in (Nguyen, 2008, Nguyen, 2000). The advantage of the RLS algorithm is that it provides the history of identification, thus the adaptive of the system can be analyzed.

For the equation *(4.5)*, it can be written into four equations in the form of $\Theta = \Phi\theta$. In this

equation, Θ is the value of estimated force or moment, Φ is the vector containing speed and acceleration products, θ is the vector of hydrodynamic derivatives. Once the structure of the mathematical model is determined in advance, the RLS algorithm can be used to estimate the coefficients, the procedure of using RLS based SI algorithm for hydrodynamic coefficients estimation is presented in Fig. 4. 4.

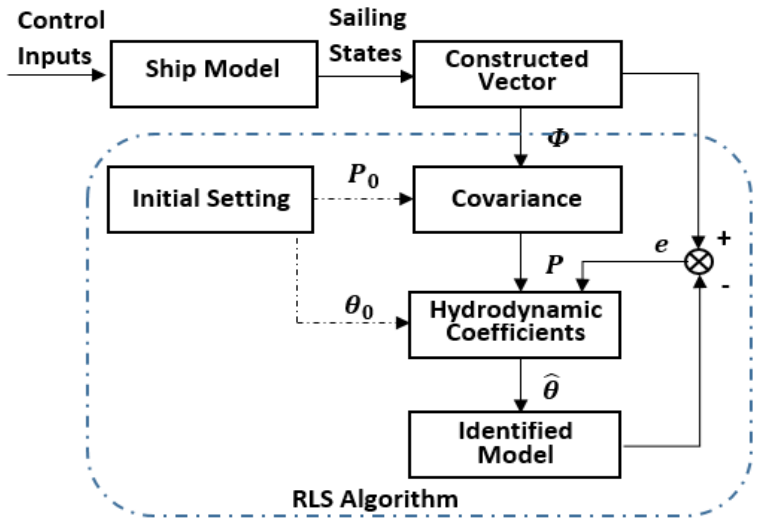

Fig. 4. 4 The RLS based system identification for ship

The data used for hydrodynamic coefficients estimation was measured from 20° starboard turning circle with sample time at 0.1 seconds. By using the above-mentioned identification algorithm, the hydrodynamic derivatives in the degree of surge, sway, yaw and roll were estimated, see in Table 4.3.

Table 4. 3 Hydrodynamic Coefficients of The Free Running Model in the Degree of Surge, Sway, Yaw and Roll

Surge	Sway	Roll	Yaw
$X_{uu}' = -0.0024$	$Y_v' = -0.0549$	$K_v' = 0.00089$	$N_v' = -0.0095$
$X_{vr}' = -0.0024$	$Y_r' = -0.00129$	$K_r' = 0.00013$	$N_r' = -0.0046$
$X_{vv}' = 0.0149$	$Y_{vvv}' = 0.02394$	$K_p' = 0.00006$	$N_r' = -0.00008$
$X_{rr}' = 0.0207$	$Y_{vvr}' = -0.242$	$K_{vvv}' = -0.0264$	$N_{vvv}' = 0.0034$
$X_{\phi\phi}' = 0.0166$	$Y_{vrr}' = -0.1299$	$K_{vvr}' = -0.008$	$N_{rrr}' = 0.0017$
	$Y_{vv\phi}' = -0.0148$	$K_{vrr}' = 0.0096$	$N_{vvr}' = -0.0216$
		$K_{vv\phi}' = -0.0103$	$N_{vrr}' = 0.0011$
		$K_{rr\phi}' = -0.00159$	$N_{vv\phi}' = -0.0191$
			$N_{v\phi\phi}' = -0.0058$
			$N_{rr\phi}' = -0.0033$

Surge	Sway	Roll	Yaw
			$N'_{r\phi\phi} = 0.0024$

4.5.2 Modelling of the Scaled Model

In order to validate the estimated hydrodynamic coefficients, the mathematical model which contains steering and manoeuvring characteristics were developed. The S-function was utilised to describe the ordinary differential equations of the model scaled ship. The time history of vessel's motion was solved by the Bogacki-Shampine method.

The simulation trajectory and roll angle of the proposed mathematical model were compared with the experimental data, as shown in Fig. 4. 5, Fig. 4. 6 and Fig. 4. 7. It is indicated that the simulated values are in good agreement with the measurements. As shown in Fig. 7, the differences of yaw rate at the beginning is affected by the uncontrollable instantaneous wind in the experiment lake. Considering the high agreement of the final value in the following time, the difference is acceptable.

According to the comparison, it can be regarded that the estimated hydrodynamic coefficients and the developed mathematical model can properly describe ship's motions.

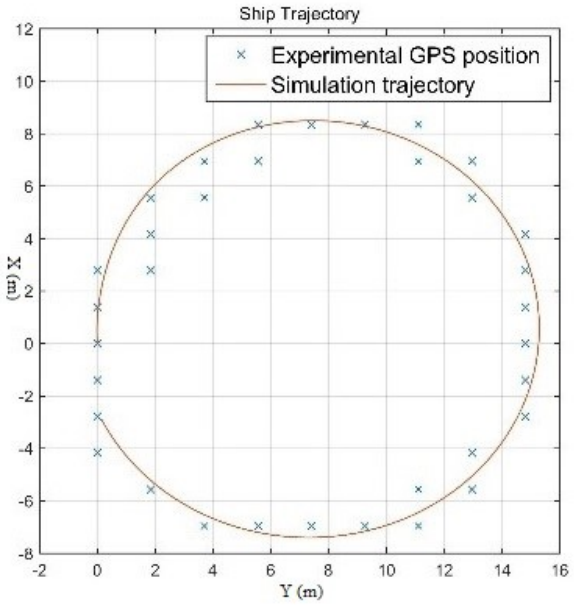

Fig. 4. 5 Comparison of the simulated trajectory and GPS measurements

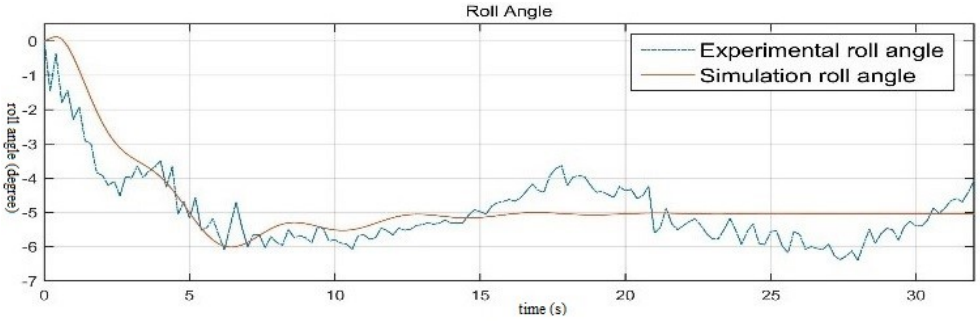

Fig. 4. 6 *Comparison of the simulated and observed roll angle*

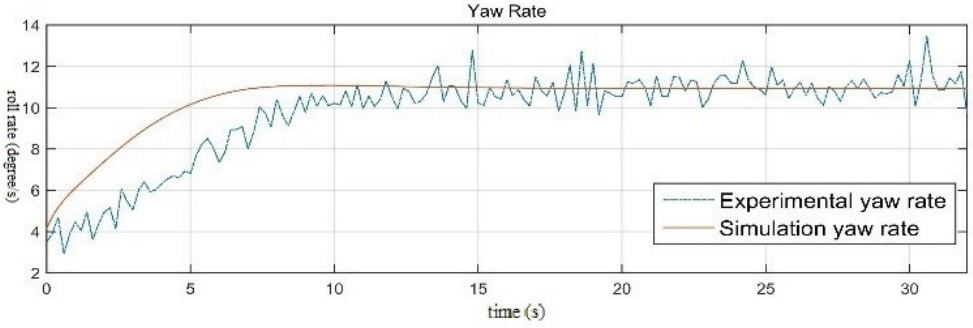

Fig. 4. 7 Comparison of the simulated and observed yaw rate

4.6 Conclusion

In this study, the hydrodynamic coefficients of a 4 DOF mathematical model have been estimated through using experiment data measured from turning circle manoeuvring tests. The

free running test was conducted by using the myRIO as the embedded computer and DAQ to measure IMU and GPS data from low cost sensors. The corresponding raw data were processed and filtered to get the smooth and continuous data. The system identification was conducted with a RLS method to get the hydrodynamic derivatives, which have been validated by the comparison between experimental data and simulation data.

It is shown that the proposed devices and method are capable of identifying the hydrodynamic coefficients and developing a mathematical model. The agreement between the experimental and simulated responses has shown that the mathematical model with estimated hydrodynamic coefficients can describe manoeuvring characteristics properly.

For the future work, captive experiments will be conducted to verify the estimated coefficients. Besides, other advanced filtering algorithms will be employed to improve the accuracy of the data processing.

Chapter 5

Experimental Studies of KFV RBFNN Based Autopilot

Based on the developed physical model 'Hoorn' in **Chapter 4**, this chapter experimentally investigates the capabilities of the control algorithm developed in **Chapter 3** to manoeuvre the ship. By using the proposed online data processing method (observer), experiments were conducted in a lake. It is worth noting that both the experimental and simulation tests were conducted with the similar environment conditions, thus the control performance of each control system can be analysed accordingly. The findings in this chapter answer the fourth research question presented in **Chapter 1**.

Part A: This subchapter has been submitted for publication in 'ISA Transactions'. The citation for the research article is:

Wang, Y., Nguyen, H. D., Chai, S., & Khan, F. (2017). *Experimental and Numerical Study of Autopilot Using Extended Kalman Filter Trained Neural Networks for Surface Vessels*. ISA Transactions.

Part B: This subchapter has been submitted for publication in 'Applied Ocean Research'. The citation for the research article is:

Wang, Y., Nguyen, H. D., Chai, S., & Khan, F. (2017). *Unscented Kalman Filter Trained Neural Network Control Design for Ship Autopilot with Experimental and Numerical Approaches*. Applied Ocean Research.

Chapter5 - Part A. Experimental Studies of EKF RBFNN Based Autopilot

Abstract of Chapter 5A: Due to the characteristics of nonlinearity and unpredictable environmental dynamics, the design of ship's steering controller is a challenge. The purpose of this study is to design an intelligent autopilot based on Radial Basis Function Neural Network (RBFNN) control algorithm only use rudder as the control actuator. The introduction of the Extended Kalman Filter (EKF) training algorithm enables a neural network based autopilot to counteract the uncertain effects of both environmental disturbances and sailing states measurements. The newly developed free running model scaled surface vessel utilising myRIO as the embedded computer and Data acquisition (DAQ) card was presented. After the implementation of signal processing and filtering, the performances of course keeping, course changing and path tracking were investigated by conducting experiments using the physical model on Lake and simulations using the corresponding mathematical model. The results demonstrated that the developed autopilot was feasible to be used for the ship's motion control in the presences of environmental disturbances. Moreover, in comparison with the Back-Propagation (BP) networks and Proportional-Derivative (PD) based control methods, the EKF RBFNN based control method showed better performance regarding course keeping and path tracking for sailing ships.

5A.1 Introduction

For the seagoing vessels, the autopilot is widely utilised in various aspects and circumstances. The adoption of autopilot is of vital importance in reducing operating costs and human risks as it is helpful to release officer duty on the bridge to other works. Moreover, the feasible autopilot would enhance the vehicle's motion control reliability, especially for the ship sailing in constrained waters like straits, coastal waters, and area of traffic separation scheme. It is also essential for the ship to increase the capability in accomplishing special tasks and conducting special operations like placing cables and delivering supplies to vessels at sea. In addition, the developing of multitasking autopilot will speed up the applications of unmanned ship to perform exploration, survey, monitoring and data collection tasks.

Considering the reliability and simplification of the conventional proportional-integrative-derivative (PID) controller, it has been extensively employed in designing autopilot. However,

the control performance varies with loading conditions and sailing uncertainties, including both of the external disturbances and measurements. Generally, the PID approaches rely on gain scheduling method to overcome the unpredictable behaviours in the process control (Tannuri et al., 2010). Nevertheless, when the ship encounters complicated environmental disturbances, the control performance of the PID autopilot will be obviously affected. Therefore, the autopilot needed to be switched to Manual mode when sailing in severe seas.

It is known that the adaptive control is more suitable to achieve better control performance and disturbance rejection. Some control algorithms, such as linear quadratic Gaussian control (Miller, 1973), optimal feedback control (Parsons and Cuong, 1980) and stochastic control (Rios-Neto and da Cruz, 1985) have been employed to stabilise the system and provide necessary robustness. However, it is indicated that the structure of these control methods are complex and the application requires a huge number of prior information (Unar and DavidJ, 1999). In recent decades, due to the development of the modern control theory, various control strategies, including H-infinite algorithm (Morawski and Pomirski, 1998), genetic algorithm (McGookin et al., 2000), cascade control (Lefeber et al., 2003), back-stepping control (Skjetne et al., 2005, Yi and Zhang, 2016), and fuzzy logic control (Rigatos and Tzafestas, 2006) have been carried out to enhance the ship's automatic steering capability. Despite the benefits of the above mentioned control strategies are attractive, some disadvantages are needed to be addressed, such as the time consumption of generation propagation, the unexpected tracking error generated from the previous error conditions, and the difficulties in formulating the fuzzy control rules based on trial-and-error based human knowledge (Sun et al., 2014).

Prompted by the development of the computing technology, the neural network based control became applicable in engineering practice without known complete prior information. Owing to the satisfactory capability in approximating, neural networks control algorithms have also been introduced to design the autopilot (Unar and DavidJ, 1999, Wu et al., 2012, Dai et al., 2012, Leonessa et al., 2006, Wang and Er, 2015). In comparison with some multilayer feed-forward neural networks, it is found that the RBFNN is feasible in approximating unknown functions (Park and Sandberg, 1991). Also, the RBFNN has simple architecture and good generalisation capability, which is beneficial to avoid unnecessary and lengthy calculation (Liu, 2013). Thus, this architecture was employed in this study.

The training algorithm is essential in constructing the proposed neural network controller for ship's automatic steering. Generally, besides the extensively utilised BP training algorithm

(Duro and Reyes, 1999), other corresponding methods such as fully supervised gradient descent (Karayiannis, 1999) and back-stepping (Yahui et al., 2004) have been widely used to train artificial neural networks. Although some of these algorithms have been proved to be effective, some drawbacks, including the possibilities of converging to local minima as well as the slow converging speed, are needed to be addressed.

From another point of view, the process of neural networks training can be considered as a parameter estimation problem. The Kalman Filter (KF) or its variant is an alternative with the capability in providing an online approach to estimate the states of the networks (Sanchez et al., 2008). Among them, the EKF algorithms for training neural networks can provide an online mechanism in which the parameters can be updated immediately (Simon, 2002). Contrary to some other higher-order training methods, the EKF based training algorithms for networks do not require batch processing, making it more suitable for online usage. It is indicated that the converge speed is improved and the number of tuning parameters is decreased when the EKF training algorithm is applied to train proposed neural networks (Haykin, 2001).

The main objectives of this study are

- to propose the EKF RBFNN based autopilot which is responsible for calculating the rudder angle to control the surface vessel;
- to introduce the configuration and signal processing method of a newly developed free running model scaled vessel constructed by the platform named myRIO;
- to conduct the experimental and numerical validation of the proposed autopilot based upon the scaled model; and
- to analyses the control performance of the developed autopilot through the comparison with that of BP RBFNN and PD based systems.

The paper is organised as follows: the section 2 briefly introduces the model of the process including ship motion equations as well as the numerical model of waves acting on the ship. The design of EKF RBFNN based autopilot is presented in section 3 with regard to the ship's course keeping and path tracking. The experiment setup and signal processing method are expressed in the following two sections. Subsequently, experimental and numerical validations are presented to validate the feasibility of the proposed controller. Finally, the corresponding conclusions are drawn in the last section.

5A.2. Dynamic Model of Ship Motions

In this section, the ship's motion formulations and the numerical model of waves are briefly introduced. The states of the model contain two components: kinetic states and the kinematic states defined in body-fixed coordinates and earth-fixed coordinate. The relevant items can be seen in Fig. 5A. 1.

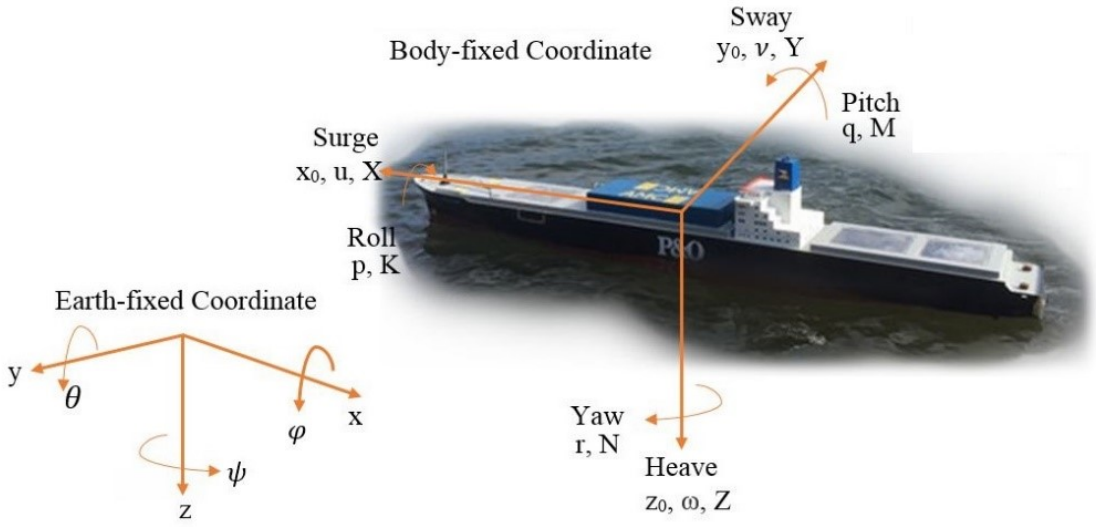

Fig. 5A. 1 The Body-fixed Coordinate and Earth-fixed Coordinate of the surface vessel

Derived from Newton-Euler's law, dynamic model of ship motions in six degrees of freedom (DOF) can be expressed as (Fossen, 1994b):

$$M\dot{\nu} + C(\nu)\nu + D(\nu)\nu + g(\eta) = \tau + \tau_E \qquad (5A.1)$$

where $\nu = (u, v, w, p, q, r)^T$ is the velocity items of the ship's translated and rotation motion, including surge, sway, heave velocity, and roll, pitch, yaw speed; M the inertia matrix; $C(\nu)$ the matrix of Coriolis and centripetal terms containing the added mass; D the matrix of damping terms; $g(\eta)$ the vector of restoring forces and moments arisen from gravity and buoyancy and η ship's position and orientation; τ the vector of control inputs; τ_E represents the vector of environment forces and moments. Generally, the motions of pitch and heave could be disregarded for the surface vessels, because these items are not commonly being utilised in practice rather than the motions of surge, sway, yaw and roll. Thus the nonlinear four DOF non-dimensional model is sufficient to describe the dynamic motions of the surface vessel (Son and Nomoto, 1982).

To describe waves disturbance acting on the ship, the modified Pierson-Moskowitz (PM) wave spectrum model recommended by ITTC and outlined in Perez (2006) can be utilised as:

$$G(S) = h(S) \times W_h = \frac{2\xi w_e \delta_w S}{S^2 + 2\xi w_e S + {w_e}^2} \times W_h;\ w_e = w_0 - \frac{{w_0}^2}{g} U cos\beta \qquad (5A.2)$$

where w_0 is the wa frequency, w_e the encounter wave frequency with speed at U and encounter angle β, ξ the damping coefficient, δ_w the wave intensity, and W_h a zero-mean Gaussian white noise process for generating the transfer function. According to the research of Sgobbo and Parsons (1999b), the forces and moments generated by waves can be inserted into the right hands of the motion equations to express the nonlinear environmental disturbances.

5A.3. EKF Trained RBFNN Autopilot Design

The main advantage of utilising neural networks for controller design is not necessary to know the accurate mathematical model of the plant in practical applications, even in the presence of undesired uncertainties. In this study, the proposed RBFNN (shown in Fig. 3A. 1) is employed in addressing the vessel's complicated

For the ship advancing with external disturbance, the EKF RBFNN based autopilot can be developed to achieve the function of course keeping and path tracking. The architecture of the system is illustrated in Fig. 5A. 2. It is indicated that the desired angle ψ_d and the actual yaw angle ψ are adopted to build the input matrix of RBFNN based controller. Specifically, when the system is switched to the Course Keeping Loop, the constant desired angle for course keeping is utilised directly; on the other side, when the system is switched to the Path tracking Loop, the dynamic desired angle will be calculated by the Enclosure-Based-Steering Line-of-Sight (EBS LOS) guidance method incorporated with actual position and pre-set waypoints. Subsequently, the input matrix will be transited to the following controller to get the control law for rudder, which is used to make the ship sailing based on the desired requirements.

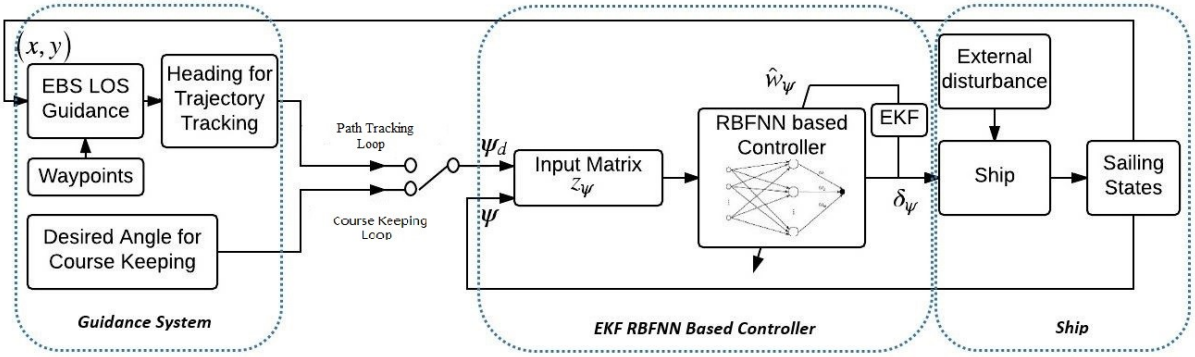

Fig. 5A. 2 Illustration of the Guidance System and EKF-RBFNN based control system for ship with external disturbance

The output of the course keeping controller has the following forms:

$$\delta_\psi = \hat{U}_\psi(z_\psi) = \frac{1}{\beta}\sum_{i=1}^{m} \hat{w}_{\psi(EKF)}^T h(z_\psi)$$

$$= \frac{1}{\beta}[\hat{w}_{\psi 1(EKF)} h_1(z_\psi) + \hat{w}_{\psi 2(EKF)} h_2(z_\psi) + \cdots + \hat{w}_{\psi m(EKF)} h_m(z_\psi)] \qquad (5A.3)$$

where z_ψ denotes the input matrix of the RBFNN based controller, β is the limitation item of control output to constraint the command rudder angle,m is the total number of neuron nodes in the hidden layer, $\hat{w}_{\psi(EKF)}$ is the estimated weights updated by the EKF algorithm, which can be seen in Table 5A. 1:

Table 5A. 1 Implementation of the EKF estimation algorithm to neural networks training

Initialization	
Initialize with:	$\hat{w}_0 = E[w_0], P_0 = E[(w_0 - \hat{w}_0)(w_0 - \hat{w}_0)^T]$, observation and process noise covariance R, Q

Executing and estimating recursively

Prediction transformation

Weights Predicted: $\widehat{w}_{k|k-1} = f(\widehat{w}_{k-1})$

Jacobin Matrices 1: $F_{k-1} = \partial f / \partial \widehat{w}_{k-1}$

Covariance of predicted weights: $P_{k|k-1} = F_{k-1} P_{k-1} {F_{k-1}}^T$

Observation transformation:

Jacobin Matrices 2: $H_k = (h_m)_k$

Covariance of measurement: $P_k^1 = H_k P_{k|k-1} {H_k}^T + R$

$P_k^2 = P_{k|k-1} {H_k}^T$

Extended Kalman Filter calculation and update functions

$K_k = P_k^2 / P_k^1$

$\widehat{w}_k = \widehat{w}_{k|k-1} + K_k s$

$P_{k+1} = P_{k|k-1} - K_k {H_k}^T P_k + Q$

where K_k represents Kalman gain matrix for weights training, P_k is the approximate error covariance matrix, $\widehat{w}_k$ is the estimation weights, H_k is the Jacobian matrix which is derived from the partial derivatives of the output of the system in relation to the weights, R and Q are the observation noise and artificial process noise which is beneficial to avoid numerical divergence, s is the augmented error containing the errors and relevant derivatives.

As mentioned formerly, the purpose of the controller in both situations is to change the heading of the vessel by changing the deflection of the rudder, because the path tracking relies on the dynamic reference heading which is generated by the EBS LOS guidance algorithm. This method can be realised by introducing a virtual circle with radius R, which normally equals to 2 times or 3 times of ship's length (Alfi et al., 2015), encloses the vessel when it sails between two pre-set waypoints $p_k(x_k, y_k)$ and $p_{k+1}(x_{k+1}, y_{k+1})$. The intersection nearby the waypoint p_{k+1} represents the LOS point, see Fig. 3A. 4. Thus the ship's dynamic desired course angle x_d can be calculated by using the LOS point $p_{LOS}(x_{los}, y_{los})$:

$$x_d = tan^{-1}\left(\frac{y_{los} - y}{x_{los} - x}\right) \qquad (5A.4)$$

Moreover, the deviation between the ship's dynamic position and the planned track can be obtained by the following equation (Wang et al., 2017a):

$$E_0 = (y - y_k)cos(\alpha_k) - (x - x_k)sin(\alpha_k) \quad (5A.5)$$

where E_0 represents the tracking error, α_k represents the angle of the pre-set trajectory. more details can be seen in **Chapter 3A.3**

To evaluate the capability of the control system further, the cost functions of yaw error C_{Yaw}, rudder deflection C_{Rudder} were employed in this study as follows (Burns, 1995):

$$C_{Yaw} = \sum_{i=0}^{N}(\Delta\psi_i)^2; C_{Rudder} = \sum_{i=0}^{N}\delta_i^2 \quad (5A.6)$$

where N is the total amount of the iterations, $\Delta\psi_i$ and δ represent the yaw angle error and rudder deflection of the ith iteration respectively.

5A.4. Free Running Model and Signal Processing Methods

In this study, the experimental tests were implemented by using a physical scaled model of a container ship on the Trevallyn Lake in Launceston (Tasmania, Australia). The model scaled vessel is a replica of the 'M/V Nedlloyd Hoorn' and it was built on the 1:100 scale, see in Fig. 5A. 1. The hydrodynamic design and loading condition follows the properties of the full scale ship in fully loaded conditions, the main characteristics of the model scaled ship can be seen in Table 4. 1. Thus, the geometric, kinetic and dynamic similarity principles were preserved. Furthermore, it is needed to be mentioned that the results of experiments can be recalculated to refer to real objects using the known relations (Morawski and Pomirski, 1998). In this section, the details of Hoorn are described, focusing on its system configurations and the signal processing algorithms.

5A.4.1 Configurations of Hoorn

The mechanical and electronic facilities of the ship were newly updated in the Control Lab of Australian Maritime College in 2016. The configurations of the physical model are shown in Fig. 5A. 3 with the following five sub-systems:

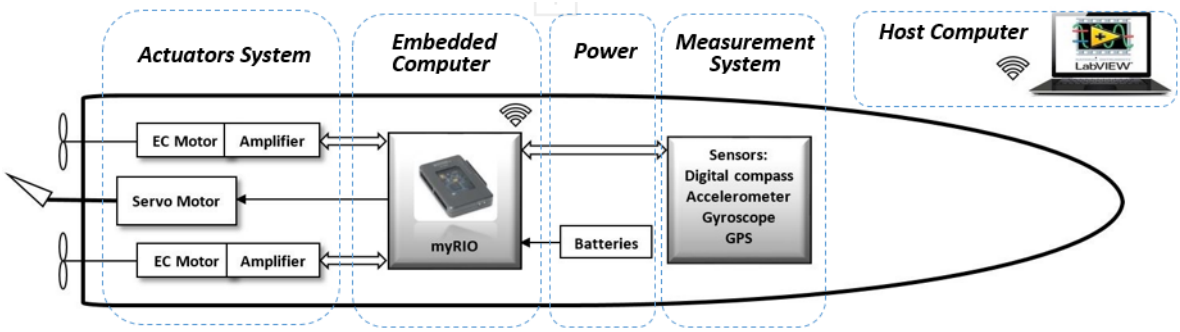

Fig. 5A. 3 The configuration of the free running model Hoorn

1). Power supply system: 6 lead acid batteries were being carried on the ship to provide power at 36V to the electronic devices and actuators including propellers and rudder. 2). Actuators system: Twin propellers were driven by two independent brushless direct current (BLDC) motors controlled by two sets of ESCON 50/5 amplifiers. The deflection of the rudder was determined by a medium speed servo motor driven by the pulse signal. 3). Embedded computer platform: The device named myRIO was utilised as the embedded computer and real-time (RT) I/O platform. The myRIO features a 667 MHz dual-core programmable processor and a customizable Xilinx programmable gate array (FPGA), incorporating with onboard memory and built-in Wi-Fi module, to allow the users to deploy applications remotely and run them in use of LabVIEW. Various data acquisition card ports were used to support the connection of SPI, PWM and I^2C. 4). Measurement system: The measurements were accomplished by using the low-cost sensors. The measured data would be transmitted and logged in myRIO to reflect the sailing states. 5) Host computer: Host computer installing the software LabVIEW was used to control the model, and deploy the control algorithm and signal processing methods remotely.

5A.4.2. Online Signal Processing and Data Filtering

As usual, the measurements collected from low-cost sensors cannot be utilised directly before implementing calibration, as these measurements are easily subjected to the effects of distortion, declination and coloured noises. Thus, the signal processing and data filtering are required before the execution of control experiments.

As a magnetometer module, the employed digital compass is needed to do the calibration to compensate the declination and magnetic distortions by using the following equation (Fang et al., 2011):

$$\psi = arctan\left(\frac{y_c}{x_c}\right) + \psi_{declination} \quad (5A.7)$$

where ψ is the calibrated yaw angle, x_c and y_c are the calibrated least significant bit (LSB) magnetometer data from the digital compass, and the $\psi_{declination}$ is the magnetic declination. Besides, the signal conditioning also includes conversion of default LSB data to the data in the unit of degree per second. A practical description of the signal processing method for low-cost sensors can be seen in **Chapter 4.4**.

For the proposed control system, the reliability and stability of the measured yaw angle are essential to the corresponding performance. In order to deal with the uncertainties and high-frequency coloured noise in the measurements, the KF was developed for states estimation by using two kinds of observations from digital compass and gyroscope. Previous tests indicated that the proposed conventional KF is sufficient to estimate the yaw angle as its inherent change is at low frequency. The working principle can be presented as considering the current observation and using the previous states to optimise the most likely current states. The details can be seen in Table 5A. 2:

Filtering method: execution of yaw angle filtering:

Table 5A. 2 Implementation of the KF estimation algorithm to yaw angle filtering

Predict states	$\hat{\psi}_t^- = \hat{\psi}_{t-1} + \Delta t \times r_z$	$\hat{\psi}_t^-$ is the predicted yaw angle, $\hat{\psi}_{t-1}$ is the yaw angle in the last interval, Δt is the time interval, r_z is the yaw rate measured from the gyroscope.
Predict covariance	$P_t^- = P_{t-1} + Q'$	P_t^- is the predicted error covariance, Q' is the covariance of the process noise.
Kalman gain	$K_\psi = \frac{P_t^-}{P_t^- + R'}$	K_ψ is the Kalman gain, R' is the covariance of observation noise.
Update estimate	$\hat{\psi}_t = \hat{\psi}_t^- + K_\psi \times (z_\psi - \hat{\psi}_t^-)$	$\hat{\psi}_t$ is the estimated yaw angle.
Update covariance	$P_t = (1 - K_\psi)P_t^-$	P_t is the updated covariance for the next step.

In use of the developed signal conditioning and data filtering methods, the smoothed and reliable values of angle and angle rate were available for the following control applications.

5A.6. Experiment Results and Discussion

During the experiments, the model scaled vessel was fully loaded and its average speed was about 0.7 m/s. The approximate direction of the wind generated waves was approximately at 45 $degrees$, the speed of the south-west wind did not exceed 4 m/s, but the occasional wind was strong around the Trevallyn Lake. The experiment program was developed by using LabVIEW and communicated between onboard myRIO and host computer onshore. The proposed control algorithm was written in M-language in use of the Mathscript Node Module. The control law for rudder alternation was constrained within ± 15 $degrees$ and the maximum gradient was limited within ± 10 $degree/s$ to match the configuration of the servo motor. Once the program was deployed into the myRIO, the signal processing would work with the sampling rate at 10 Hz and the control algorithm would also work in the loop with interval time at *0.1 seconds*. The methods of online signal processing were programmed in an independent Mathscript to estimate the actual sailing states. Because the insufficient accuracy of the low-cost GPS data, only the course keeping experimental tests were reported in this study.

The adopted courses are straight lines to guide the ship sailing forward, so the direction of the ship will stabilise on the corresponding yaw angle, which is expressed by the rotation around Z axis in Fig. 5A. 1. To validate the control performance of the proposed autopilot, two experiment scenarios with different course at 225° and 255° were implemented (see in Fig. 5A. 4), thus the wave/current encounter angles for the two case studies were 180° and 150° respectively. The parameters of the EKF training algorithm were set at $R = 1, Q = 0.1$, and $\beta = 50$ was adopted in the RBFNN based controller to constrain the rudder angle in acceptable range. In order to verify the performance of the proposed control system, the BP RBFNN based controller developed in Wang et al. (2015) was employed for comparison.

Fig. 5A. 4 Experiment under the control of EKF RBFNN

The performance of the proposed control systems was demonstrated by the results of the experiments reported in Fig. 5A. 5 and Fig. 5A. 6. The cost values calculated by the equation *(5A. 6)* about yaw error and rudder actions, as well as the corresponding maximum absolute values, are outlined in the Table 5A. 3. It is worth noting that the remote control range was limited due to the WIFI range at 100 meters, thus experiment results in 100 seconds were reported. The results indicated that both control algorithms have successfully made the model scaled vessel advancing on the desired course. In more detail, the experiment of EKF RBFNN based control with the desired course at 225° was firstly conducted, resulting in converging to the desired course smoothly. On the other hand, the BP RBFNN based algorithm and PD based algorithm also controlled the ship sailing on the preferred course, but there existed the deviations at about 0.71° and 0.97°. Moreover, the EKF RBFNN based controller has lower rudder action cost in comparison with the BP RBFNN and PD based one, which has been corroborated by the values of rudder action costs. The second set of experiments with desired course angle at 255° were conducted nearby the cape with larger external disturbances. Thus the capability of the controller in counteracting heavier disturbances was verified. It is indicated that, during the sailing process adopting EKF RBFNN based controller, the deviation from the desired course did not exceed 0.5°, which was smaller than that of the BP RBFNN and PD based controller. Although the heavier external disturbance resulted in large rudder actions to compensate the effects, the rudder actions of using EKF RBFNN autopilot was smaller than that of the BP RBFNN and PD autopilot. According to the above-mentioned discussion, the EKF RBFNN based controller was demonstrated to be more capable of getting higher control accuracy and coping with the nonlinear disturbances with more efficient rudder actions.

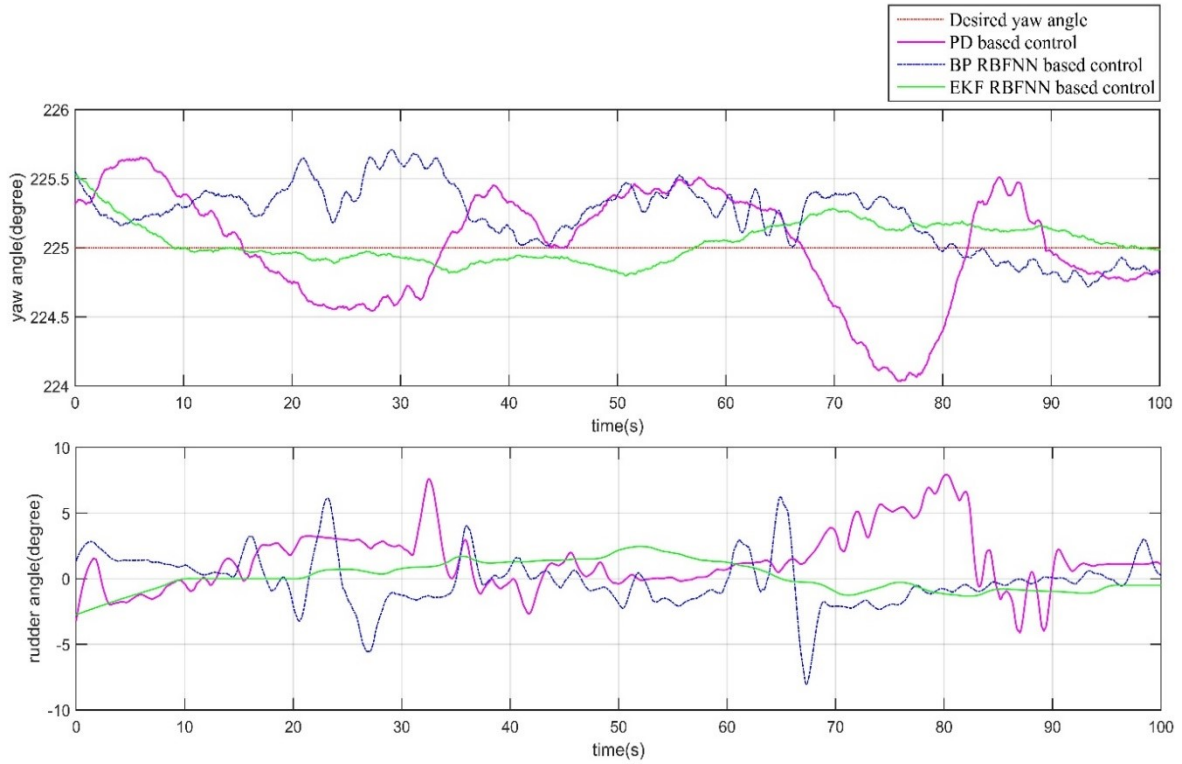

Fig. 5A. 5 Yaw angle and rudder action under the PD, BP RBFNN and EKF RBFNN based control with desired course at 225°

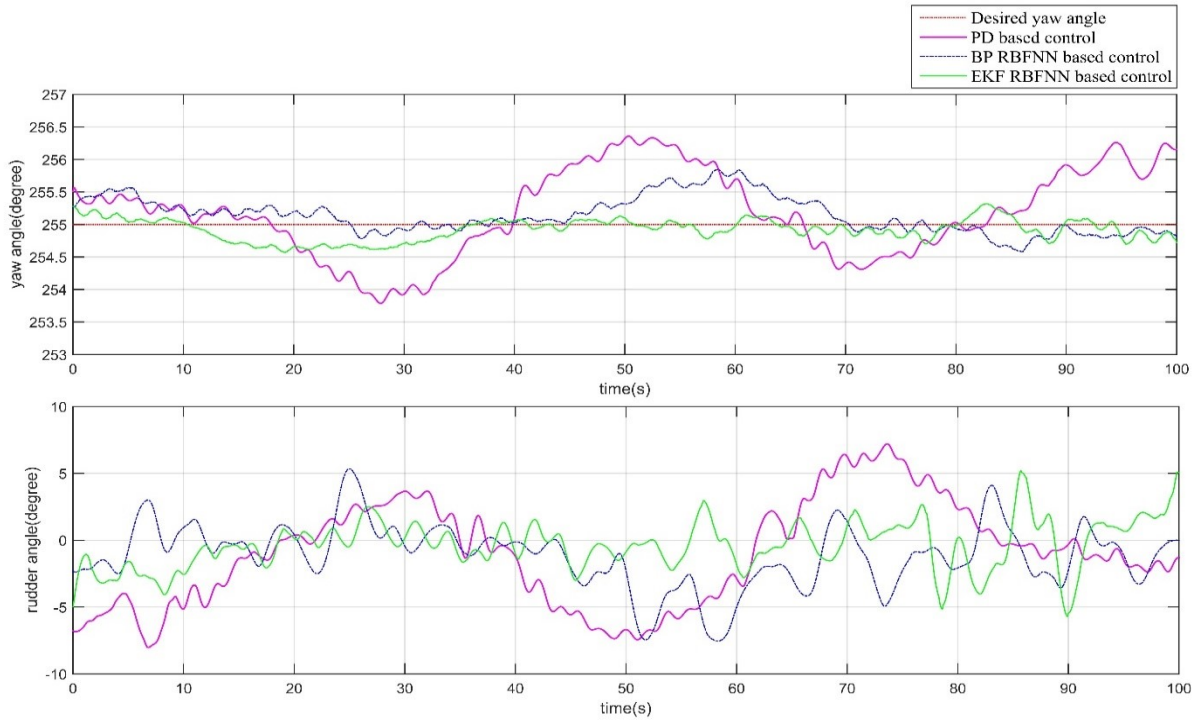

Fig. 5A. 6 Yaw angle and rudder action under the PD, BP RBFNN and EKF RBFNN based control with desired course at 255°

Table 5A. 3 The cost values and maximum values of yaw error and rudder action with yaw angle at 225°and 255°

Scenario	Controller	Yaw error cost	Maximum yaw error	Rudder action cost	Maximum rudder angle
225^0	EKF RBFNN	21.21	0.53	1317.71	2.7
	BP RBFNN	107.54	0.71	3883.35	8.0
	PD	164.64	0.97	6923.75	7.9
255^0	EKF RBFNN	34.50	0.43	3379.35	5.7
	BP RBFNN	97.31	0.85	6806.92	7.5
	PD	477.43	1.36	15621.65	8.1

5A.7. Simulation Results and Discussion

In order to further validate the feasibility of the proposed EKF trained RBFNN based control algorithm in path tracking, the simulations studies were conducted as the current utilised low-cost GPS module was not sufficient to supply smooth and accurate position data for online feedback control. The hydrodynamic parameters of Hoorn's nonlinear mathematical model can be seen in Wang et al. (2017b). For the developed mathematical model, the rudder angle, shaft speed of propeller and the Pierson-Moskowitz wave spectrum constructed the input. The maximum rudder deflection was limited within $\pm 15°$ on both portside and starboard, the slew rate limitation was set to $\pm 10\ °/s$ according to the configuration of the servo motor. The shaft speed of the propeller was set to $900\ rpm$. The external disturbance generated from random waves was acted on the ship's motion equations, and the water depth was assumed to be infinite to disregard shallow water effects and band effects. The Bogacki-Shampine method was adopted to solve the simulation of the ship's motion responses in time series, including the velocity of surge, sway, yaw and roll, the angle of yaw and roll, the position of ship and the rudder angle.

When the control system was switched to the 'Path tracking Loop', the EBS LOS guidance module would provide the dynamic desired yaw angle to track the trajectory planned by the pre-set waypoints. The trajectory was planned from the initial waypoint at (0, 0) to the following waypoint (-200, -200) before heading to the next point at (-360,-800). The

parameters in the EKF training algorithms and RBFNN architectures were consisted with that in the experiments.

The positions of the ship advancing according to the pre-set trajectory are shown in Fig. 5A. 7. Considering the limitation of the chart scale, the motion responses of the vessel controlled by three types of controllers are illustrated in Fig. 5A. 8. What needed to be explained is that the unsmooth inflexions in the figure of path tracking error were generated from the change of newly referred track. According to the evaluation of the maximum deviation and standard deviation of the path tracking in Table 5A. 4, it was shown that the RBFNN based control systems worked well on the path tracking. In order to attain the similar level of control performance, the PD based control system utilised high frequency rudder actions. The differences between the BP RBFNN and EKF RBFNN based trajectory tracks can be explained as the learning speed of each algorithm. When the third waypoint was selected for the guidance, the angle of the pre-set trajectory was 255°. The change of the waves encounter angle affected the path tracking performance. The corresponding weights of both controllers were optimised to encounter the increased forces and moments. As shown in the Fig. 5A. 8, the settling speed of using EKF RBFNN based controller was quicker than that of the BP RBFNN based controller and PD based controller after the new steer-point was selected. In addition, during the sailing between two waypoints, the rudder actions of using EKF training algorithm are more rational than that of the BP training method and conventional PD based control method. Consequently, the controllability of the ship using EKF RBFNN based autopilot was validated regarding the path tracking capability in counteracting unpredictable environmental disturbances.

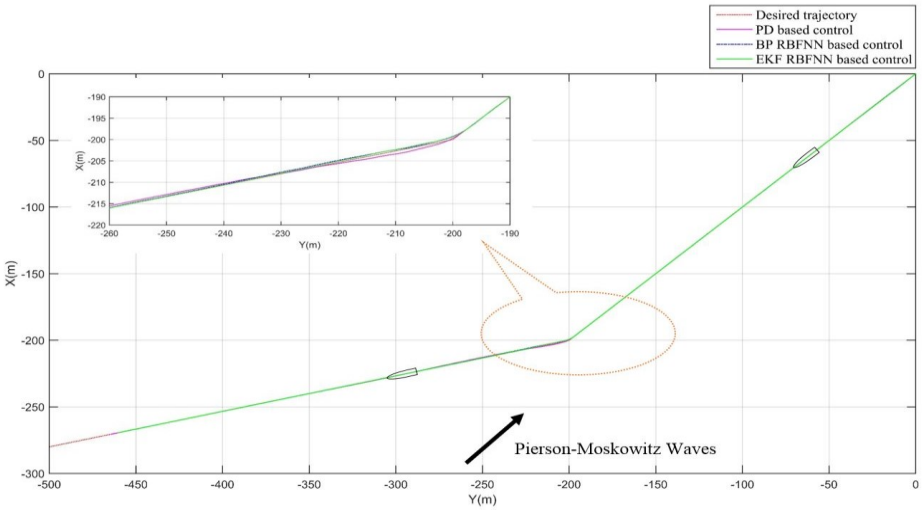

Fig. 5A. 7 Path tracking of ship controlled by PD, BP RBFNN and EKF RBFNN based

controller

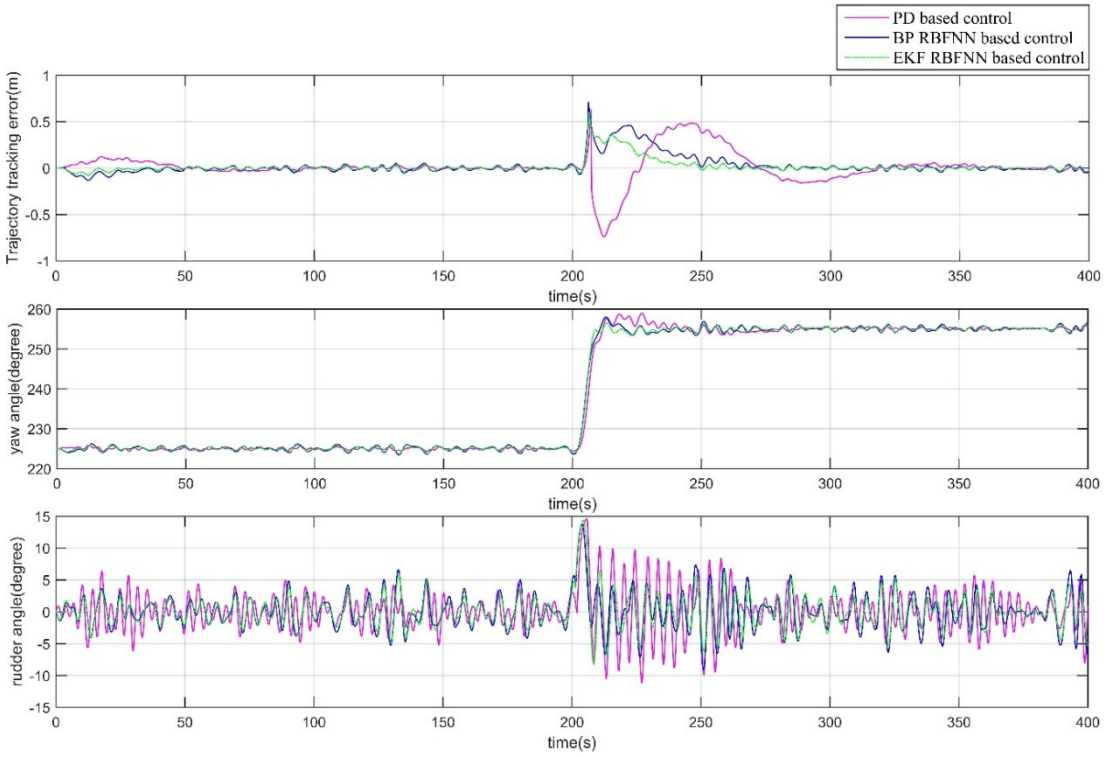

Fig. 5A. 8 The ship response under the control of PD, BP RBFNN and EKF RBFNN controller based on the designed trajectory

Table 5A. 4 The maximum deviation and standard deviation of path tracking for the EFK RBFNN, BP RBFNN and PD based controllers

Controller types	**Maximum Deviation (*m*)**	**Standard Deviation**
EKF RBFNN	0.35	0.0729
BP RBFNN	0.45	0.1007
PD	0.74	0.1617

Based on the numerical studies concerning path tracking and different waves encounter angles, the robustness of the proposed EKF RBFNN steering control system on the aspects of path tracking was verified. In comparison with the BP trained RBFNN control system and PD based control system, the priorities of the EKF trained RBFNN system consist of the capability of effective rudder actions and short settling time coping with dynamical changes.

5A.8. Conclusion

In this study, the EKF RBFNN based ship steering control system has been developed and

investigated. The newly developed free running scaled model was introduced and employed for validation. The robustness of the developed autopilot has been verified by analysing the motion responses of proposed ship advancing with random environmental disturbances only utilising rudder as the only actuator. In order to investigate the performance of proposed EKF RBFNN based control system, two kinds of control algorithms, namely BP trained RBFNN control and conventional PD based control, have been employed. The experimental and numerical results have indicated that the EKF RBFNN based autopilot was feasible to accomplish the tasks of path tracking, course keeping and course changing with small overshoot and short settling time. According to the comparison with the BP RBFNN based controller and PD based controller, the main advantages of the proposed controller lied in its faster learning speed and good disturbance rejection. It is worth noting that the design parameters of EKF RBFNN are fewer than that of the BP RBFNN, which will reduce the complexity of the initial tuning. Simultaneously, the action of rudder using EKF RBFNN based controller was smaller and softer than that of the BP RBFNN based controller.

From the view of commercial utilisation, the experimental and simulated results indicate that the developed autopilot scheme and the signal processing methods can be executed on the currently employed computing platform of marine vessels. Thus low-cost intelligent autopilot can be designed. In the future studies, further investigation will be focused on the installation of the positioning sensor with higher accuracy to experimentally achieve the task of path tracking control and other complicated manoeuvres. Also, remote communication technique with longer range would be adopted to extend the experiment time to investigate the reliability of the control system.

Chapter5 - Part B. Experimental Studies of UKF RBFNN Based Autopilot

Abstract of Chapter 5B: In the recent decades, the application and research of unmanned surface vessels are experiencing considerable growth, which have caused the demands of intelligent autopilots to grow along with the ever-growing requirements. In this study, the design of an autopilot based on Unscented Kalman Filter (UKF) trained Radial Basis Function Neural Networks (RBFNN) was presented. The modified UKF was proposed as the weights training mechanism to provide satisfactory control performance for surface vessels with random external disturbances. To enable the experimental studies, the configurations of the newly developed free running scaled model, as well as the online signal processing method, were introduced. The experimental and numerical tests were carried out through using the physical scaled model and corresponding mathematical model to validate the capability of the designed control system under various sailing conditions. The results indicated that the UKF RBFNN based autopilot satisfied the functionalities of course keeping, course changing and path tracking only using the rudder as the actuator. It was concluded that the developed control scheme was effective to track the desired states and robust against unpredictable external disturbances. Moreover, in comparison with Back-Propagation (BP) RBFNN and Proportional-Derivative (PD) based autopilots, the UKF RBFNN based autopilot has the comparable capability in the aspects of providing smooth and effective control laws.

5B.1. Introduction

The development of digital connectivity and advanced control scheme has sparked interests in the automatic steering system of various vehicles including cars and planes, and now ships. The beneficiary of the latest autopilot system will be the autonomous surface vessels, which can be widely used for oceanographic exploration, mine hunting and coastal patrols. Moreover, the increased capability of the proposed autopilot will benefit the path tracking accuracy of the ship passing through the dense traffic areas, such as narrow straits and area of traffic separation scheme. In addition, the feasibility of the control system will promote the ship to fulfil the complex voyage planning and execute some special operations including cable placing and underway replenishment. So the new challenges of autopilot design have been put forward in consideration of the high degree of manoeuvrability and controllability required by these demanding tasks.

However, considering the nonlinear hydrodynamic characteristics associated with the ship motions as well as the under-actuation, i.e. with fewer control actuators than the variables to be controlled, the ship's control has been a long-standing problem. When the Proportional-Integral-Derivative (PID) based control system became available commercially, the autopilot system made a significant contribution to turning the automatic steering of vessels into reality. Almost all designed autopilots were developed based on this control algorithm until the 1980s. Yet, the disadvantages are that the control parameters are tedious to be determined under the varying operating conditions and it can only provide satisfied control at the fixed points it is optimised for (Tannuri et al., 2010). Especially, when the ship is advancing in severe seas, the conventional autopilot needed to be switched to 'Manual' mode because it is hard to compensate the effects of complicated environmental disturbances.

To compensate the effects of external disturbance, the adaptive approaches can be utilised to handle the hydrodynamic and kinematic behaviours of the systems. A series of adaptive control algorithms, including stochastic control method (Rios-Neto and da Cruz, 1985), linear quadratic Gaussian method (Katebi and Byrne, 1988), feedback linearization method (Fossen and Paulsen, 1992), adaptive PID method (García and Castelo, 1995), and batch adaptive method (Park et al., 2000) have been investigated by many researchers. However, it is shown that some of the adaptive control methods call for substantial prior information (Tulunay, 1991). Moreover, adaptive control would fail when the dynamics changing speed is beyond its adapting capability (Sun et al., 2014). These shortcomings provided motivations for the applications of other modern control theories, including H-infinite algorithm (Morawski and Pomirski, 1998), genetic algorithm (McGookin et al., 2000), fuzzy logic control (Rigatos and Tzafestas, 2006), and sliding mode control (Tannuri et al., 2010). Although the merits of the above mentioned control strategies are desirable, there existed some drawbacks, including the time consumption of generation propagation, the unexpected tracking error generated from the previous error conditions, the requirement of trial-and-error based human knowledge in formulating the fuzzy control rules (Sun et al., 2014).

Impelled by the development of the computing technology, the neural network became applicable in engineering practice. Considering the features of unknown approximating and robustness against system noises, neural networks control is one of the competent approaches to achieve good control performance and disturbance rejection. Therefore, in order for the autopilot to render good helmsman behaviour, neural networks based control algorithms have

been introduced to design the intelligent autopilot (Dai et al., 2012, Wu et al., 2012, Unar and DavidJ, 1999, Wang and Er, 2015, Leonessa et al., 2006). Amongst the present multilayer feedforward neural networks, the RBFNN is an efficient neural networks architecture to fix the multivariable interpolation problem (Hardy, 1971, Powell, 1985, Broomhead and Lowe, 1988). The following applications indicated that the RBFNN has the features of simple architecture and good generalisation capability, which is essential to avoid unnecessary and lengthy calculation (Liu, 2013). Thus this scheme was employed in this study.

When the RBFNN is determined as the control scheme, the training algorithm is important in constructing the neural network based ship steering controller. In the present work, some training methods, e.g. BP training algorithm (Duro and Reyes, 1999), fully supervised gradient descent (Karayiannis, 1999), back-stepping (Yahui et al., 2004), have been proved to be feasible and effective. Yet, the above-mentioned methods have some potential drawbacks, such as the limited converging speed, the possibilities of converging to local minima and the limitations of applying to the various neural network architectures (Choi et al., 2005a).

In order to overcome the flaws, the KFV, which is capable of estimating parameters, was considered as one alternative to the training of the neural network controller (de Oliveira, 2012b). In which, the UKF training method is a strategy that determines weights in each interval by solving a weighted least squares minimisation problem. The main feature of the UKF method is the adoption of a set of particularly determined ‘sigma points’ (Julier and Uhlmann, 1997a). When these points propagate through the nonlinear system, they are capable of capturing the true mean and covariance of the Gaussian random variables through the system dynamics. It was indicated that the UKF was accurate up to third order in capturing the mean and covariance with high training velocity (Hongli et al., 2010). In comparison with the linear or linearise Kalman Filter, the deterministic sampling method adopted in UKF method achieved a better level of estimation accuracy (Wan and Van Der Merwe, 2000).

The main objectives of this study are

- to propose the intelligent autopilot based on UKF trained RBFNN control algorithm to achieve the functionalities of course keeping and path tracking;
- to outline the configuration of a newly developed free running model scaled surface vessel based on the platform myRIO and describe the relevant signal processing methods;

- to verify the capability of the proposed autopilot based upon the developed ship through experimental and numerical tests; and
- to investigate the performance of the developed control scheme according to the comparison with that of BP RBFNN and PD based control.

The paper is organised as follows: in section 2, the configurations of the newly developed free running scaled model as well as the relevant mathematical model in waves are presented. In the following section, the design of UKF RBFNN based autopilot is introduced regarding the functionalities of course keeping and path tracking incorporated with Enclosure-Based-Steering Line-of-Sight (EBS LOS) guidance algorithm. The experiment setup and the corresponding online signal processing methods are briefly outlined in section 4. In the following section, the experimental and numerical studies are presented to validate the feasibility of the proposed controller. Finally, the conclusions are drawn in the last section.

5B.2. The Control Plant and Relevant Mathematical Model

The employed model scaled surface vessel is a floating replica of the 'M/V Nedlloyd Hoorn' built on the 1:100 scale. The hull was constructed of fabric glass with the geometric, kinetic and hydrodynamic similarity principles fully preserved. Thus, the results of hydrodynamic and control investigations can be recalculated to refer to real objects using the known relations (Morawski and Pomirski, 1998). The main particulars of the scaled model are outlined in Table 4. 1. A brief description of the free running scaled model setup and the relevant nonlinear mathematical model in waves are given in this section.

2.1. Configurations of Hoorn

The mechanical and electronics facilities of the vessel were newly updated in the Control Lab of Australian Maritime College. The configurations of the physical model can be outlined as five sub-systems in Fig. 5B. 1.

More information about the components in Power supply system, Actuators system, Embedded computer platform, Measurement system and Host computer can be seen in **Chapter 5A.4**. The details and the type of the electrical and electronic devices can be seen in Appendix II**.**

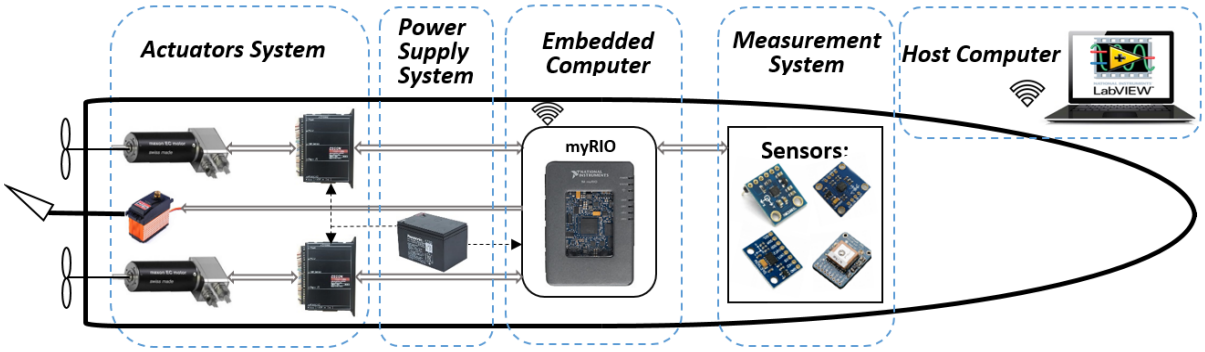

Fig. 5B. 1 The configuration of the free running model Hoorn

2.2. The Mathematical Model of Hoorn

The mathematical model of Hoorn includes hydrodynamic and manoeuvring characteristics. As the reverse motion dynamics are quite different, the forward motions of the vessel are considered. The motions of the Hoorn are defined in two interrelated coordinates, named Earth-fixed coordinate and Body-fixed coordinate (Fossen, 1994a) shown in Fig. 5B. 2.

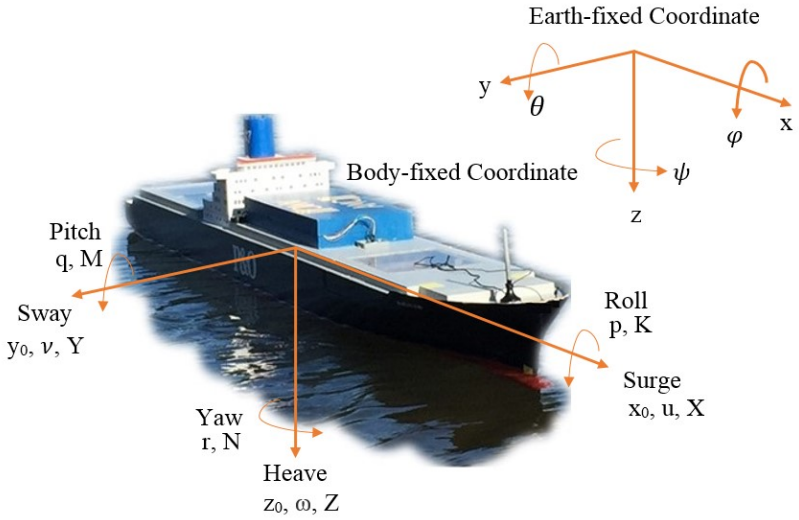

Fig. 5B. 2 The Body-fixed Coordinate and Earth-fixed Coordinate of the surface vessel

The mathematical model of Hoorn was developed based on experimental approaches (Wang et al., 2017b). The conservation of linear and angular momentum, as well as the models of rudder and propeller can be expressed as the following equations:

$$M\dot{\nu} + C(\nu)\nu + D(\nu)\nu + g(\eta) = \tau + \tau_E \qquad (5B.1)$$

$$\dot{\delta} = \delta_c - \delta \qquad (5B.2)$$

$$\dot{n} = \frac{1}{T_n}(n_c - n) \qquad (5B.3)$$

where $v = (u, v, w, p, q, r)^T$ denotes the velocity items of the ship's translated and rotation motion, including surge, sway, heave velocity, and roll, pitch, yaw speed; M the inertia matrix; $C(v)$ the matrix of Coriolis and centripetal terms containing the added mass; D the matrix of damping terms; $g(\eta)$ the vector of restoring forces and moments arisen from gravity and buoyancy, η ship's position and orientation; τ the vector of control inputs; τ_E the vector of environment forces and moments; δ_c the commanded rudder angle; δ the actual rudder angle; T_n, n_c and n are the time constants, commanded shaft speed and current shaft speed, respectively. For the rudder, the boundary of the slew rate and the maximum rudder deflection angle can be set according to the practical requirements and weather conditions.

To verify the capability of the designed controller in compensating environmental disturbances, the modified Pierson-Moskowitz (PM) wave spectrum model recommended by ITTC and outlined in Perez (2006) was employed in this study.

5B.3. Design of UKF RBFNN Based Autopilot

The RBFNN (see Fig. 3A. 1) based control algorithm is with the advantages of not necessarily to know the mathematical model of the plant in practical applications, as well as coping with the unexpected external uncertainties in the control process. In this study, the UKF trained RBFNN is adopted to design the autopilot consisting of two interrelated control functionalities, i.e. course keeping and path tracking.

When the proposed UKF RBFNN based control algorithm is employed in the application of ship motion control, the configuration of the autopilot can be illustrated in Fig. 5B. 3. There are three components in the system: the guidance system, the UKF RBFNN based controller and the ship subjecting to external disturbance. The functionality of guidance system can be determined by switching between two modes: when the system is switched to the Course Keeping Loop, the constant desired angle for course keeping will be supplied; on the other hand, when the system is switched to the Path tracking Loop, the instant desired yaw angle would be computed by the EBS LOS guidance method using actual measured position and pre-set way-points. In the part of UKF RBFNN based controller, the desired angle ψ_d provided by guidance system and the actual yaw angle ψ measured from the sensors/observer are adopted to construct the input matrix for RBFNN based controller. After that, the control law is

approximated cooperating with the UKF training algorithm. The control law will be transmitted to change the rudder angle and make the ship sailing on the desired course or trajectory.

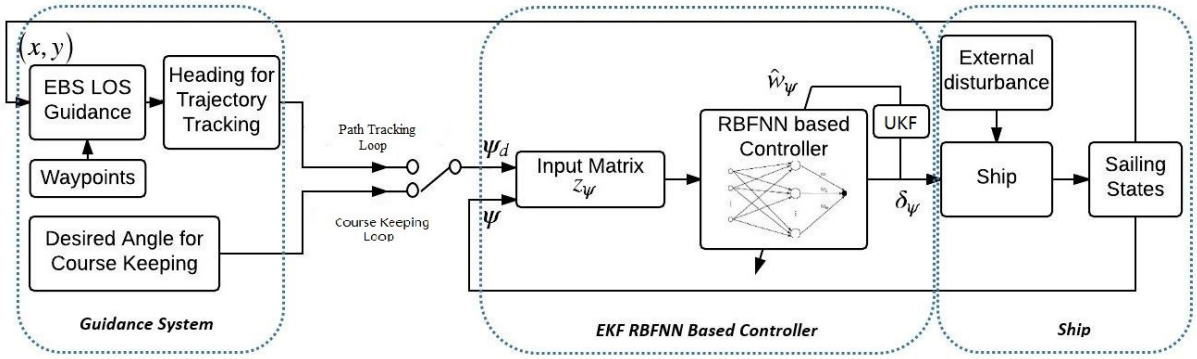

Fig. 5B. 3 Illustration of the Guidance System and UKF-RBFNN based control system for ship with external disturbance

Particularly, the output of the UKF RBFNN controller can be expressed by the following equations:

$$\delta_\psi = \hat{U}_\psi(z_\psi) = \frac{1}{\beta}\sum_{i=1}^{m} \hat{w}_{\psi(UKF)}^T h(z_\psi)$$

$$= \frac{1}{\beta}[\hat{w}_{\psi 1(UKF)} h_1(z_\psi) + \hat{w}_{\psi 2} h_{2(UKF)}(z_\psi) + \cdots + \hat{w}_{\psi m(UKF)} h_m(z_\psi)] \qquad (5B.4)$$

where z_ψ denotes the input matrix of the UKF RBFNN based controller, β is the limitation item of control law to constrain the rudder angle within practical value, m is the total number of neuron nodes in the hidden layer, $\hat{w}_\psi$ is the estimated weights updated by UKF algorithm. The implementation are summarised in Table 5B. 1.

Table 5B. 1 Implementation of the UKF method to train neural networks

Initialization	
Define the weights vector:	$\eta^M = \left[\frac{\lambda}{m+\lambda}, \left(\frac{\lambda}{2(m+\lambda)}\right)_i\right], i = 2, \ldots, 2m+1;$
	$\eta^C = [\frac{\lambda}{m+\lambda} + 1 - \alpha^2 + \beta, \left(\frac{\lambda}{2(m+\lambda)}\right)_i], i = 2, \ldots, 2m+1$
Initialize with:	$\hat{W}_0 = E[\hat{w}_0], P_{\hat{W}_0} = E[(\hat{w} - \hat{w}_0)(\hat{w} - \hat{w}_0)^T]$

Executing and filtering recursively

Generate sigma points: $\widehat{W} = \left[\widehat{w}, \widehat{w} + \left(\sqrt{m+\lambda}\sqrt{P}\right)_i, \widehat{w} - \left(\sqrt{m+\lambda}\sqrt{P}\right)_i\right]$

Prediction transformation

Mean of predicted weights: $\widehat{W}_{Mean} = \sum_{i=1}^{2m+1} \widehat{W}_i \eta_i^M$

Covariance of predicted weights: $P_{\widehat{W}} = \sum_{i=1}^{2m+1} \eta_i^M (\widehat{W}_i - \widehat{W}_{Mean})(\widehat{W}_i - \widehat{W}_{Mean})^T + Q$

Measurement update transformation

Mean of propagated sigma points: $U_{Mean} = \sum_{i=1}^{2m+1} U_i \eta_i^M$

Covariance of measurement: $P_{UU} = \sum_{i=1}^{2m+1} \eta_i^C (U_i - U_{Mean})(U_i - U_{Mean})^T + R$

Cross-covariance of measurement: $P_{\widehat{W}U} = \sum_{i=1}^{2m+1} \eta_i^C (\widehat{W}_i - \widehat{W}_{Mean})(U_i - U_{Mean})^T$

Unscented Kalman Filter calculation and update functions

$$K = P_{\widehat{W}U}/P_{UU}$$

$$\widehat{w} = \widehat{W}_{Mean} + Ks$$

$$P = P_{\widehat{W}} - KP_{UU}K^T$$

In the above-mentioned process, K denotes the Kalman gain matrix for weights group, P is the matrix of approximate error covariance, $\widehat{w}$ is the estimated weights, Q and R are the artificial process noise and observation noise which are useful to avoid numerical divergence, s is the modified augmented error item which contains the error and relevant derivatives to compensate the effects of high inertia and under-actuation.

Moreover, the path tracking involves automatic calculation of the heading angle by collecting instant positions and using it to determine the dynamic heading, which is achieved by using the EBS LOS guidance algorithm (The calculation details can be seen in **Chapter 3A.3**).

In order to numerically evaluate the performance of the control system, the cost function of yaw tracking error denoted by C_{Yaw} and the cost function of rudder actions denoted by C_{Rudder} were adopted in this study (Burns, 1995). The evaluation principle can be seen as equation *(5A.6)*.

5B.4. Experiment setup and Online Signal Processing

In this study, experiments of the proposed UKF RBFNN autopilot were carried out on the Trevallyn Lake in Launceston (Tasmania, Australia). During the experiments, the free running scaled model was fully loaded, and its average speed was approximately $0.7\ m/s$. The speed

of the south-west wind did not exceed $4\ m/s$, but the occasional wind was strong around the experiment site. The waves varied as the change of geography characteristic and the discharging conditions of the dam. The experiment program was developed in LabVIEW and communicated between onboard myRIO and host computer. The proposed control algorithm was written in M-language using the Mathscript Node Module. The control law for rudder deflection was constrained within $\pm 15\,°$ and the slew rate was limited within $\pm 10\,°/s$ considering the configuration of the servo motor.

Contrary with the offline processing in the open-loop experiments for system identification, online signal processing is required in the close-loop control process to eliminate the distortion, declination and coloured noises in the raw data collected from low-cost sensors.

The processing of rotation rate and accelerations measured by gyroscope and accelerometer focus on the conversion from default *least significant bit* to the value in the unit of *degree per second* by considering the value of bit-rate. The calibration of the digital compass is complicated as it subject to the influence of declination and magnetic distortions, which can be fixed by using the following equation (Fang et al., 2011)

$$\psi = \psi_{declination} + arctan\left(\frac{y_c}{x_c}\right) \qquad (5B.5)$$

$$\begin{bmatrix} x_c \\ y_c \\ z_c \end{bmatrix} = M \times \left(\begin{bmatrix} x_{raw} \\ y_{raw} \\ z_{raw} \end{bmatrix} - B \right) = \begin{bmatrix} 1.031 & -0.044 & 0.013 \\ 0.058 & 1.011 & -0.003 \\ 0.028 & 0.015 & 1.096 \end{bmatrix} \times \left(\begin{bmatrix} x_{raw} \\ y_{raw} \\ z_{raw} \end{bmatrix} - \begin{bmatrix} -65.826 \\ -98.788 \\ 63.286 \end{bmatrix} \right) \qquad (5B.6)$$

where ψ is the calibrated yaw angle, the $\psi_{declination} = 0.2467\ rad$ is the magnetic declination determined by the experiment site, $[x_c \quad y_c \quad z_c]^T$ and $[x_{raw} \quad y_{raw} \quad z_{raw}]^T$ are the calibrated and raw data in relevant axis. The matrix *M* and *B* are calculated through the experiment approach. More details about the sensors calibrations can be seen in **Chapter 4.4**.

Data filtering is of great importance in the case of ship control systems since the reliable and stable data will construct the input matrix of the proposed controller. To cope with the uncertainties and high frequency coloured noise in the yaw angle, the KF was developed by using the measurements from both digital compass and gyroscope for states estimation. The methodology can be considered as using the current observation and the previous states to optimise the most likely current states. Considering the low-frequency configuration of yaw

motion as well as the computational expense, conventional KF filter is sufficient to be employed as the observer algorithm to estimate the yaw angle of the scaled model.

In the proposed autopilot experiment program, an independent Mathscript Loop was employed to programme the developed signal processing and filtering methods. Thus, the smoothed and stable data were available for the following control application. After remotely deploying the developed program into the myRIO, the neural network based controller would work in the Time Loop with interval time at *0.1 seconds* and use the processed data with the sampling rate at 10 Hz. Considering the accuracy limitation of the employed low-cost GPS, only the course keeping experimental tests were reported in this study.

5B.5. Experiment Results and Discussion

The aim of the experiments is to maintain the ship sailing forward with fixed yaw angle. Thus the direction of the ship will stabilise on the corresponding yaw angle, which is explained as the rotation around Z axis in Fig. 5B. 2. In order to validate the control performance of the proposed autopilot, two experiment scenarios with different course at $225°$ and $255°$ were conducted (see Fig. 5B. 4). It is worth noting that the remote control range was limited due to the practical WIFI range at 100 meters, thus experiment results in 100 seconds were reported. The parameters of the UKF training algorithm were set at $R = 1, Q = 0.1$, and $\beta = 50$ was chosen for the controller output to constrain the rudder angle in practical level. In order to highlight the performance of the proposed control system, the experiments of BP RBFNN based controller developed in Wang et al. (2015) were also performed for comparison.

Fig. 5B. 4 Course keeping experiment under the control of UKF RBFNN

The first set of experiments using UKF RBFNN, BP RBFNN and PD based controller were implemented with the desired yaw angle at $225°$. During these experiments, the dam was

discharging flood which generated large starboard-bow-quartering current from the tributary. The time histories of heading angle and rudder deflection were plotted in Fig. 5B. 5. The Table 5B. 2 outlined the numerical valuation of the control performance, namely yaw error costs and rudder action costs, in use of the equations *(5A.6)*. The results indicated that the scaled model using both control scheme were capable of tracking the desired yaw angle with rudder deflection around 2°~7.5° to compensate the constant disturbance of the current. Although the BP RBFNN and PD based controller also successfully made the ship to advance on the desired course, the yaw tracking error was higher than that of the UKF RBFNN based control system. In addition, the UKF RBFNN based controller had smaller and smoother rudder actions in comparison with the BP RBFNN and PD based one, which have been corroborated by the costs values in the Table 5B. 2.

Table 5B. 2 The value of yaw error cost and rudder action cost at yaw angle 225°

Scenario	Controller	Yaw error cost	Maximum yaw error	Rudder action cost	Maximum rudder angle
225°	UKF RBFNN	8.86	0.23	13579.33	5.95
	BP RBFNN	30.15	0.45	28151.47	7.52
	PD	73.22	0.60	29574.73	10.14

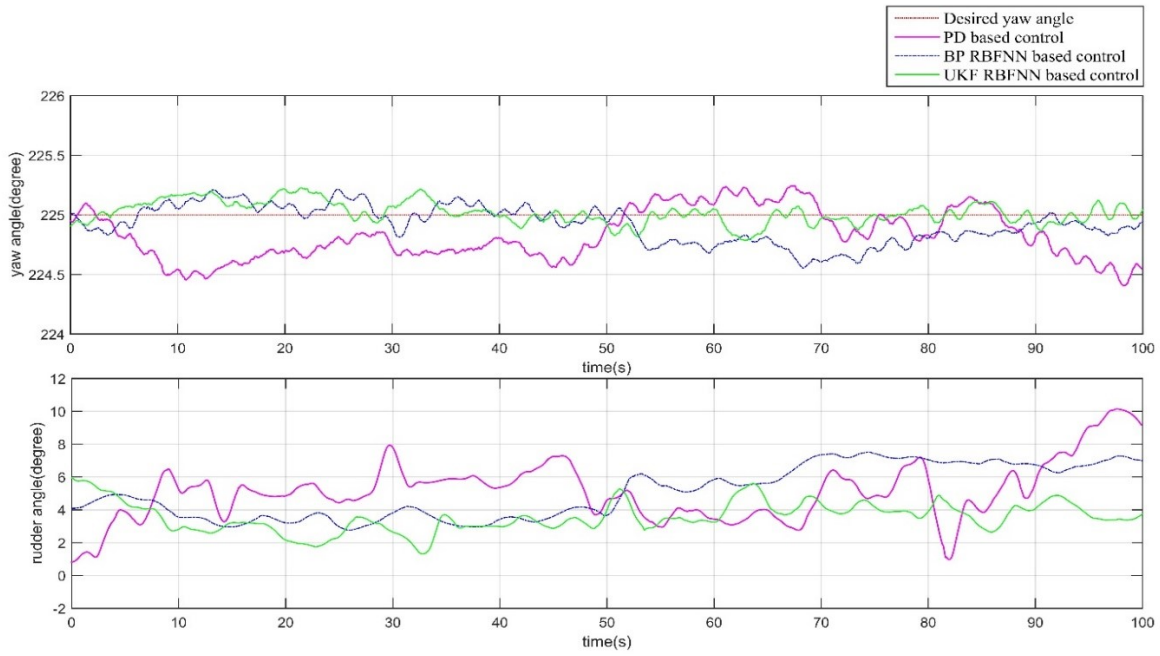

Fig. 5B. 5 Yaw angle and rudder action under the PD, BP RBFNN and UKF RBFNN based control with desired course at 225°

The second set of experiments with the desired course at 255° were conducted nearby the cape, where there were existing the wind generated waves. The waves encounter angle was approximate 150°. The controllability of the proposed control systems are presented by the Fig. 5B. 6 and Table 5B. 3. The conclusion expressed previously can be applied to this scenario since the UKF RBFNN based controller also showed small course keeping error and smooth rudder actions. The time series plots of the course keeping error and rudder actions indicated that the UKF RBFNN based controller had obviously better performance in course keeping in comparison with that of the BP RBFNN and PD based controller.

Table 5B. 3 The value of yaw error cost and rudder action cost at yaw angle 255°

Scenario	Controller	Yaw error cost	Maximum yaw error	Rudder action cost	Maximum rudder angle
255°	UKF RBFNN	23.18	0.39	1445.82	2.72
	BP RBFNN	97.31	0.85	6806.92	7.50
	PD	477.43	1.36	15621.65	8.10

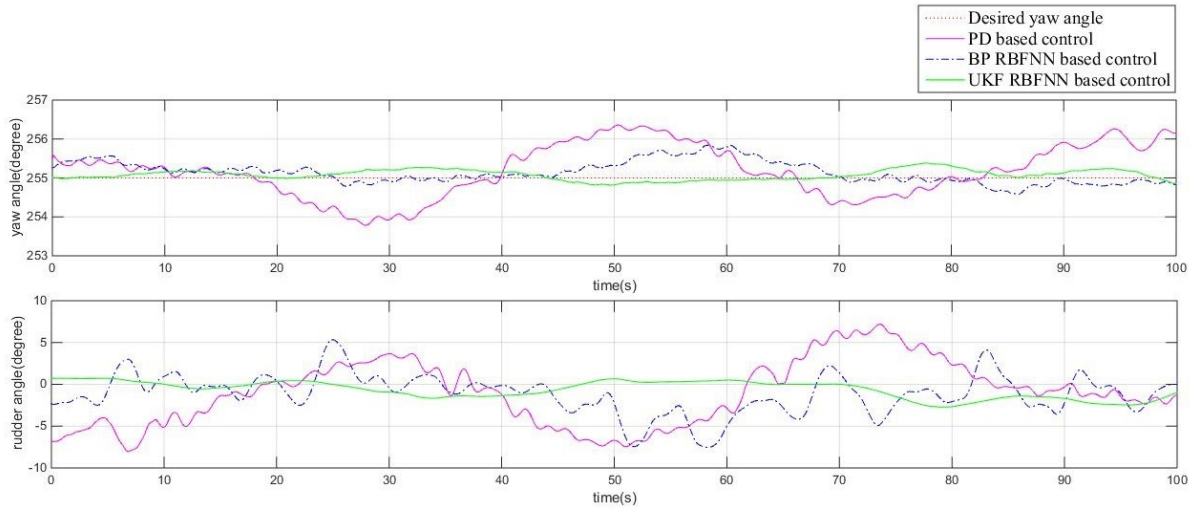

Fig. 5B. 6 Yaw angle and rudder action under the PD, BP RBFNN and UKF RBFNN based control with desired course at 255°

The two sets of experiments gave the comparison of the course keeping performance using the UKF RBFNN, BP RBFNN and PD based controller. The results showed that the performance

of proposed controller was acceptable. It is indicated that the main qualities of the UKF RBFNN based controller were its good disturbance rejection and smooth control output.

5B.6. Simulation Results and Discussion

As previously mentioned, the current utilised low-cost GPS module was not sufficient to supply smooth and accurate position data for online feedback control. Thus, in order to validate the path tracking functionality of UKF RBFNN autopilot, the simulation studies were conducted using Hoorn's mathematical model. In the mathematical model, the input contained the rudder angle, shaft speed of propeller and the Pierson-Moskowitz wave spectrum reflecting the external disturbances. To meet the requirement of practical engineering, the rudder had a saturation constraints as $-15°\sim15°$, the slew rate limitation was set to $\pm10\,°/s$ according to the features of the servo motor. The external disturbance generated from the random waves was acted on the ship, and the water depth was assumed to be infinite to disregard shallow water effects and band effects. The shaft speed of the propeller was set to $r = 900\,rpm$. The Bogacki-Shampine method was adopted to solve the response of the ship motions in time series. The velocity of surge, sway, yaw and roll, the angle of yaw and roll, the position of the ship and the actual rudder angle would be calculated.

The path tracking was achieved by switching the system to the mode of 'Path tracking Loop'. In that case, the EBS LOS guidance module would provide the instant desired yaw angle to make the ship converging on the pre-planned trajectory. The reference trajectory was planned from the initial waypoint at (0, 0) to the following waypoint (-200, -200) and then to the next point at (-360,-800). The similar parameters tuned in the experiments were applied in the simulation studies.

The recorded trajectories of the ship controlled by three types of control schemes were presented in the Fig. 5B. 7. It is easy to observe that the controllers have successfully tracked the pre-set trajectory, but the tracking performance using UKF RBFNN autopilot is better than that of the BP RBFNN and PD based autopilot. Furthermore, Fig. 5B. 8 showed the results of path tracking errors, yaw angle along with the rudder deflections in time series. In order to highlight the merits of the UKF RBFNN based controllers with regard to the accuracy of the path tracking, the standard deviations and maximum deviations (except the region around point of inflexion) of the controllers are evaluated and outlined in Table 5B. 5. The differences in these tracking performances are obvious since the control mechanisms are different. It is worth

mentioning that the big rudder angles, as well as the unsmooth inflexions in the plot of tracking error, were caused by the changes of reference way-point for guidance. To obtain the similar tracking performance, the PD based controller utilised high-frequency rudder actions. When the third way-point was chosen for the guidance, the waves encounter angle changed to 150°, which affected the path tracking accuracy in some extents. The results demonstrated that the UKF RBFNN controller had shortened the time of training to compensate the increased environmental forces and moments. Also, the UKF RBFNN based autopilot still had stable and smooth control efforts, which was essential and meaningful for the algorithm to be applied in practice. Therefore, the controllability of the ship with the UKF RBFNN control system was proved to be effective than that of the BP RBFNN and PD based controller.

In summary, the numerical studies have validated the capability of UKF RBFNN based control system in the aspect of path tracking with environmental disturbance. In comparison with the BP RBFNN and PD based control system, it can be seen from the results that the priorities of the proposed autopilot consist of softer rudder actions and shorter settling time in coping with dynamical uncertainties.

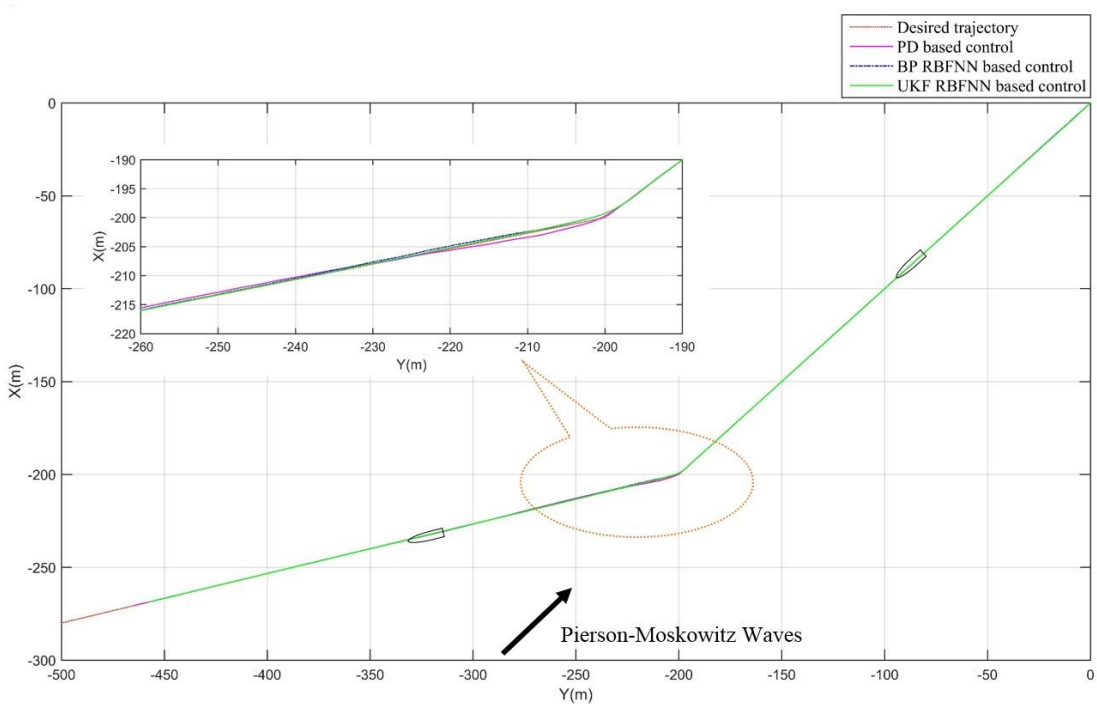

Fig. 5B. 7 Path tracking of ship controlled by PD, BP RBFNN and UKF RBFNN based controller

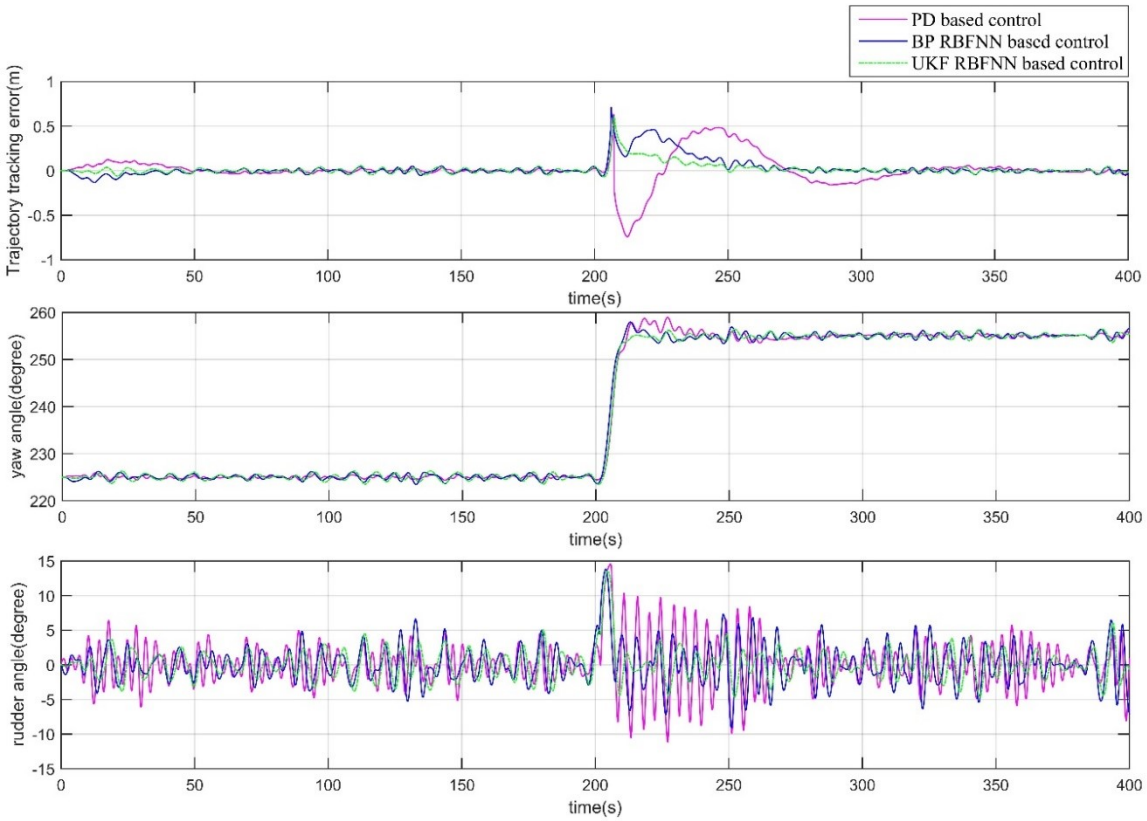

Fig. 5B. 8 The ship response under the control of PD, BP RBFNN and UKF RBFNN controller based on the designed trajectory

Table 3B. 5

Table 5B. 4 The maximum deviation and standard deviation of path tracking for the UFK RBFNN, BP RBFNN and PD based controllers

Controller types	**Maximum Deviation (*m*)**	**Standard Deviation**
UKF RBFNN	0.29	0.0619
BP RBFNN	0.45	0.1007
PD	0.74	0.1617

5B.7. Conclusion and Future Work

In this study, the UKF RBFNN based ship steering control algorithm has been proposed, implemented, and tested experimentally and numerically. The control was achieved using the rudder as the only actuator, in which the control law was approximated by RBFNN incorporated with UKF training algorithm. The design approach of the free running scaled model Hoorn, as well as the signal processing process, were introduced. The experimental and

numerical results showed that the developed control scheme was promising to ship's motions control and capable of enhancing the controllability when the ship is advancing with dynamic disturbances. Meanwhile, the corresponding case studies using BP RBBFNN and PD based control methods were employed to highlight the performance of the UKF RBFNN based control method in the aspects of faster learning procedure and good disturbance rejection. It can be concluded that the developed UKF RBFNN based control system can satisfy the functionalities of course keeping and path tracking quite well, showing smooth control actions and robustness.

Further study is currently underway to investigate the installation of the positioning sensor with higher accuracy to fulfil the task of path tracking and other complicated manoeuvres. In addition, to investigate the reliability of the control system, other remote communication techniques with longer range or autonomous control mode of computing platform would be adopted to extend the experiment time.

Chapter 6

Summary, Conclusions and Future Work

This chapter provides an overall summary of this thesis, bringing together the findings in each chapter and drawing the conclusions accordingly. It also highlights applicability, significance, benefits of the project and the recommendations for further researches.

6.1 Summary

This project aimed to apply the EKF and UKF trained RBFNN control strategies to improve the ship's controllability and robustness in coping with the unpredicted environmental disturbances and system nonlinearities. The main research objective was proposed to solve the main research question "how to develop the EKF/UKF RBFNN based autopilot to improve the capability of controlling the surface vessels?"

The review of the literature, which related to the development of commercial autopilots and the current developed intelligent autopilots, were conducted to clarify the motivations for this project. Although different kinds of advanced control algorithms have been employed by the researchers to design the intelligent autopilot, there remains some improvement place in the aspects of improving converge speed and robustness against the variable disturbances. Thus, to meet the increasing requirement of the ship's control accuracy and feasibility, new control strategies are required to design the autopilots to safely and efficiently control the under-actuated ships even in the presence of the server weather.

To solve the research questions, the novelty control algorithms, namely EKF RBFNN and the UKF RBFNN, were applied to control the surface vessels' motions, including course keeping,

path tracking and rudder-roll damping. Also, the newly developed free running model scaled ship was also proposed to enable the experimental research. The effectiveness of the developed control systems was validated through both numerical and experimental investigations. Therefore, the research objectives have been achieved, comprising the following components:

- Development of the BP RBFNN, EKF RBFNN and UKF RBFNN based ship's motions control system to improve the control capability of course-keeping, path tracking and roll damping only use the rudder as the actuator (**Chapter 2** and **3**);
- Modelling of the newly developed free running scaled model 'Hoorn' as well as the investigation of relevant signal processing methods (**Chapters 4**); and
- Investigation of the developed autopilots through the experimental approach using the physical model of 'Hoorn' and the mathematical model developed in the previous chapter (**Chapter 5**).

According to the above-mentioned investigations, the results have indicated that the research questions mentioned in **Chapter 1** have been answered.

6.2 Main Findings

As a result of the investigations and discussions presented in this thesis, the findings can be summarised in the relevant areas below:

6.2.1 Performance of the developed control systems

Conventional BP RBFNN based ship's control system

The modified BP RBFNN based ship's motions control system, which contains the functionalities of course keeping and roll damping, was firstly developed (**Chapter 2**). In this phase, the nonlinear mathematical model of a full scale container ship with manoeuvring characteristics was employed to simulate the motion responses of the vessel in waves. The results showed that the BP RBFNN based control system could make the vessel advancing on the desired course and stabilise the roll motion in variable sailing conditions. Also, the performance with the influences of waves and observation noises indicated that the NN based control system is superior to the conventional PID based control system.

EKF RBFNN based autopilot

To improve the converging speed and decrease the tuning complexity in designing BP RBFNN

controller, the EKF trained RBFNN control algorithm was proposed to achieve the automatic steering of the surface vessels only use the rudder as the manoeuvring actuator (**Chapter 5A**), and validated by using the newly developed free running model scaled ship. The experimental and numerical results have indicated that the EKF RBFNN based autopilot was competent to fulfil the proposed tasks, including path tracking, course keeping and course changing, with small overshoot and short settling time. It is obvious show that the EKF RBFNN based autopilot was capable of generating smaller and softer rudder actions than that of the BP RBFNN based controller. It is worth noting that the design parameters of EKF RBFNN are decreased. Thus a simple scheme was achieved in reducing the design efforts.

UKF RBFNN based autopilot

To refine the control performance, the UKF RBFNN based autopilot has been proposed, implemented, and tested experimentally and numerically. In the proposed control loop, the ship is manoeuvred by the rudder deflection, which was driven by the control law approximated by RBFNN incorporated with UKF training algorithm. The experimental and numerical results showed that the developed autopilot was sufficient to control the ship's motions and enhance the controllability when the ship was advancing with dynamic disturbances. It can be seen that the UKF RBFNN based control system satisfies the functionalities of course keeping and path tracking with smooth control actions and robustness.

Based on the comparison between the results in **Chapter 5A** and **Chapter 5B**, the control improvements of the UKF RBFNN based autopilot in the aspects of faster learning procedure and good disturbance rejection were demonstrated.

EKF RBFNN based rudder roll stabilisation system

In order to investigate the capability of the EKF RBFNN control algorithm in coping with complicated manoeuvring tasks, it was adopted to develop the rudder roll stabilisation system, which contains course keeping controller and roll damping controller implemented in parallel. The performance of the designed rudder roll stabilisation system was validated by employing a container ship's nonlinear mathematical model, which was adequate to show the motion responses of the ship in waves. The results verified the capability and flexibility of the developed roll damping stabiliser. The comparison between the BP RBFNN and EKF RBFNN based control systems were presented. It is indicated that the EKF RBFNN based stabiliser requires fewer rudder actions, but it is more effective to reduce roll motions and adaptive to compensate the external disturbances generated by random waves.

UKF RBFNN based rudder roll stabilisation system

In this project, the UKF trained RBFNN based control strategies also have been employed in designing the ship's rudder-roll stabilisation system. The results of this investigation showed that the UKF RBFNN based roll stabiliser, as well as course keeping/path tracking controller, were capable and flexible to accomplish the purposes of path tracking and roll reduction simultaneously only through rudder actions. The comparison with the BP RBFNN and PD based stabiliser highlighted the significant advantages of the UKF RBFNN based stabiliser. It is needed to mention that the reduction of actual speed generated by the rudder actions under the control of UKF RBFNN based stabiliser is acceptable at approximate 1%.

Further findings can be gotten from the comparison between the results in **Chapter 3A** and **Chapter 3B**. It is indicated that the UKF RBFNN based control system is much more capable of eliminating the effects of external disturbances and effective to drive the rudder to make the ship sailing on the desired states.

6.2.2 Performance of the developed free running platform

Performance of the newly developed free running model scaled vessel

The newly developed free running scaled model 'Hoorn' was successfully utilised to conduct the relevant experiments. In details, the platform provided reliable data measurements for modelling during the open-loop experiments, while it supplied qualified capabilities to implement the online NN based control algorithms during the closed-loop experiments.

The originally proposed configuration of the free running ship has several advantages. Firstly, the employment of the embedded computer unit, i.e. myRIO, provided promising reliability and feasibility to satisfy the operations of the physical ship with reduced fabrication costs. In comparison with the previous control structure, which combined different kinds of software and hardware, the new control structure successfully avoided the unreliability and incompatibility. Secondly, the usage of the software LabVIEW allowed the user to easily deploy and modify the signal processing and control algorithms without reprogramming the microcontroller. Moreover, the newly updated actuators, including twin EC motors for propelling and high torque servo motor for steering, are qualified and reliable, which have been demonstrated in the experiments in **Chapter 4** and **Chapter 5**.

Low-cost sensors measurements and signal processing algorithm

The original open-loop experiment results in **Chapter 4** have shown that the raw data from the low-cost IMU sensors are easily subject to the distortions and coloured noises, thus the signal processing methods were required. The corresponding calibration methods and Kalman filter were employed to process the raw data and eliminate the noise from sensors. The experiment results indicated that the disturbances in the raw signal data were effectively eliminated as the processed data were smooth and stable to carry out the system identification (**Chapter 4**) and the experimental validations for developed autopilots (**Chapter 5A** and **Chapter 5B**).

Modelling of the free running model scaled ship

As a sequence of the satisfactory signal processing, the 4 DOF mathematical model of 'Hoorn' has been estimated through using experiment data measured from turning circle manoeuvring tests (**Chapter 4**). The scheme of the mathematical model of the surface vessel was proposed based on the relationship between the kinetics and kinematics. The system identification was carried out by using the RLS method to get the hydrodynamic derivatives. It is shown that the experimental results have a good agreement with the simulated responses.

6.3 Conclusions

The findings identified in this thesis lead to the subsequent conclusions under the relevant aspects below:

KFV trained RBFNN based control algorithms for the ship's motion control

According to experimental and numerical investigations, the effectiveness and flexibility of the developed EKF RBFNN and UKF RBFNN based control systems in coping with the ship's motion control were demonstrated. The findings in designing both rudder roll stabilisation system and classical autopilot have shown that the advantages of the KFV RBFNN based controllers lain in their fast learning speed and good disturbance rejection. It can be concluded that the modified RBFNN control algorithms are adaptive to variable sailing states, and robust against the unpredictable environmental disturbances and measurement uncertainties when they are adopted to develop control systems for ships' motions.

Comparison between EKF RBFNN and UKF RBFNN based control systems

According to the comparisons between the investigations in **Chapter 3A/Chapter 3B** and **Chapter 5A/Chapter 5B**, it can be concluded that the UKF RBFNN based control systems have the advantages in achieving better tracking accuracy, and generating effective and

smoother control laws/rudder actions. Also, the control accuracy and the environmental rejection capabilities of the UKF RBFNN based control systems are better than that of the EKF RBFNN based ones, as the adoption of the 'Sigma points' in UKF based training algorithms are successfully used to address the potential propagating errors during the training process.

Although the UKF training algorithm has increased design complexity, its performance is obviously increased in comparison with EKF based one. It is suggested that the selection between the EKF and UKF training algorithms can be determined by the trade-off between the specification of the control tasks and the hardware computational capability.

Effectiveness of the newly developed free running model scaled ship

The open-loop and the closed-loop experiments indicated that the relevant electronic and mechanical components, as well as the employed sensors and signal processing method, are reliable. In addition, the 4 DOF mathematical model of model scaled vessel with full coefficients was firstly developed through experimental approaches. Therefore, it can be concluded that the developed experiment platform is sufficient to be employed to investigate the hydrodynamic characteristics of the hull and to experimentally validate the design of intelligent control systems for the ship's motions.

6.4 Applicability, Significance and Benefits of the Research Outcomes

The results of this project supply a support and basis for the development of the more capable intelligent autopilot based upon the EKF and UKF trained RBFNN to control the ship's motions. The simulation results indicate the possibility of adopting the developed control scheme to maintain the course and path tracking while reducing the roll motion in the presence of large disturbances only use the rudder as the actuator. Thus enhance the safety of seafarers, ships, cargoes and environment. The development of 'Hoorn' enables the experimental and numerical validations of the developed autopilots. The results showed that developed controllers provide the choice to design the autopilots with improved control accuracy and smooth servo motor actions.

The benefits of the developed control algorithms can be concluded as the accessibility and easy application. Firstly, the corresponding experimental investigations showed that the KFV trained RBFNN control systems had acceptable computational complexity. They are available to be deployed in the computer memory and executed by the microprocessor in the current

autopilot system, thus the intelligent autopilot with improved control performance can be designed with low-costs. Secondly, the developed rudder roll stabilization strategies provide an alternative for the ship to reduce roll motion. So for the ship without specific roll stabilisation facilities, the deck officers duty on the bridge have the choice to take positive actions to reduce roll while keeping course or trajectory without too much speed reduction.

This study also contains development and the modelling of the free running scaled model. The employed embedded myRIO demonstrates its computational capability, which allows the programmer to deploy the qualified signal processing method and complex control strategies. Moreover, the benefits of the free running model scaled ship lie in the low-cost in fabrication but effective to be employed in further applications. Additionally, the proposed experimental system identification approach is sufficient to develop the mathematical model, which can be used to speed up the investigations of an advanced control scheme for the ship's motions. Therefore, it is indicated that the developed free running model scaled ship provides a suitable way for industry and academic university to investigate the hydrodynamic characteristics and intelligent autopilots.

6.5 Future Works Recommendations

Based upon the achievement of this project, the following extensions for further investigation can be outlined below:

- To investigate the theoretical methods to prove the stability of the developed control algorithms in course keeping, path tracking and roll motion. Therefore the stability analysis can be conducted to generalise the control algorithm and extend to control other marine vehicles including autonomous underwater vehicle (AUV) and remotely operated vehicle (ROV).
- Further, to update the free running scaled model 'Hoorn'. Focusing on the installation of the positioning sensor with higher accuracy to experimentally achieve the tasks of path tracking control and other complicated manoeuvres, including automatic berthing, mooring and dynamic positioning control. Also, remote communication technique with longer range can be adopted to extend the experiment time to investigate the reliability of the control system.
- To investigate the CFD and captive test approaches to validate the mathematical model. Thus the approach of constructing the free running scaled model for modelling can be

generalised as a low-cost but efficient way to investigate the hydrodynamic characteristics of a class of vessels.

- To design a feasible SI toolbox based on the employed hardware and software. In the proposed kit, the high-order nonlinear filtering methods, such as Particle filter, can be applied to improve the accuracy and optimum of the estimation of the state. The pursuit purpose is to conduct the mathematical model automatically with the input of experimental results.
- To introduce the predictive control algorithm in the proposed system to determine the trade-off between parameter c_ψ and c_ϕ, which are the weights reflecting the emphasis of control performance. By optimizing the parameters on-line, the rudder roll stabilization will be good at identifying the potential huge roll angle to be counteracted, and avoiding useless deflections in compensating small roll angles.
- To combine the closed-loop of speed control in the proposed system to maintain the sailing speed of the vessel, especially for the merchant vessel operating with a strict linear schedule.
- To investigate the speed reduction of other facilities, i.e. stabilizing fins, to support the merits of the designed rudder roll stabilization system.
- To conduct more experiments, including the test of rudder roll stabilisation system, to further validate the capability of the developed control systems.

The long-term objective of this study is to apply the developed control strategies to the hardware of the full scale ship and refine the capability in sea trails. Moreover, the control system is expected to integrate with the ECDIS, thus the complex marine tasks can be conducted with improved control accuracy and robustness against severe weathers.

Bibliography

ALARCIN, F. & GULEZ, K. 2007. Rudder roll stabilization for fishing vessel using neural network approach. *Ocean engineering,* 34**,** 1811-1817.

ALFI, A., SHOKRZADEH, A. & ASADI, M. 2015. Reliability analysis of H-infinity control for a container ship in way-point tracking. *Applied Ocean Research,* 52**,** 309-316.

ANTONELLI, G., CACCAVALE, F. & CHIAVERINI, S. 2004. Adaptive tracking control of underwater vehicle-manipulator systems based on the virtual decomposition approach. *IEEE Transactions on Robotics and Automation,* 20**,** 594-602.

ANTONELLI, G., CHIAVERINI, S., SARKAR, N. & WEST, M. 2001. Adaptive control of an autonomous underwater vehicle: experimental results on ODIN. *IEEE Transactions on Control Systems Technology,* 9**,** 756-765.

ARAKI, M., SADAT-HOSSEINI, H., SANADA, Y., TANIMOTO, K., UMEDA, N. & STERN, F. 2012. Estimating maneuvering coefficients using system identification methods with experimental, system-based, and CFD free-running trial data. *Ocean Engineering,* 51**,** 63-84.

ASHRAFIUON, H., MUSKE, K. R., MCNINCH, L. C. & SOLTAN, R. A. 2008. Sliding-mode tracking control of surface vessels. *IEEE Transactions on Industrial Electronics,* 55**,** 4004-4012.

BRINK, A., BAAS, G., TIANO, A. & VOLTA, E. 1979. Adaptive automatic course-keeping control of a supertanker and a containership-a simulation study. *lllilill. ll***,** 1.

BROOMHEAD, D. S. & LOWE, D. 1988. Radial basis functions, multi-variable functional interpolation and adaptive networks. DTIC Document.

BRUZZONE, A. & SIGNORILE, R. 1998. Simulation and genetic algorithms for ship planning and shipyard layout. *Simulation,* 71**,** 74-83.

BURNS, R. 1995. The use of artificial neural networks for the intelligent optimal control of surface ships. *IEEE Journal of Oceanic Engineering,* 20**,** 65-72.

CHEN, S., WU, Y. & LUK, B. 1999. Combined genetic algorithm optimization and regularized orthogonal least squares learning for radial basis function networks. *IEEE Transactions on Neural Networks,* 10**,** 1239-1243.

CHOI, J., DE C LIMA, A. & HAYKIN, S. Unscented Kalman filter-trained recurrent neural equalizer for time-varying channels. Communications, 2003. ICC'03. IEEE International Conference on, 2003. IEEE, 3241-3245.

CHOI, J., LIMA, A. C. C. & HAYKIN, S. 2005a. Kalman filter-trained recurrent neural equalizers for time-varying channels. *Communications, IEEE Transactions on,* 53**,** 472-480.

CHOI, J., LIMA, A. C. C. & HAYKIN, S. 2005b. Kalman filter-trained recurrent neural equalizers for time-varying channels. *IEEE transactions on communications,* 53**,** 472-480.

DAI, S.-L., WANG, C. & LUO, F. 2012. Identification and learning control of ocean surface ship using neural networks. *IEEE Transactions on Industrial Informatics,* 8**,** 801-810.

DE OLIVEIRA, M. A. 2012a. An application of neural networks trained with kalman filter variants (ekf and ukf) to heteroscedastic time series forecasting. *Applied Mathematical Sciences,* 6**,** 3675-3686.

DE OLIVEIRA, M. A. 2012b. An application of neural networks trained with kalman filter variants (ekf and ukf) to heteroscedastic time series forecasting. *Appl. Math. Sci,* 6**,** 3675-3686.

DO, K. D., JIANG, Z.-P. & PAN, J. 2004. Robust adaptive path following of underactuated ships. *Automatica,* 40**,** 929-944.

DU, J., GUO, C., YU, S. & ZHAO, Y. 2007. Adaptive autopilot design of time-varying uncertain ships with completely unknown control coefficient. *IEEE Journal of Oceanic Engineering,* 32**,** 346-352.

DURO, R. J. & REYES, J. S. 1999. Discrete-time backpropagation for training synaptic delay-based artificial neural networks. *IEEE Transactions on Neural Networks,* 10**,** 779-789.

FANG, J., SUN, H., CAO, J., ZHANG, X. & TAO, Y. 2011. A novel calibration method of magnetic compass based on ellipsoid fitting. *IEEE Transactions on Instrumentation and Measurement,* 60**,** 2053-2061.

FANG, M.-C., LIN, Y.-H. & WANG, B.-J. 2012a. Applying the PD controller on the roll reduction and track keeping for the ship advancing in waves. *Ocean Engineering,* 54**,** 13-25.

FANG, M.-C. & LUO, J.-H. 2007a. On the track keeping and roll reduction of the ship in random waves using different sliding mode controllers. *Ocean engineering,* 34**,** 479-488.

FANG, M.-C., ZHUO, Y.-Z. & LEE, Z.-Y. 2010a. The application of the self-tuning neural network PID controller on the ship roll reduction in random waves. *Ocean Engineering,* 37**,** 529-538.

FANG, M. C., LIN, Y. H. & WANG, B.-J. 2012b. Applying the PD controller on the roll reduction and track keeping for the ship advancing in waves. *Ocean Engineering,* 54**,** 13-25.

FANG, M. C. & LUO, J. H. 2007b. On the track keeping and roll reduction of the ship in random waves using different sliding mode controllers. *Ocean Engineering,* 34**,** 479-488.

FANG, M. C., ZHUO, Y. Z. & LEE, Z.-Y. 2010b. The application of the self-tuning neural network PID controller on the ship roll reduction in random waves. *Ocean Engineering,* 37**,** 529-538.

FOSSEN, T. I. 1991. *Nonlinear modelling and control of underwater vehicles.* Norwegian University of Science and Technology.

FOSSEN, T. I. 1994a. *Guidance and control of ocean vehicles*, Wiley New York.

FOSSEN, T. I. 1994b. *Guidance and control of ocean vehicles*, John Wiley & Sons Inc.

FOSSEN, T. I. 2011. *Handbook of marine craft hydrodynamics and motion control*, John Wiley & Sons.

FOSSEN, T. I. & PAULSEN, M. J. Adaptive feedback linearization applied to steering of ships. Control Applications, 1992., First IEEE Conference on, 1992. IEEE, 1088-1093.

GARC A, R. F. & CASTELO, F. P. 1995. Adaptive PID Controller Applied on Marine DP Control using Frequency Analysis Techniques. *IFAC Proceedings Volumes,* 28**,** 356-361.

GE, HANG, C. C., LEE, T. H. & ZHANG, T. 2010. *Stable adaptive neural network control*, Springer Publishing Company, Incorporated.

GE, S., HANG, C. & ZHANG, T. 1999. A direct method for robust adaptive nonlinear control with guaranteed transient performance. *Systems & control letters,* 37**,** 275-284.

GIERUSZ, W., VINH, N. C. & RAK, A. 2007. Maneuvering control and path tracking of very large crude carrier. *Ocean Engineering,* 34**,** 932-945.

HARDY, R. L. 1971. Multiquadric equations of topography and other irregular surfaces. *Journal of geophysical research,* 76**,** 1905-1915.

HAUN, E. 2014. ASV Debuts New Unmanned Surface Vehicle [Online]. Marine Technology news. Available: https://www.marinetechnologynews.com/news/debuts-unmanned-surface-vehicle-487078 [Accessed].

HAYKIN, S. S. 2001. *Kalman filtering and neural networks*, Wiley Online Library.

HONGLI, L., JIANG, W., YANQIU, C., HAIYANG, W. & YINGYUAN, C. On neural network training algorithm based on the unscented Kalman filter. Control Conference (CCC), 2010 29th Chinese, 2010. IEEE, 1447-1450.

IRWIN, G. W., WARWICK, K. & HUNT, K. J. 1995. *Neural network applications in control*, Iet.

JULIER, S. J. The scaled unscented transformation. American Control Conference, 2002. Proceedings of the 2002, 2002. IEEE, 4555-4559.

JULIER, S. J. & UHLMANN, J. K. New extension of the Kalman filter to nonlinear systems. AeroSense'97, 1997a. International Society for Optics and Photonics, 182-193.

JULIER, S. J. & UHLMANN, J. K. A new extension of the Kalman filter to nonlinear systems. Int. symp. aerospace/defense sensing, simul. and controls, 1997b. Orlando, FL, 182-193.

K LLSTR M, C. G., ÅSTR M, K. J., THORELL, N., ERIKSSON, J. & STEN, L. 1979. Adaptive autopilots for tankers. *Automatica,* 15**,** 241-254.

KANDEPU, R., FOSS, B. & IMSLAND, L. 2008. Applying the unscented Kalman filter for nonlinear state estimation. *Journal of Process Control,* 18**,** 753-768.

KARAYIANNIS, N. B. 1999. Reformulated radial basis neural networks trained by gradient descent. *IEEE Transactions on Neural Networks,* 10**,** 657-671.

KATEBI, M. & BYRNE, J. 1988. LQG adaptive ship autopilot. *Transactions of the Institute of Measurement and Control,* 10**,** 187-197.

LAUVDAL, T. & FOSSEN, T. I. Rudder roll stabilization of ships subject to input rate saturation using a gain scheduled control law. Proc. of the IFAC Conference on Control Applications in Marine Systems (CAMS'98), Fukuoka, Japan, 1998. 121-127.

LEFEBER, E., PETTERSEN, K. Y. & NIJMEIJER, H. 2003. Tracking control of an underactuated ship. *IEEE transactions on control systems technology,* 11**,** 52-61.

LEONESSA, A., VANZWIETEN, T. & MOREL, Y. 2006. Neural network model reference adaptive control of marine vehicles. *Current trends in nonlinear systems and control***,** 421-440.

LI, H., GUO, C. & LI, X. Ship roll stabilization using supervision control based on inverse model wavelet neural network. Intelligent Control and Automation (WCICA), 2010 8th World Congress on, 2010. IEEE, 4829-4833.

LI, Y., QIANG, S., ZHUANG, X. & KAYNAK, O. 2004. Robust and adaptive backstepping control for nonlinear systems using RBF neural networks. *IEEE Transactions on Neural Networks,* 15**,** 693-701.

LI, Z., SUN, J. & OH, S. 2009. Design, analysis and experimental validation of a robust nonlinear path following controller for marine surface vessels. *Automatica,* 45**,** 1649-1658.

LIU, J. 2013. *Radial Basis Function (RBF) Neural Network Control for Mechanical Systems: Design, Analysis and Matlab Simulation*, Springer Berlin Heidelberg.

LLOYD, A. 1975. Roll stabilization by rudder.

MARINE, S. 2014. The NAVIPILOT 4000 [Online]. Available: http://www.ship-technology.com/products/the-navipilot-4000 [Accessed].

MCGOOKIN, E. W., MURRAY-SMITH, D. J., LI, Y. & FOSSEN, T. I. 2000. Ship steering control system optimisation using genetic algorithms. *Control Engineering Practice,* 8**,** 429-443.

MEDAGAM, P. V. & POURBOGHRAT, F. Optimal control of nonlinear systems using RBF neural network and adaptive extended Kalman filter. American Control Conference, 2009. ACC'09., 2009. IEEE, 355-360.

MESSINA, G., NABERGOJ, R. & TRINCAS, G. Designing and operating safer fishing vessels. Proceedings of the 6th International Symposium on Technics and Technology in fishing vessels" Ancona [Italy] pp, 1997. 192-209.

MILLER, H. Modern Control Theory Applied to Ship Steering. Ship Operation Automation, IFAC/IFIP Symposium, 1973.

MINORSKY, N. 1922. Directional stability of automatically steered bodies. *Naval Engineers Journal,* 32.

MORAWSKI, L. & POMIRSKI, J. 1998. Ship track-keeping: Experiments with a physical tanker model. *Control Engineering Practice,* 6**,** 763-769.

MOREIRA, L., FOSSEN, T. I. & SOARES, C. G. 2007. Path following control system for a tanker ship model. *Ocean Engineering,* 34**,** 2074-2085.

MORENO-SALINAS, D., CHAOS, D., DE LA CRUZ, J. M. & ARANDA, J. 2013. Identification of a surface marine vessel using LS-SVM. *Journal of Applied Mathematics,* 2013.

NARENDRA, K. S. & THATHACHAR, M. A. 2012. *Learning automata: an introduction*, Courier Corporation.

NEJIM, S. Rudder roll damping system for ships using fuzzy logic control. OCEANS 2000 MTS/IEEE Conference and Exhibition, 2000. IEEE, 1137-1143.

NGUYEN, H. 2000. *Self-tuning pole assignment and optimal control systems for ships.* Ph. D thesis. Tokyo University of Marine Science and Technology, Tokyo, Japan. 2001. C721, C724, C729 References C732.

NGUYEN, H. D. Multitask automatic manoeuvring systems using recursive optimal control algorithms. Communications and Electronics, 2008. ICCE 2008. Second International Conference on, 2008. IEEE, 54-59.

NGUYEN, P.-H. & JUNG, Y.-C. 2007. Neural Network Based Rudder-Roll Damping Control System for Ship. *Journal of Korean navigation and port research,* 31**,** 289-293.

NOMOTO, K. 1972. Paper 1. Problems and Requirements of Directional Stability and Control of Surface Ships. *Journal of Mechanical Engineering Science,* 14**,** 1-5.

ODA, H., HYODO, T., OHTSU, K., ITO, M., HIROSE, N., PARK, J. & SATO, H. 1999. Designing advanced rudder roll stabilization system-high power with small size hydraulic system and adaptive control. *Proc of 12 SCSS*.

ODA, H. & OHTSU, K. 1991. ROLL STABILISATION BY RUDDER CONTROL THROUGH MULTI-VARIATE AUTO-REGRESSIVE MODEL.

ODA, H., OHTSU, K., SASAKI, M., SEKI, Y. & HOTTA, T. 1992. Rudder Roll Stabilization Control System through Multivariate Auto Regressive Model. *Proc. of CAMS'92*, 113-127.

PAO, Y. 1989. Adaptive pattern recognition and neural networks.

PARK, J. & SANDBERG, I. W. 1991. Universal approximation using radial-basis-function networks. *Neural computation,* 3, 246-257.

PARK, J. S., OHTSU, K. & KITAGAWA, G. 2000. Batch - adaptive ship's autopilots. *International Journal of Adaptive Control and Signal Processing,* 14, 427-439.

PARSONS, M. G. & CUONG, H. T. 1980. Adaptive Path Control of Surface Ships in Restricted Waters. MICHIGAN UNIV ANN ARBOR DEPT OF NAVAL ARCHITECTURE AND MARINE ENGINEERING.

PEREIRA, J. & DUNCAN, A. System identification of underwater vehicles. Underwater Technology, 2000. UT 00. Proceedings of the 2000 International Symposium on, 2000. IEEE, 419-424.

PEREZ, T. 2005. Rudder Roll Stabilisation of Ships. *Constrained Control and Estimation: An Optimisation Approach*, 323-346.

PEREZ, T. 2006. *Ship motion control: course keeping and roll stabilisation using rudder and fins*, Springer Science & Business Media.

PEREZ, T. & BLANKE, M. 2002. *Mathematical ship modelling for control applications*, Ørsted-DTU, Automation.

PEREZ, T. & BLANKE, M. 2012. Ship roll damping control. *Annual Reviews in Control,* 36, 129-147.

PETTERSEN, K. Y. & NIJMEIJER, H. 2001. Underactuated ship tracking control: theory and experiments. *International Journal of Control,* 74, 1435-1446.

POLKINGHORNE, M., ROBERTS, G., BURNS, R. & WINWOOD, D. 1995. The implementation of fixed rulebase fuzzy logic to the control of small surface ships. *Control Engineering Practice,* 3, 321-328.

POWELL, M. J. Radial basis function for multivariable interpolation: a review. IMA Conference on Algorithms for the Approximation of Functions ans Data, 1985, 1985. RMCS.

PUSKORIUS, G. & FELDKAMP, L. Model reference adaptive control with recurrent networks trained by the dynamic DEKF algorithm. Neural Networks, 1992. IJCNN., International Joint Conference on, 1992. IEEE, 106-113.

PUSKORIUS, G. V. & FELDKAMP, L. 1994. Neurocontrol of nonlinear dynamical systems with Kalman filter trained recurrent networks. *Neural Networks, IEEE Transactions on,* 5, 279-297.

RHUDY, M. & GU, Y. 2013. Understanding Nonlinear Kalman Filters, Part II: An Implementation Guide. *Interactive Robotics Letters*.

RIGATOS, G. & TZAFESTAS, S. 2006. Adaptive fuzzy control for the ship steering problem. *Mechatronics,* 16, 479-489.

RIOS-NETO, A. & DA CRUZ, J. 1985. A stochastic rudder control law for ship path-following autopilots. *Automatica,* 21, 371-384.

ROBERTS, G. 1992. Ship motion control using a multivariable approach.

ROBERTS, G., SHARIF, M., SUTTON, R. & AGARWAL, A. 1997. Robust control methodology applied to the design of a combined steering/stabiliser system for warships. *IEE Proceedings-Control Theory and Applications,* 144, 128-136.

SANCHEZ, E. N., ALAN S, A. Y. & LOUKIANOV, A. G. 2008. *Discrete-time high order neural control: trained with Kalman filtering*, Springer Science & Business Media.

SGOBBO, J. N. & PARSONS, M. G. 1999a. Rudder/fin roll stabilization of the USCG WMEC 901 class vessel. *Marine Technology,* 36, 157-170.

SGOBBO, J. N. & PARSONS, M. G. 1999b. Rudder/fin roll stabilization of the USCG WMEC 901 class vessel. *Marine Technology and SNAME news,* 36, 157.

SIMON, D. 2002. Training radial basis neural networks with the extended Kalman filter. *Neurocomputing,* 48, 455-475.

SKJETNE, R., FOSSEN, T. I. & KOKOTOVIĆ, P. V. 2005. Adaptive maneuvering, with experiments, for a model ship in a marine control laboratory. *Automatica,* 41, 289-298.

SON, K.-H. & NOMOTO, K. 1982. On the Coupled Motion of Steering and Rolling of a High-speed Container Ship. *Naval Architecture and Ocean Engineering,* 20, 73-83.

SPERRY, E. A. 1922. *Automatic steering*, Society of Naval Architects and Marine Engineers.

STAPLES, N. 2013. Tobruk's underway replenishment [Online]. Navy daily: Navy daily. Available: http://news.navy.gov.au/en/Dec2013/Fleet/748/Tobruk%27s-underway-replenishment.htm#.Wdq9MVV9670 [Accessed].

SUM, J., LEUNG, C.-S., YOUNG, G. H. & KAN, W.-K. 1999a. On the Kalman filtering method in neural network training and pruning. *IEEE Transactions on Neural Networks,* 10**,** 161-166.

SUM, J., LEUNG, C.-S., YOUNG, G. H. & KAN, W.-K. 1999b. On the Kalman filtering method in neural network training and pruning. *Neural Networks, IEEE Transactions on,* 10**,** 161-166.

SUN, B., ZHU, D. & YANG, S. X. 2014. A bioinspired filtered backstepping tracking control of 7000-m manned submarine vehicle. *IEEE Transactions on Industrial Electronics,* 61**,** 3682-3693.

TANNURI, E., AGOSTINHO, A., MORISHITA, H. & MORATELLI, L. 2010. Dynamic positioning systems: An experimental analysis of sliding mode control. *Control Engineering Practice,* 18**,** 1121-1132.

TEE, K. P. & GE, S. S. 2006. Control of fully actuated ocean surface vessels using a class of feedforward approximators. *IEEE Transactions on Control Systems Technology,* 14**,** 750-756.

TREAKLE, T. W., MOOK, D. T., LIAPIS, S. I. & NAYFEH, A. H. 2000. A time-domain method to evaluate the use of moving weights to reduce the roll motion of a ship. *Ocean engineering,* 27**,** 1321-1343.

TREBATICK , P. Recurrent neural network training with the extended kalman filter. IIT. SRC 2005: Student Research Conference, 2005. 57.

TULUNAY, E. 1991. Introduction to neural networks and their application to process control. *Neural Networks: Advances and Applications.* Elsevier Amsterdam.

UNAR, M. A. & DAVIDJ, M. S. 1999. Automatic steering of ships using neural networks. *International journal of adaptive control and signal processing,* 13**,** 203-218.

VAN AMERONGEN, J. 1984. Adaptive steering of ships—A model reference approach. *Automatica,* 20**,** 3-14.

VAN AMERONGEN, J. & VAN NAUTA LEMKE, H. 1978. Optimum steering of ships with an adaptive autopilot. *Fifth Ship Control Systems Symposium.* Annapolis, USA.

VAN DER MERWE, R. & WAN, E. A. Efficient derivative-free Kalman filters for online learning. ESANN, 2001. 205-210.

WAN, E. A. & VAN DER MERWE, R. The unscented Kalman filter for nonlinear estimation. Adaptive Systems for Signal Processing, Communications, and Control Symposium 2000. AS-SPCC. The IEEE 2000, 2000. Ieee, 153-158.

WAN, E. A. & VAN DER MERWE, R. 2002. The Unscented Kalman Filter. *Kalman Filtering and Neural Networks.* John Wiley & Sons, Inc.

WANG, N. & ER, M. J. 2015. Self-constructing adaptive robust fuzzy neural tracking control of surface vehicles with uncertainties and unknown disturbances. *IEEE Transactions on Control Systems Technology,* 23**,** 991-1002.

WANG, Y., CHAI, S., KHAN, F. & NGUYEN, H. D. 2017a. Unscented Kalman Filter trained neural networks based rudder roll stabilization system for ship in waves. *Applied Ocean Research,* 68**,** 26-38.

WANG, Y., CHAI, S. & NGUYEN, H. D. Modelling of a surface vessel from free running test using low cost sensors. Control, Automation and Robotics (ICCAR), 2017 3rd International Conference on, 2017b. IEEE, 299-303.

WANG, Y., NGUYEN, H. D., CHAI, S. & KHAN, F. Radial basis function neural network based rudder roll stabilization for ship sailing in waves. Control Conference (AUCC), 2015 5th Australian, 2015. IEEE, 158-163.

WU, J., PENG, H., OHTSU, K., KITAGAWA, G. & ITOH, T. 2012. Ship's tracking control based on nonlinear time series model. *Applied Ocean Research,* 36**,** 1-11.

XIANKU, Z., YICHENG, J., CHENGEN, Y. & LIKUN, Z. A kind of robust rudder roll-damping system. Systems and Control in Aerospace and Astronautics, 2006. ISSCAA 2006. 1st International Symposium on, 2006. IEEE, 4 pp.-1154.

YAHUI, L., SHENG, Q., XIANYI, Z. & OKYAY, K. 2004. Robust and adaptive backstepping control for nonlinear systems using RBF neural networks. *IEEE Transactions on Neural Networks,* 15**,** 693-701.

YI, B. & ZHANG, W. 2016. A nonlinear updated gain observer for MIMO systems: design, analysis and application to marine surface vessels. *ISA transactions,* 64**,** 129-140.

YOON, H. K., SON, N. S. & LEE, G. J. 2007. Estimation of the roll hydrodynamic moment model of a ship by using the system identification method and the free running model test. *IEEE Journal of Oceanic Engineering,* 32**,** 798-806.

ZHAN, R. & WAN, J. 2006. Neural network-aided adaptive unscented Kalman filter for nonlinear state estimation. *IEEE Signal Processing Letters,* 13**,** 445-448.

ZHANG, G. & ZHANG, X. 2015. A novel DVS guidance principle and robust adaptive path-following control for underactuated ships using low frequency gain-learning. *ISA transactions,* 56**,** 75-85.

ZHANG, R., CHEN, Y., SUN, Z., SUN, F. & XU, H. 2000. Path control of a surface ship in restricted waters using sliding mode. *IEEE Transactions on Control Systems Technology,* 8**,** 722-732.

ZHANG, X., JIN, Y., YANG, C. & ZHANG, L. A kind of robust rudder roll-damping system. Systems and Control in Aerospace and Astronautics, 2006. ISSCAA 2006. 1st International Symposium on, 2006. IEEE, 4 pp.-1154.

ZHAO, J., ZHU, X., WANG, W. & LIU, Y. 2013. Extended Kalman filter-based Elman networks for industrial time series prediction with GPU acceleration. *Neurocomputing,* 118**,** 215-224.

ZIRILLI, A., ROBERTS, G., TIANO, A. & SUTTON, R. 2000. Adaptive steering of a containership based on neural networks. *International Journal of Adaptive Control and Signal Processing,* 14**,** 849-873.

Appendix I -- Mathematical model of a full scale container ship coding in MATLAB S-function

```
function [sys,x0,str,ts] = ContainerModel(t,x,u,flag)
% ContainerVessel.m, Version 1.1
% Made by Hung Nguyen in 2007
% References:
% Fossen (1994, 2002)

switch flag
case 0,
   [sys,x0,str,ts] = mdlInitializeSizes;
case 1,
    sys=mdlDerivatives(t,x,u);
case 3,
   sys = mdlOutputs(t,x,u);
case {2, 4, 9},
   sys = [];
otherwise
   error(['Unhandled flag = ',num2str(flag)]);
end

function [sys,x0,str,ts] = mdlInitializeSizes

sizes = simsizes;
sizes.NumContStates = 10;
sizes.NumDiscStates = 0;
sizes.NumOutputs = 10;
sizes.NumInputs = -1;
sizes.DirFeedthrough = 1;
sizes.NumSampleTimes = 1;
sys = simsizes(sizes);
```

```
% Initial values of state vector:
x0 = [8.0 0 0 0 0 pi/3 0 0 0 80]';
str = [];
ts = [0 0];
% end of mdlInitializeSizes

function sys=mdlDerivatives(t,x,u)

% [xdot,U] = container(x,ui) returns the speed U in m/s (optionally) and the
% time derivative of the state vector: x = [ u v r x y psi p phi delta n ]'  for
% a container ship L = 175 m, where
% u     = surge velocity         (m/s)
% v     = sway velocity          (m/s)
% r     = yaw velocity           (rad/s)
% x     = position in x-direction (m)
% y     = position in y-direction (m)
% psi   = yaw angle              (rad)
% p     = roll velocity          (rad/s)
% phi   = roll angle             (rad)
% delta = actual rudder angle    (rad)
% n     = actual shaft velocity  (rpm)
%
% The input vector is :
% ui      = [ delta_c n_c ]'  where
% delta_c = commanded rudder angle   (rad)
% n_c     = commanded shaft velocity (rpm)

% Reference:  Son og Nomoto (1982). On the Coupled Motion of Steering and
%             Rolling of a High Speed Container Ship, Naval Architect of Ocean Engineering,
%             20: 73-83. From J.S.N.A. , Japan, Vol. 150, 1981.
% Author:    Trygve Lauvdal
% Date:      12th May 1994
% Revisions: 18th July 2001 (Thor I. Fossen): added output U, changed order of x-vector
```

```
%          20th July 2001 (Thor I. Fossen): changed my = 0.000238 to my = 0.007049
% References: Fossen (1994, 2002).
% Revisions:  12 July 2007 by Hung Nguyen: modified into S-function for Simulink

% Check of input and state dimensions
if (length(x) ~= 10),error('x-vector must have dimension 10 !');end
if (length(u) ~= 2),error('u-vector must have dimension  2 !');end

% Normalization variables
L = 175;                  % length of ship (m)
U = sqrt(x(1)^2 + x(2)^2);   % service speed (m/s)

% Check service speed
if U <= 0,error('The ship must have speed greater than zero');end
if x(10) <= 0,error('The propeller rpm must be greater than zero');end

delta_max  = 30;          % max rudder angle (°)
Ddelta_max = 5;           % max rudder rate (°/s)
n_max      = 160;         % max shaft velocity (rpm)

% Non-dimensional states and inputs
delta_c = u(1);
n_c     = u(2)/60*L/U;
noi = u(3);

u1    = x(1)/U;   v   = x(2)/U;
p     = x(7)*L/U; r   = x(3)*L/U;
phi   = x(8);     psi = x(6);
delta = x(9);     n   = x(10)/60*L/U;

% Parameters, hydrodynamic derivatives and main dimensions
m  = 0.00792;    mx     = 0.000238;   my = 0.007049;
Ix = 0.0000176;  alphay = 0.05;       lx = 0.0313;
```

```
ly = 0.0313;    Ix    = 0.0000176;  Iz = 0.000456;
Jx = 0.0000034;  Jz    = 0.000419;   xG = 0;

B    = 25.40;   dF = 8.00;    g    = 9.81;
dA   = 9.00;    d  = 8.50;    nabla = 21222;
KM   = 10.39;   KB = 4.6154;  AR   = 33.0376;
Delta = 1.8219;  D  = 6.533;   GM   = 0.3/L;
rho  = 1025;    t  = 0.175;   T    = 0.0005;
W    = rho*g*nabla/(rho*L^2*U^2/2);

Xuu    = -0.0004226;  Xvr   = -0.00311;    Xrr    = 0.00020;
Xphiphi  = -0.00020;    Xvv   = -0.00386;

Kv     =  0.0003026;  Kr    = -0.000063;   Kp     = -0.0000075;
Kphi   = -0.000021;   Kvvv  =  0.002843;   Krrr   = -0.0000462;
Kvvr   = -0.000588;   Kvrr  =  0.0010565;  Kvvphi  = -0.0012012;
Kvphiphi = -0.0000793;  Krrphi = -0.000243;   Krphiphi =  0.00003569;

Yv     = -0.0116;    Yr    =  0.00242;    Yp     =  0;
Yphi   = -0.000063;   Yvvv  = -0.109;      Yrrr   =  0.00177;
Yvvr   =  0.0214;     Yvrr  = -0.0405;     Yvvphi  =  0.04605;
Yvphiphi =  0.00304;    Yrrphi =  0.009325;   Yrphiphi = -0.001368;

Nv     = -0.0038545;  Nr    = -0.00222;    Np     =  0.000213;
Nphi   = -0.0001424;  Nvvv  =  0.001492;   Nrrr   = -0.00229;
Nvvr   = -0.0424;     Nvrr  =  0.00156;    Nvvphi  = -0.019058;
Nvphiphi = -0.0053766;  Nrrphi = -0.0038592;  Nrphiphi =  0.0024195;

kk   =  0.631;  epsilon =  0.921;  xR   = -0.5;
wp   =  0.184;  tau   =  1.09;   xp   = -0.526;
cpv  =  0.0;    cpr   =  0.0;    ga   =  0.088;
cRr  = -0.156;  cRrrr  = -0.275;  cRrrv =  1.96;
cRX  =  0.71;   aH    =  0.237;  zR   =  0.033;
```

```
xH    = -0.48;
a11   = 6.65;  a22   = 0.119;  a33   = 0.145;

% Masses and moments of inertia
m11 = (m+mx);
m22 = (m+my);
m32 = -my*ly;
m42 = my*alphay;
m33 = (Ix+Jx);
m44 = (Iz+Jz);

% Rudder saturation and dynamics
if abs(delta_c) >= delta_max*pi/180,
  delta_c = sign(delta_c)*delta_max*pi/180;
end

delta_dot = delta_c - delta;

if abs(delta_dot) >= Ddelta_max*pi/180,
  delta_dot = sign(delta_dot)*Ddelta_max*pi/180;
end

% Shaft velocity saturation and dynamics
n_c = n_c*U/L;
n   = n*U/L;
if abs(n_c) >= n_max/60,
  n_c = sign(n_c)*n_max/60;
end

if n > 0.3,Tm=5.65/n;else,Tm=18.83;end
n_dot = 1/Tm*(n_c-n)*60;

% Calculation of state derivatives
```

```
 vR     = ga*v + cRr*r + cRrrr*r^3 + cRrrv*r^2*v;
 uP     = cos(v)*((1 - wp) + tau*((v + xp*r)^2 + cpv*v + cpr*r));
  J     = uP*U/(n*D);
 KT     = 0.527 - 0.455*J;
 uR     = uP*epsilon*sqrt(1 + 8*kk*KT/(pi*J^2));
 alphaR = delta + atan(vR/uR);
 FN     = - ((6.13*Delta)/(Delta + 2.25))*(AR/L^2)*(uR^2 + vR^2)*sin(alphaR);
 T      = 2*rho*D^4/(U^2*L^2*rho)*KT*n*abs(n);

% Forces and moments
 X    = Xuu*u1^2 + (1-t)*T + Xvr*v*r + Xvv*v^2 + Xrr*r^2 + Xphiphi*phi^2 + ...
        cRX*FN*sin(delta) + (m + my)*v*r + m*a11*noi*tan(psi);

 Y    = Yv*v + Yr*r + Yp*p + Yphi*phi + Yvvv*v^3 + Yrrr*r^3 + Yvvr*v^2*r + ...
        Yvrr*v*r^2 + Yvvphi*v^2*phi + Yvphiphi*v*phi^2 + Yrrphi*r^2*phi + ...
        Yrphiphi*r*phi^2 + (1 + aH)*FN*cos(delta) - (m + mx)*u1*r + m*a11*noi;

 K    = Kv*v + Kr*r + Kp*p + Kphi*phi + Kvvv*v^3 + Krrr*r^3 + Kvvr*v^2*r + ...
        Kvrr*v*r^2 + Kvvphi*v^2*phi + Kvphiphi*v*phi^2 + Krrphi*r^2*phi + ...
        Krphiphi*r*phi^2 - (1 + aH)*zR*FN*cos(delta) + mx*lx*u1*r - W*GM*phi
        + m*a22*L*noi;

 N    = Nv*v + Nr*r + Np*p + Nphi*phi + Nvvv*v^3 + Nrrr*r^3 + Nvvr*v^2*r + ...
        Nvrr*v*r^2 + Nvvphi*v^2*phi + Nvphiphi*v*phi^2 + Nrrphi*r^2*phi + ...
        Nrphiphi*r*phi^2 + (xR + aH*xH)*FN*cos(delta) + m*a33*L*noi;

% Dimensional state derivatives  xdot = [ u v r x y psi p phi delta n ]'
detM = m22*m33*m44-m32^2*m44-m42^2*m33;

xdot =[                  X*(U^2/L)/m11
       -((-m33*m44*Y+m32*m44*K+m42*m33*N)/detM)*(U^2/L)
        ((-m42*m33*Y+m32*m42*K+N*m22*m33-N*m32^2)/detM)*(U^2/L^2)
             (cos(psi)*u1-sin(psi)*cos(phi)*v)*U
```

```
            (sin(psi)*u1+cos(psi)*cos(phi)*v)*U
                    cos(phi)*r*(U/L)
        ((-m32*m44*Y+K*m22*m44-K*m42^2+m32*m42*N)/detM)*(U^2/L^2)
                      p*(U/L)
                    delta_dot
                      n_dot              ];

% Return values for S-function:
sys = xdot;
% End of mdlDerivatives

function sys = mdlOutputs(t,x,u)

sys = x;

% End of function mdlOutputs
```

Appendix II -- Electronic configuration of model scaled vessel 'Hoorn'

This appendix outlines the electronic components of the free running scaled model Hoorn in this project. The model is consisted of five subsystems: Power supply system, propelling and steering system, embedded computer platform, sensors and host computer. The details are presented as following in Table Appendix 1.

Table Appendix 1 Electronic components employed in developing 'Hoorn'

Subsystem	Devices	Figure	Roles
Power supply system	Panasonic LC-RC1212PG Lead Acid Battery (12 V) 6 sets with 36V output		Power supply
Propelling and steering system	Maxon EC motor 136208 2 sets		Propellers drive
	ESCON Amplifier 50/5 2 sets		Amplify direct current and measurement of motors' shaft speed
	CYS-S8218 servo motor 40Kg torque 1 set		Rudder drive
Embedded computer platform	NI myRIO 1900 1 set		Embedded computer, DAQ, microprocesser, WIFI communication

Sensors	HMC5883L Digital Compass	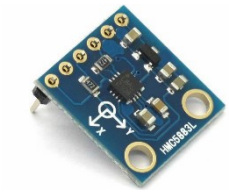	Measurement of yaw angle
	ADXL345 Accelerometer		Measurement of kinetic acceleration on 3 axis
	L3G4200D Gyroscope		Measurement of rotation rate on 3 axis
	MTK3339 GPS		Measurement of positioning
Host computer and WIFI module	D-LINK DI-524UP		WIFI communication router
	Laptop with LabVIEW 2014		Terminal device, RT operatiom, monitoring

Appendix III -- Mathematical model of 'Hoorn' coding in MATLAB S-function

```
% Modelling, System Identification from the Free Running Model Test of Hoorn
% Version 1.3 (23/05/2017)
% Developed by Yuanyuan Wang and Hung Duc Nguyen in 2016

function [sys,x0,str,ts] = HoornModel2(t,x,u,flag)

switch flag
case 0,
   [sys,x0,str,ts] = mdlInitializeSizes;
case 1,
    sys=mdlDerivatives(t,x,u);
case 3,
   sys = mdlOutputs(t,x,u);
case {2, 4, 9},
   sys = [];
otherwise
   error(['Unhandled flag = ',num2str(flag)]);
end

function [sys,x0,str,ts] = mdlInitializeSizes

sizes = simsizes;
sizes.NumContStates = 11;
sizes.NumDiscStates = 0;
sizes.NumOutputs = 11;
sizes.NumInputs = -1;
sizes.DirFeedthrough = 1;
sizes.NumSampleTimes = 1;
sys = simsizes(sizes);
```

```
% Initial values of state vector:
x0 = [1 0 0 0 0 0 0 0 0 1 -1]';
%x = [ u v r x y psi p phi delta n1 n2]'
str = [];
ts = [0 0];
% end of mdlInitializeSizes

function sys=mdlDerivatives(t,x,u)
% [xdot,U] = container(x,ui) returns the speed U in m/s (optionally) and the
% time derivative of the state vector: x = [ u v r x y psi p phi delta n ]'  for
% a free running model Hoorn L = 2.47 m, where
% u     = surge velocity         (m/s)
% v     = sway velocity          (m/s)
% r     = yaw velocity           (rad/s)
% x     = position in x-direction (m)
% y     = position in y-direction (m)
% psi   = yaw angle              (rad)
% p     = roll velocity          (rad/s)
% phi   = roll angle             (rad)
% delta = actual rudder angle    (rad)
% n1    = propeller 1   (rpm)
% n2    = propeller 2   (rpm)
% The input vector is :
% ui      = [ delta_c n_c ]'  where
% delta_c = commanded rudder angle   (rad)
% n_c     = commanded shaft velocity (rpm)

% Check of input and state dimensions
if (length(x) ~= 11),error('x-vector must have dimension 11 !');end
if (length(u) ~= 3),error('u-vector must have dimension  3 !');end

% Normalization variables
L = 2.47;                  % length of ship (m)
```

```
U = sqrt(x(1)^2 + x(2)^2);   % service speed (m/s)

% Check service speed
%if U <= 0,error('The ship must have speed greater than zero');end
%if x(10) <= 0,error('The propeller rpm must be greater than zero');end

delta_max  = 30;            % max rudder angle (°)
Ddelta_max = 20;            % max rudder rate (°/s)
Nc_max     = 1000;

% Non-dimensional states and inputs
delta_c = u(1);
n1_c    = u(2);
n2_c    = u(3);

u1    = x(1)/U;   v   = x(2)/U;
p     = x(7)*L/U; r   = x(3)*L/U;
phi   = x(8);     psi = x(6);
delta = x(9);
n1    = x(10);
n2    = x(11);

% Parameters, hydrodynamic derivatives and main dimensions
m = 0.0084;     mx = 0.00031514;   my = 0.0075;
alphay = 0.05;  lx = 0.0313;       ly = 0.0313;
Ix = 0.000077279;  Iz = 0.0020;
Jx = 0.000015456;  Jz = 0.0020;   xG = 0;
B = 0.32; g = 9.81;  d  = 0.12; Cb = 0.69;
weights = 63.4; AR = 0.0006; rho   = 1000;
D = 0.06; GM = 0.00875/L;
W     = weights*g/(rho*L^2*U^2/2);

Xuu     = -0.0024;    Xvr    = -0.0024;   Xvv    = 0.0149;
```

```
Xrr      = 0.0207;    Xphiphi  = 0.0166;

Yv = -0.0492; Yr = 0; Yp = 0;
Yphi = 0; Yvvv = 0.02394; Yrrr = 0;
Yvvr = -0.2422; Yvrr = -0.1299; Yvvphi = -0.0148;
Yvphiphi = 0; Yrrphi = 0; Yrphiphi = 0;

Kv =  0.00089; Kr =  0.00013; Kp = -0.000062;
Kphi = 0; Kvvv = -0.0264; Krrr =0;
Kvvr = -0.0080; Kvrr =0.0096; Kvvphi = -0.0103;
Kvphiphi =0; Krrphi = -0.00159; Krphiphi = 0;

Nv       = -0.0095;  Nr     = -0.00455;    Np =0;
Nphi = 0; Nvvv   = 0.0034;   Nrrr     = 0.0017;
Nvvr     = -0.0216;     Nvrr   =  0.0011;    Nvvphi = -0.0191;
Nvphiphi = -0.0058; Nrrphi = -0.0033; Nrphiphi = 0.0024;
% Masses and moments of inertia
m11 = (m+mx);
m22 = (m+my);
m32 = -my*ly;
m42 = my*alphay;
m33 = (Ix+Jx);
m44 = (Iz+Jz);

% Rudder saturation and dynamics
if abs(delta_c) >= delta_max*pi/180,
   delta_c = sign(delta_c)*delta_max*pi/180;
end
delta_dot = delta_c - delta;
if abs(delta_dot) >= Ddelta_max*pi/180,
   delta_dot = sign(delta_dot)*Ddelta_max*pi/180;
end
%n_dot = 0;
```

```
n1_dot = n1_c - n1;
n2_dot = n2_c - n2;

if abs(n1_dot) >= Nc_max,
   n1_dot = sign(n1_dot)*Nc_max;
end
if abs(n2_dot) >= Nc_max,
   n2_dot = sign(n2_dot)*Nc_max;
end

% Calculation of state derivatives
T = (n1^2*sign(n1)-n2^2*sign(n2))*6.3545*10^(-6)/(0.5*L^2*U^2*1000)*1;
Npropeller=(n1^2*sign(n1)+n2^2*sign(n2))*6.3545*10^(-6)*590/(0.5*L^3*U^2)*1;
%Yaw moments generated from propellers

%Calculation of Rudder force
deltap = 10.4569/U^2;
krudder2 = 1 + 0.6*deltap;
FN = -0.006*0.3610*krudder2*(6.13*1.67/(2.25+1.67))/L^2*sin(delta)*1;

aH = 0.237;xR = -0.5;xH = -0.45;zR = 0.033;cRX = 0.6175;
% Forces and moments
% surge
  X    = Xuu*u1^2 + T + Xvr*v*r + Xvv*v^2 + Xrr*r^2 + Xphiphi*phi^2 + ...
         cRX*FN*sin(delta) + (m + my)*v*r;
% sway
  Y    = Yv*v + Yr*r + Yp*p + Yphi*phi + Yvvv*v^3 + Yrrr*r^3 + Yvvr*v^2*r + ...
         Yvrr*v*r^2 + Yvvphi*v^2*phi + Yvphiphi*v*phi^2 + Yrrphi*r^2*phi + ...
         Yrphiphi*r*phi^2 + (1 + aH)*FN*cos(delta) - (m + mx)*u1*r;
% roll
  K    = Kv*v + Kr*r + Kp*p + Kphi*phi + Kvvv*v^3 + Krrr*r^3 + Kvvr*v^2*r + ...
         Kvrr*v*r^2 + Kvvphi*v^2*phi + Kvphiphi*v*phi^2 + Krrphi*r^2*phi + ...
```

```
        Krphiphi*r*phi^2 - (1 + aH)*zR*FN*cos(delta) + mx*lx*u1*r - W*GM*phi;
% yaw
  N    = Nv*v + Nr*r + Np*p + Nphi*phi + Nvvv*v^3 + Nrrr*r^3 + Nvvr*v^2*r + ...
         Nvrr*v*r^2 + Nvvphi*v^2*phi + Nvphiphi*v*phi^2 + Nrrphi*r^2*phi + ...
         Nrphiphi*r*phi^2 + (xR + aH*xH)*FN*cos(delta)+Npropeller;
% Dimensional state derivatives  xdot = [ u v r x y psi p phi delta n ]'
detM = m22*m33*m44-m32^2*m44-m42^2*m33;

xdot =[              X*(U^2/L)/m11;
       -((-m33*m44*Y+m32*m44*K+m42*m33*N)/detM)*(U^2/L);
        ((-m42*m33*Y+m32*m42*K+N*m22*m33-N*m32^2)/detM)*(U^2/L^2);
            (cos(psi)*u1-sin(psi)*cos(phi)*v)*U;
            (sin(psi)*u1+cos(psi)*cos(phi)*v)*U ;
                  cos(phi)*r*(U/L)          ;
        ((-m32*m44*Y+K*m22*m44-K*m42^2+m32*m42*N)/detM)*(U^2/L^2);
                    p*(U/L);
                   delta_dot;
                    n1_dot;
                    n2_dot];

% Return values for S-function:
sys = xdot;

% End of mdlDerivatives
function sys = mdlOutputs(t,x,u)
sys = x;
% End of function mdlOutputs
```

Appendix III -- EBS LOS coding in MATLAB S-function

Step 1 Initialization

```
% Initialization.m
clear
global waypointx waypointy count L1 count1 index

%%%%%% length of ship %%%%%%
L1 = 175.00;

%%%%%% waypoint database%%%%%%
x2 =[0 1000 2000 2000 1000 0];
y2 =[0 0 1000 2000 3000 3000];
waypointx = x2';  waypointy = y2';
count = 2;count1=1; index = 0;
% End of file
```

Step 2 Waypoints selection

```
function [sys,x0,str,ts] = LosSFunction(t,x,u,flag)

% SquarePatternSFunction.m
%
switch flag
case 0
  [sys,x0,str,ts] = mdlInitializeSizes;
case 3
  sys = mdlOutputs(t,x,u);
case { 1, 2, 4, 9}
  sys = [];
otherwise
  error(['Unhandled flag = ',num2str(flag)]);
end
% End of function myfun
```

```
function [sys,x0,str,ts] = mdlInitializeSizes
sizes = simsizes;
sizes.NumContStates = 0;
sizes.NumDiscStates = 0;
sizes.NumOutputs = 6;
sizes.NumInputs = -1;
sizes.DirFeedthrough = 1;
sizes.NumSampleTimes = 1;
sys = simsizes(sizes);
x0 = [];
str = [];
ts = [-1 0];
% end of mdlInitializeSizes

function sys = mdlOutputs(t,x,u)
global waypointx waypointy count L1 count1
xxpos = u(1);
yypos = u(2);

% Coref = psi_ref(count)*pi/180;
xx = waypointx(count);yy = waypointy(count);
xxp = waypointx(count1);yyp = waypointy(count1);
R0 = sqrt((xx-xxpos)^2 + (yy-yypos)^2);

if R0 <= 2*L1
    count = count+1;
    count1=count1+1;
    xx = waypointx(count);
    yy = waypointy(count);
    xxp = waypointx(count1);
    yyp = waypointy(count1);
end
```

```
sys = [xxp yyp xx yy xxpos yypos]';    % Reference cource
% End of function mdlOutputs
```

Step 3 LOS processing

```
function yy = fcn(u1,u2,u3,u4,u5,u6)

%items definition
x_k = u3;
y_k = u4;
x_k_1 = u1;
y_k_1 = u2;
x = u5;
y = u6;
Lpp = 175;
delta_x = x_k - x_k_1;
delta_y = y_k - y_k_1;

if( delta_x==0 )
   x_los = x_k_1;

   if( delta_y > 0)
      y_los = y + 2*Lpp;
   else
      y_los = y - 2*Lpp;
   end

else % delta_x ~= o
   d = delta_y / delta_x;
   e = x_k_1;
   f = y_k_1;
   g = -d*e + f;
   a = 1 + d^2;
   b = 2*(d*g - d*y -x);
```

```
    c = x^2 + y^2 +g^2 - (2*Lpp)^2 - 2*g*y;

    if(delta_x > 0)
        x_los = (-b + sqrt(abs(b^2 - 4*a*c)))/(2*a);
    else
        x_los = (-b - sqrt(abs(b^2 - 4*a*c)))/(2*a);
    end
        y_los = d*x_los + g;
end

r1 = atan2((y_los - y),(x_los - x));
yy = [r1];
%dynamic desired yaw angle calculated by EBS LOS guidance algorithm
```